Characterization of photolyases from Sulfolobus solfataricus

Binjawhar, Dalal

Award date:
2013

Awarding institution:
University of Bath

Characterization of photolyases from *Sulfolobus solfataricus*

Submitted by

Dalal Binjawhar

A thesis submitted for the degree of Doctor of Philosophy

University of Bath

Department of Biology and Biochemistry

April 2013

COPYRIGHT

Acknowledgments

It has been a wonderfully enlightening experience working on this project. It is the result of many efforts that cannot go unmentioned. I would like to start off by thanking Allah for granting me the blessing of knowledge. Without his guidance and direction I wouldn't be able to accomplish this work. I would also like to express my gratitude and appreciation to my supervisors, Momna Hejmadi, David Hough and Michael Danson, whose contribution to this study cannot be measured. My words fail to express how thankful I am for their wisdom, thoughtful patience, tolerance and brilliant supervision. I truly believe I am blessed with the best supervisors this department has to offer. I would also like to thank my colleagues in Lab 1.33 for their support and for making the work environment enjoyable. Especially, KarlPayne, Winnie Wu, Charlie, Philippe, Carolyn, Chris Hillier, Chris Vennard, Tracey, John, Dima and Giannina. I would like to extend my thanks to Prof.r. Carlos Menck for providing me with the recombinant rat kangaroo *phr* gene in pCY4B. Many thanks to all staff in the teaching lab, in this department, for their kind cooperation for letting me using many machines even during busy times. Also I don't want to forget to thank the University of Bath for giving me the opportunity to do my PhD in the department of Biology and Biochemistry.

I am very grateful to my country and especially to the Ministry of Higher Education in Saudi Arabia for funding my study.

Most of all I would like to thank my parents who made me the person I am today, their understanding, insight, patience and upbringing are the reasons this study is even possible. A very special thanks to my husband, Hani, for his help, support, patience and for sharing all the moments of happiness and sadness during all these years and especially for being with me and helping me get through the hard times. I would also like to extend my thanks to my sisters, Laila, Hind, Anood and Wejdan, who always encouraged me and stood by me through thick and thin. Also thanks to my brothers and my little boy for the lovely times I spent with them.

Last but not least, I thank my lovely friends, Fada, Mona and Maha for supporting me, listening to my complaints and for adding an entertainment value of my PhD.

Thank you all, and I hope for a chance to be able to give back part of what you have given to me.

Table of contents

Abbreviations

ºC	Degree Celsius
8-HDF	8-hydroxy-5-deazaflavin
APS	Ammonium persulphate
ATCC	American Type Culture Collection
BLAST	Basic Local Alignment Search Tool
bp	base pair
BSA	bovine serum albumin
CMV	cytomegalovirus
CO_2	carbon dioxide
CPD	cyclobutane pyrimidine dimer
CS	cockayne's syndrome
DF	DreamFect (transfection reagent)
DMEM	Dulbecco's Modified Eagle's Medium
DMSO	dimethyl sulphoxide
DNA	deoxynucleic acid
dATP	Deoxyadenosine triphosphate
dNTPs	deoxynucleoside triphosphate
DTT	dithiothreitol
EDTA	ethylenediamine tetracetic acid
ES	enzyme-substrate complex
et al.	And others (*et alia*)
FAD	flavin adenine dinucleotide
$FADH^-$	reduced flavin adenine dinucleotide
FBS	fetal bovine serum
FMN	flavin mono nucleotide
G1P	glycerol-1-phosphate
G3P	glycerol-3-phosphate
GFP	green fluorescent protein
hr	hour
IPTG	isopropyl β-D-thiogalactopyranoside
kb	kilo base
KDa	kilodalton
KRK	lysine arginine lysine
LB	Luria broth medium
M	molar
MCS	multiple cloning sequence
MilliQ water	ultrapurified water
min	minute
MPa	megapascal (pressure measurement)
MSH6	human mismatch repair protein
MTHF	5, 10-methenyltetrahydrofolate
MTT	(3-[4, 5-dimethylthiazol-2-y]-2, 5-diphenyltetrazolium bromide)
M_r	relative molecular mass
NER	nucleotide excision repair

NLS	nuclear localization sequence
OD_{600}	Optical density at 600 nm
PAGE	polyacrylamide gel electrophoresis
PCR	polymerase chain reaction
PP	photoproducts
RK	rat kangaroo
P/S	penicillin/streptomycin
rpm	revolutions per minute
rRNA	ribosomal ribonucleic acid
s	seconds
SDS	Sodium dodecyl sulphate
SS	*Sulfolobus solfataricus*
SSU	small subunit
TAE	tris-acetate EDTA
Taq	*Thermophilus aquaticus* (DNA polymerase)
TEMED	*N,N* tetramethylethylenediamine
Temp	temperature
Tris	Tris(hydroxymethyl)methylamine
TTD	tricothiodystrophy
U	unit (of enzyme activity)
***vs*.**	*versus*
UV	ultraviolet
UVB	Ultraviolet light at 290-320 nm
UVC	Ultraviolet light at 100-290 nm
w/v	Weight per volume
X-Gal	5-bromo-4-chloro-3-indoyl-β-D-galactopyranoside
XP	xeroderma pigmentosum

Abstract

Ultraviolet light induces DNA damage in the form of photoproducts, leading to increased genomic instability, if left unrepaired. Photoreactivation, catalysed by the enzyme photolyase, is the simplest and most efficient mechanism of repairing UV-induced DNA damage. Interestingly however, the gene encoding photolyase has been lost through evolution in all placental mammals including humans. *Sulfolobus solfataricus*, is a thermophilic archaeon that is highly tolerant to high doses of UV light in their natural environment. However, the mechanism underlying this tolerance or the role of photoreactivation remains uncharacterised.

This study, identifies a novel putative *S. solfataricus phr* gene, and its expression was functionally characterised in *E.coli* both *in vivo* and *in vitro*. The optimum temperature for the activity of the enzyme was determined to be 90 ºC.

The archaeal *phr* gene was also transfected in a photolyase-deficient human cell line, HeLa cells, using a mammalian expression vector (pDs-Red Monomer as a fusion tag). In parallel, two photolyase genes from *E.coli* and rat kangaroo (closest non-placental mammal which expresses photolyase) were used in similar systems as positive controls. The results showed no photoreactivation of UV treated cells following illumination with white light in the transfected HeLa cells with *phr* genes from the three organisms. This suggests that either the proteins were not expressed or not folded successfully in the cells. The results and findings are discussed in the context and compared with the other findings in the literature on the investigation of photoreactivation system in *S. solfataricus* and other organisms.

Chapter 1: Introduction

1.1 UV light and DNA damage

Ultraviolet light (UV), which is a component of sun light, induces severe damage to all living organisms, ranging from prokaryotic bacteria to humans (Sinha and Hader 2002). Depletion of the ozone layer increases UV radiation at Earth's surface; particularly the spectral regions of UV-B (290-320 nm) and UV-C (100-290 nm), which have the most deleterious effects on living organisms (Sinha and Hader 2002; Friedberg *et al.* 1995). This type of solar radiation induces several biological effects such as inhibition in growth and survival, protein degradation plus reduction in photosynthesis in several living cells (Herndl 1997; Klaper *et al.* 1996). Cellular DNA is the most endangered because its nucleic acid bases absorb UV light spectrum efficiently (Patrick 1977; Sancar 1990; Sancar and Sancar 1988). When the DNA is exposed to UV radiation, two major types of DNA lesions are induced: Cyclobutane pyrimidine dimers (CPDs) and (6-4) pyrimidone photoproducts (6-4 PPs) (Mitchell and Karentz 1993). CPDs correspond to the formation of a cyclobutane ring involving two covalent bonds between C_5 and C_6 of the adjacent pyrimidines on the same DNA strand, whereas 6-4 PPs are produced by formation of a single covalent bond between C_6 and C_4 of the adjacent pyrimidine residues (Friedberg 2006) Fig 1.1.

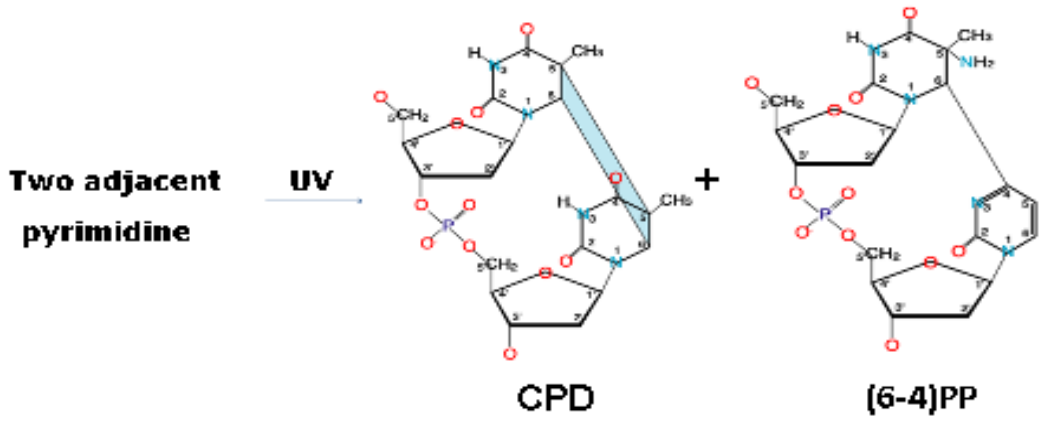

Figure1.1 UV photoproducts
Formation of CPD and (6-4)pp lesions after exposure to UV light. Adapted from (Friedberg *et al.* 1995)

These two dimers constitute 70-80 % and 20-30 % of all photoproducts induced by UV light, respectively (Friedberg *et al.* 1995). Both lesions cause distortion in the structure of the DNA molecule, which may affect DNA replication, transcription and also can block the work of DNA /RNA polymerases (Hanawalt 1994; You *et al.* 2001; Lima-Bessa *et al.* 2007). In addition, formation of CPDs might play an important role in the initiation of skin cancer (Gilchrest *et al.* 1999). This is because it was found that this lesion is associated in the generation of mutations in the tumour suppressor genes p53 in skin tumours (You *et al.* 2000; Adimoolam and Ford 2003). Moreover, UV lesions can result in a transition of C to T and CC to TT, which are considered as the most common mutations of p53 found in skin cancers of human and mouse (Ananthaswamy *et al.* 1997; Soehnge *et al.* 1997).

So, if these lesions are left unrepaired, they might interrupt essential cellular processes and consequently lead to mutagenesis, carcinogenesis and cell death (Sinha and Hader 2002). In addition, if the damage is severe in a cell and cannot be repaired, apoptosis will be induced to get rid of the mutant cell in eukaryotes (Hill *et al.* 1999). Therefore, all living cells have evolved various strategies that are capable of maintaining their genetic integrity (Weber 2005). This includes developing efficient repair mechanisms in order to eliminate the lethal effects of UV lesions (Sinha and Hader 2002). There are numbers of repair mechanisms known for repairing UV-induced DNA lesions. The following section describes these DNA repair mechanisms in detail.

1.2 DNA repair mechanisms for UV-induved DNA damage

Three main DNA repair mechanisms in repairing UV damage will be described here. Nucleotide excision repair (NER), repair mechanism by UV-endonucleases and photoreactivation. An overview of interaction between these three mechanisms can be seen in Fig 1.2.

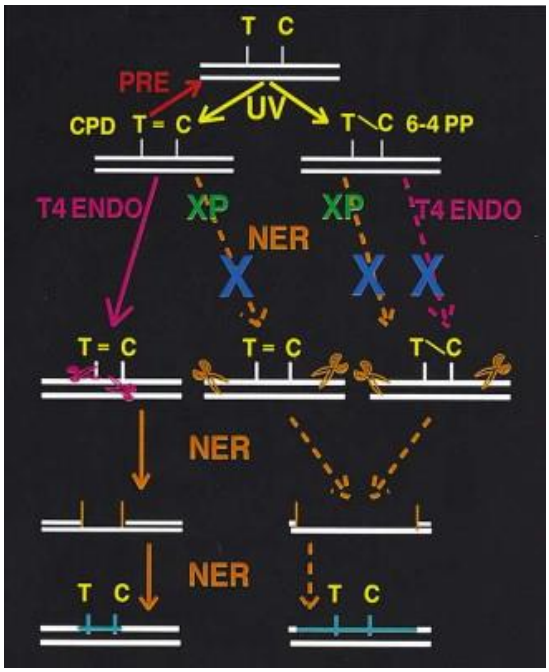

Figure 1.2 comparisons between the repair mechanism of bacterial T4 endonuclease V with photoreactivation (PRE) and mammalian NER in repairing UV lesions

UV light induces two types of DNA damage dimers, CPD and 6-4 pp. The dimers could be produced by the adjacent thymine (T) and cytosine (C). T4 endo V makes two cleavages (scissors) between the base and sugar plus another cleavage in the DNA backbone. NER (orange) then removes the lesion and the gap is refilled by adding the complementary bases from the other strand. T4 endo V cannot repair 6-4pp (dashed pink line and blue X). In the cells of XP patients, NER mechanism is unable to make the cleavage steps (dashed orange line and blue X) but can process DNA after the incision by T4 endo V. Photoreactivation can simply reverse the dimer in the presence of light (adapted fromKraemer and DiGiovanna 2002).

1.2.1 Nucleotide Excision Repair (NER):

Nucleotide excision repair, also known as a dark repair or light-independent repair, is a complex multi-step mechanism (Friedberg 2001; Weber 2005). The early reports on the discovery of NER mechanism (called cut-and-patch repair) were done in *E. coli* B/r and *E. coli* K-12 by (Setlow and Carrier 1964; Boyce and Howardflanders 1964). The NER mechanism involves numerous enzymes and proteins (around 30) that recognize and repair bulky DNA lesions such as UV photoproducts or chemical adducts induced by benzpyrene or aflatoxin (Lindahl and Wood 1999; Sinha and Hader 2002; Dorazi *et al.* 2007). NER has been found in both prokaryotes and eukaryotes but in the former the mechanism comprises only three proteins (Yasui and McCready 1998). However, archaea seem to lack the NER mechanism and homologues of bacterial NER genes were found in only few archaeal species, such as *Methanobacterium, Methanosarcina* and *Halobacterium* (McCready and Marcello 2003; Ng *et al.* 2000; Galagan *et al.* 2002; Ogrunc *et al.* 1998). NER is more efficient in repairing 6-4 PPs but its efficiency is a much less when compared with photoreactivation (Friedberg 1995; Lucas-Lledo and Lynch 2009).

NER is divided into two subpathways: transcription-coupled repair (TC-NER) which refers to the repair of active transcriped genes in DNA, and global genome repair (GG-NER) that refers to the repair of non-transcriped genes (Thoma 1999).

In eukaryotes, NER uses multiple protein complex to remove a DNA fragment of 27-30 nucleotides (Friedberg 2001). NER mechanism involves three stages, DNA damage recognition, dual incision of the lesion, and repair synthesis and ligation (Lindahl and Wood 1999). Photoproducts of UV light causes a bend or a kink in the DNA double helix and this distortion in the helical structure can be recognized by NER proteins (Posnick and Samson 2001). The first step of this mechanis in humans Fig 1.3 (proteins equivalent in yeast are indicated side by side) involves the recognition of the damage by proteins called XPC-hHR23B (in yeast called Rad4-Rad23 complex) which binds to the damage and initiates the repair mechanism (Sugasawa *et al*. 1998). The second step is the binding of several proteins XPA (Rad14), RPA (Rfa), TFIIH and XPG (Rad2) (Friedberg 2001, Thoma 1999).

TFIIH which is a general transcription factor " contains two DNA helicase activities (XPB and XPD) that unwind the DNA duplex" (Friedberg 2001). The equivalent of XPB and XPD proteins in yeast is (Rad25/Ss12) and Rad3 respectively (Thoma 1999). This unwinding generates a bubble in the DNA strand. The next step involves the binding of ERCC1-XPF (Rad1-Rad10) which makes incision at the 5' end and another incision at the 3' end made by XPG (Thoma 1999; Friedberg 2001). Finally, the fragment of 27-30 nucleotides is then removed from the genome and the gap is refilled by DNA polymerase δ or ε with accessory replication proteins (PCNA, RPA, and RFC) pluse the action of DNA ligase to restore the DNA (Friedberg 2001). "In comparison to eukaryotic NER, prokaryotic NER involves only three proteins UvrA, UvrB and UvrC which cary out the complete process of damage recognition and excision" (Sinha and Hader 2002). In prokaryotes the dual incision involves the removal of a DNA fragment comprises of 12-13 nucleotides wherease in archaea, the fragment length is 10-11 nucleotides (Ogrunc *et al*. 1998). In some archaeal species such as *M. thermoautotroph*, the NER activity was found to be similar to that of bacterial system and a homologous of UvrA and UvrB was reported (Grogan 2000). On the other hand, another archaeal species were found to have a homologous of eukaryal NER system such as homologous of Rad1, Rad2, Rad3, Rad25 and Rad27 (Aravind *et al*. 1999; Grogan 2000).

Any defects in genes involved in expressing NER proteins may result in human syndromes with photosensitivity and increased cancer risk, such as Xeroderma pigmentosum (XP),

Cockayne's syndrome (CS) and tricothiodystrophy (TTD) (Chigancas *et al.* 2004; Friedberg *et al.* 1995; Lindahl and Wood 1999; Thoma 1999; Lehmann 1995). Patients with a defective NER mechanism have 1000 times higher risk of developing skin cancer (Lindahl and Wood 1999).

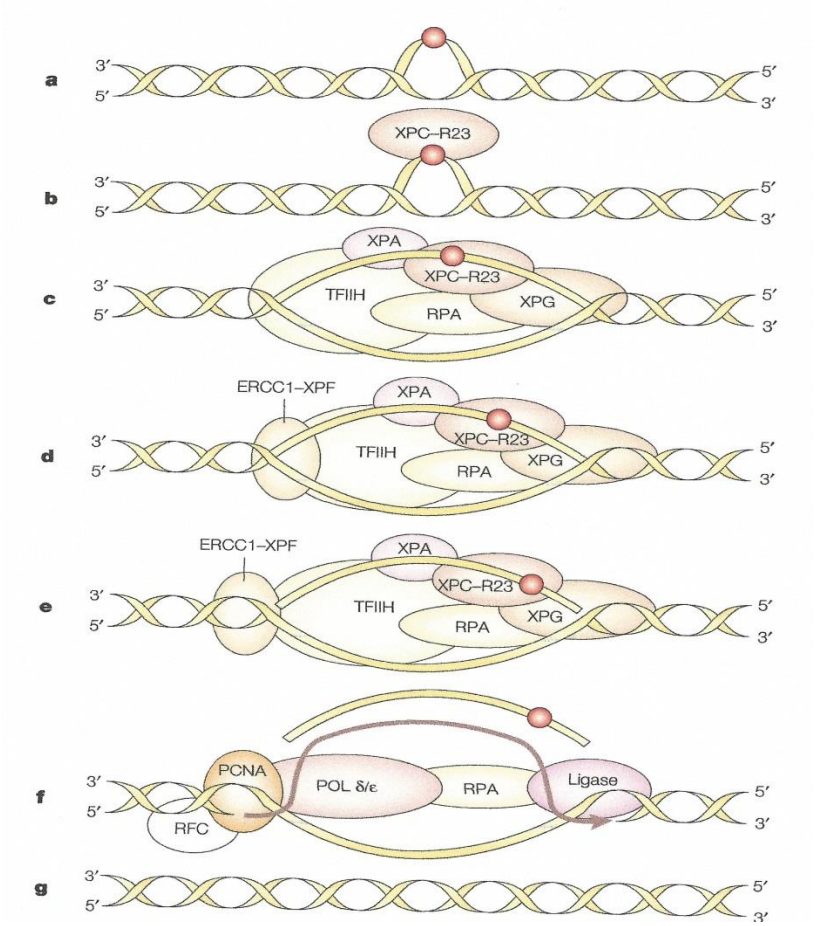

Fig 1.3 Overview of NER mechanism

a) bulky lesion on a DNA strand.
b) damage recognition by XPC-hHR23B.
c) binding of other proteins (XPA, RPA, XPG and TFIIH).
d) binding of ERCC1-XPF .
e) ERCC1-XPF makes incision at the 5' end and also XPG makes another incision at the 3' end.
f) the fragment of 27-30 nucleotides is removed and the synthesis of complementery strand is made by polymerase δ or ε with the help of PCNA, RFP and RFC accessory proteins and the strand is sealed by DNA ligase.
g) damaged DNA strand is repaired and returned to its normal confirmation (adapted from Friedberg 2001).

1.2.2 UV-endonucleases

An additional mechanism of repair of UV-induced DNA damage involves enzymes known as UV-endonucleases (Sinha and Hader 2002). These enzymes recognize the CPD lesions and cleave the *N*- glycosidic bond at the 5' end of the pyrimidine dimer followed by a cleavage of the phosphodiester bond at the AP site (Sinha and Hader 2002). These enzymes are found only in UV resistant organisms, such as *Micrococcus luteus* (Dodson *et al.* 1994). However, it was found that the *denV* gene of bacteriophage T4 coded a similar enzyme (T4 endonuclease V) and its activity was detected following expression in *S. cerevisiae* (Hamilton *et al.* 1992). T4 endonuclease V is a bacterial enzyme that functions as a DNA repair enzyme which recognizes only one type of UV damage, which is CPD (Kraemer and DiGiovanna 2002). In bacteria, there is an interaction between this repair mechanism of endonucleases and the NER mechanism, in which the resulting fragment that was cleaved by the action of endonucleases (contains the CPD lesion), is then processed by the NER system, so removing that lesion and therefore restoring the original shape of DNA Fig 1.2 (Kraemer and DiGiovanna 2002).

It was reported in 1975 that introduction of T4 endonuclease V into XP cell cultures, increased DNA repair (Tanaka *et al.* 1975). Another study also proved that the treatments with the endonuclease have beneficial effects in XP patients (Yarosh *et al.* 2001).

On the other hand, there is no interaction between NER or T4 endonuclease V and photoreactivation in bacteria (Kraemer and DiGiovanna 2002). CPD photolyase directly reverses the pyrimidine dimers in the presence of light and therefore does not involve the action of NER system (Kraemer and DiGiovanna 2002).

1.2.3 Photoreactivation

Definition

Photoreactivation is the simplest, direct and most efficient mechanism for repairing CPDs and 6-4PPs (Menck 2002; Komori *et al.* 2001). This mechanism is catalyzed by a monomeric enzyme, photolyase, which uses visible-light energy (300 - 500 nm) to reverse the UV damage (Yamamoto *et al.* 2009). All photolyases are single monomeric proteins with M_r ranging from 53-66 KDa (Sancar 1990). CPDs and 6-4PPs are repaired by CPD and 6-4 PP

photolyases, respectively, and so far no single photolyase has been shown to repair both lesions (Sancar 2003). "CPD photolyases have been found in bacteria, fungi, plants, invertebrates and many vertebrates, while 6-4 photolyases were identified in *Drosophila*, silkworm, *Xenopus laevis* and rattlesnakes, but not in *E. coli* or yeast" (Sinha and Hader 2002).

Photolyases

Photolyases are found in organisms from all three domainss of life and efficiently repair CPD lesions (Friedberg 1995). Interestingly, during evolution the photolyase gene has been lost in placental mammals including humans about 170 million years ago, after the split of marsupials and placental mammals Fig. 1.4 (Kumar and Hedges 1998; Menck 2002).

Several studies proposed another function for the photolyase enzyme because they found the enzyme binds to the DNA dimer even in the dark. In these studies they demonstrated another function for the photolyase, which is stimulation of the NER mechanism in removing UV and non UV lesions (Yamamoto *et al.* 1983; Sancar and Smith 1989; Ozer *et al.* 1995). In addition, its distribution in different tissues and in different species such as those that live in deep sea and are away from sun light, led to the same speculation that these enzymes might carry out another function (Wang 1976; Ozer *et al.* 1995). Another study proposed another function for photolyases from the plant species *Arabidopsis thaliana* and *Sinapis alba*, which is to function as a blue-light photoreceptor (Malhotra *et al.* 1995).

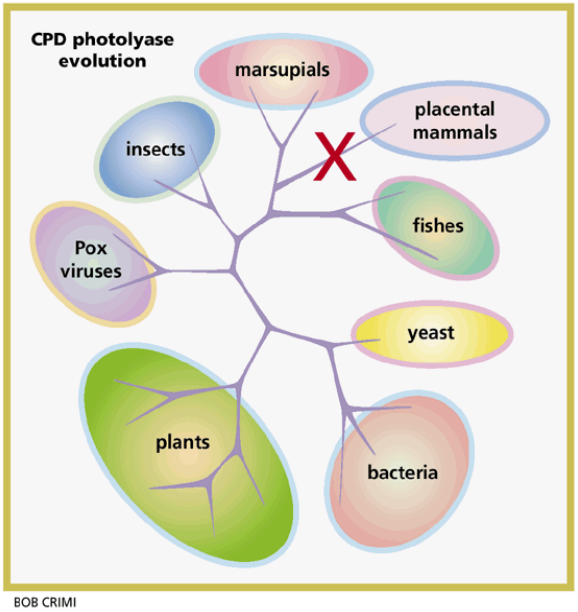

Figure 1.4 phylogenetic tree for CPD photolyase

Photolyase seems to be an ancestor enzyme found in a variety of organisms. The red cross indicates the possibility that CPD photolyase gene has been lost in placental mammals adapted from (Menck 2002).

Early history of discovery of photolyases

Kelner in 1949 found the first clear evidence for photoreactivation in which the effect of exposure to UV light at 254 nm can be reversed by illumination with visible light in *Streptomyces griseus* (Kelner 1949a). Subsequently he found the same finding in other organisms like *E. coli*, *Penicillium notatum* and *Saccharomyces cerevisiae* when they were exposed to photoreactivation light (Kelner 1949b). Also a confirmation of this finding was reported by Dulbecco in 1949 for bacteriophage (Dulbecco 1949).

These findings opened the field for further studies that demonstrated the role of photoreactivating light on reversing the effect of lethal UV-induced DNA damage (Novick and Szilard 1949; Dulbecco 1950; Rupert *et al.* 1958; Rupert 1962a; Rupert 1962b). One of these studies involves the early discovery of photoreactivation chromophores (Dulbecco 1950). This lead to detailed studies on the effect of UV light in inducing thymine dimers (later called CPDs) and the removal of this damage by photoreactivation (Wulff and Rupert 1962; Setlow and Setlow 1962; Setlow *et al.* 1965b; Setlow *et al.* 1965a).

Initially called photoreactivating enzyme (Rupert 1960, 1962a), the enzyme was later renamed as photolyase (Minato and Werbin 1972). Several attempts on the purification of this enzyme were done and the first trial was reported by (Minato and Werbin 1971), where they purified the photolyase from baker's yeast (*S. cerevisiae*). Thereafter, the chromophore of this enzyme was recognized as flavine adenine dinucleotide (FAD) and the photolyase gene from this organism was also cloned (Iwatsuki *et al.* 1980; Schild *et al.* 1984). *E. coli* photolyase was also found to have a single FAD cofactor like yeast photolyase (Sancar and Sancar 1984) and it repairs both relaxed and supercoiled DNA strands (Sancar *et al.* 1985) as well as UV-lesions on RNA strands (Kim and Sancar 1993).

Photolyases were also identified in marsupials such as *Potorous tridactylus* (Harm 1978) and *Monodelphis domestica* (Ley 1984).

In 1987 Sancar *et al* were able to purify recombinant yeast photolyase (*S. cerevisiae*) with more than 95 % purity from *E. coli* cells (Sancar *et al.* 1987). The *PHR1* gene of *S. cerevisiae* was cloned into a plasmid using recombinant techniques and the purified product revealed the presence of oxidized FAD as a chromophore with absorbance peak at 450 nm.

Chromophores and crystal structure of photolyases

Photolyases are flavoproteins and generally they are known to have two chromophores, one is a catalytic cofactor and the other is a light harvesting cofactor (Komori *et al.* 2001; Todo 1999; Sancar 2003). The light harvesting cofactor binds to the N-terminal domain whereas the C-terminal domain of the enzyme binds to the catalytic cofactor (FAD) and to the DNA (Malhotra *et al.* 1992). However, some photolyases have only one chromphore which is FAD, and this includes *T. thermophilus* (Kato *et al.* 1997) and *P. triductylus* (Yasui *et al.* 1994). The catalytic cofactor interacts directly with its substrate (UV lesion) during the photoreactivation process, whereas the light harvesting cofactor acts as an antenna in harvesting a light photon and transfering it to the catalytic cofactor (Komori *et al.* 2001). In all known photolyases the catalytic cofactor is always (FAD), whereas several light harvesting cofactors are found in different organisms, such as 5,10-methenyltetrahydrofolate (MTHF) in *E.coli* (Sancar 1994), 8-hydroxy-5-deazariboflavin (8-HDF) in *Anacystis nidulans* (Sancar 1994), FMN in *Thermus thermophilus* (Ueda et al. 2005*),* and a second molecule of FAD in *Sulfolobus tokodaii* (Fujihashi *et al.* 2007).

In 2000, Sancar outlined the presence of two chromophores in all studied photolyases, the variable one is an antenna chromophore, such as 5, 10-methenyl tetrahydrofolate (MTHF) in *E. coli* and 8-hydroxy-5-deazariboflavin (8-HDF) in *Anacystis nidulans*, while the second chromophore is always FAD (Sancar 2000). Unusually however, in thermophilic bacteria, FMN and FAD were found to be the two antenna cofactors (Ueda *et al.* 2005; Fujihashi *et al.* 2007).

Studies on photolyase crystal structure are significant in better understanding of the "structure -function relations" (Park *et al.* 1995).

In 1995, the crystal structure of *E. coli* CPD photolyase was determined by Park *et al* (Park *et al.* 1995). This work together with the work of (Sancar in 1994 and 1996 b) plus the work of (Vande Berg and Sancar 1998) demonstrated that photolyase flips the dimers out of the DNA double helix strand to fit into the active site of the enzyme.

Following the structural characterisation of *E. coli* CPD photolyase by Park *et al*, the crystal structures of CPD photolyase from *A. nidulans* (Tamada *et al*. 1997) and *Thermus thermophilus* (Komori *et al*. 2001) were reported. Both of which showed a similarity with the structure of *E. coli* photolyase in which the overall structure of the photolyases composed

of two domains: α/β domain with five parallel β strand sheets in the N-terminal region that contains the binding site for light harvesting chromophore and a helical domain at the C-terminal region contains the binding site for the catalytic cofactor FAD plus a long loop that connects both domains Fig 1.5 A, B, C (Tamada *et al.* 1997; Komori *et al.* 2001). The difference in the structures of theses three photolyases is in the type and binding site of the light harvesting cofactor. In *E. coli* the light harvesting cofactor is MTHF whereas in *A. nidulans* and *T. thermophilus* it is HDF and FMN respectively (Park *et al*. 1995; Tamada *et al*. 1997; Ueda *et al*. 2005). The crystal structure of *T. thermophilus* photolyase showed a less flexible structure as compared with the other photolyases and might explain its feature as a thermostable enzyme (Komori *et al.* 2001).

In 2007, the first crystal structure for an archaeal photolyase was determined, from *Sulfolobus tokodaii* Fig 1.5 D (Fujihashi *et al.* 2007). It also revealed a similarity with the structure of the three previously discovered photolyases plus the presence of a second FAD molecule in *S. tokodaii*, suggesting a novel light harvesting cofactor as a second chromophore (Fujihashi *et al.* 2007). The similarity in protein sequence between *S. tokodaii* photolyase and photolyases from *E. coli*, *A. nidulans* and *T. thermophilus* is 32%, 35% and 28%, respectively (Fujihashi *et al.* 2007). The purified protein from *S. tokodaii* showed a greenish-yellow solution and its overall structure showed two domains α-helical and α/β, which is similar to the three known photolyases (Fujihashi *et al.* 2007). Two cofactors were found at the same sites of those other photolyases, for the catalytic and light harvesting cofactors. It was observed also from this structure a disulphide bond between Cys3 and Cys26, and actually this pair of cysteine residues in the sequence was found only in homologous sequences from *sulfolobus* species (Fujihashi *et al.* 2007).

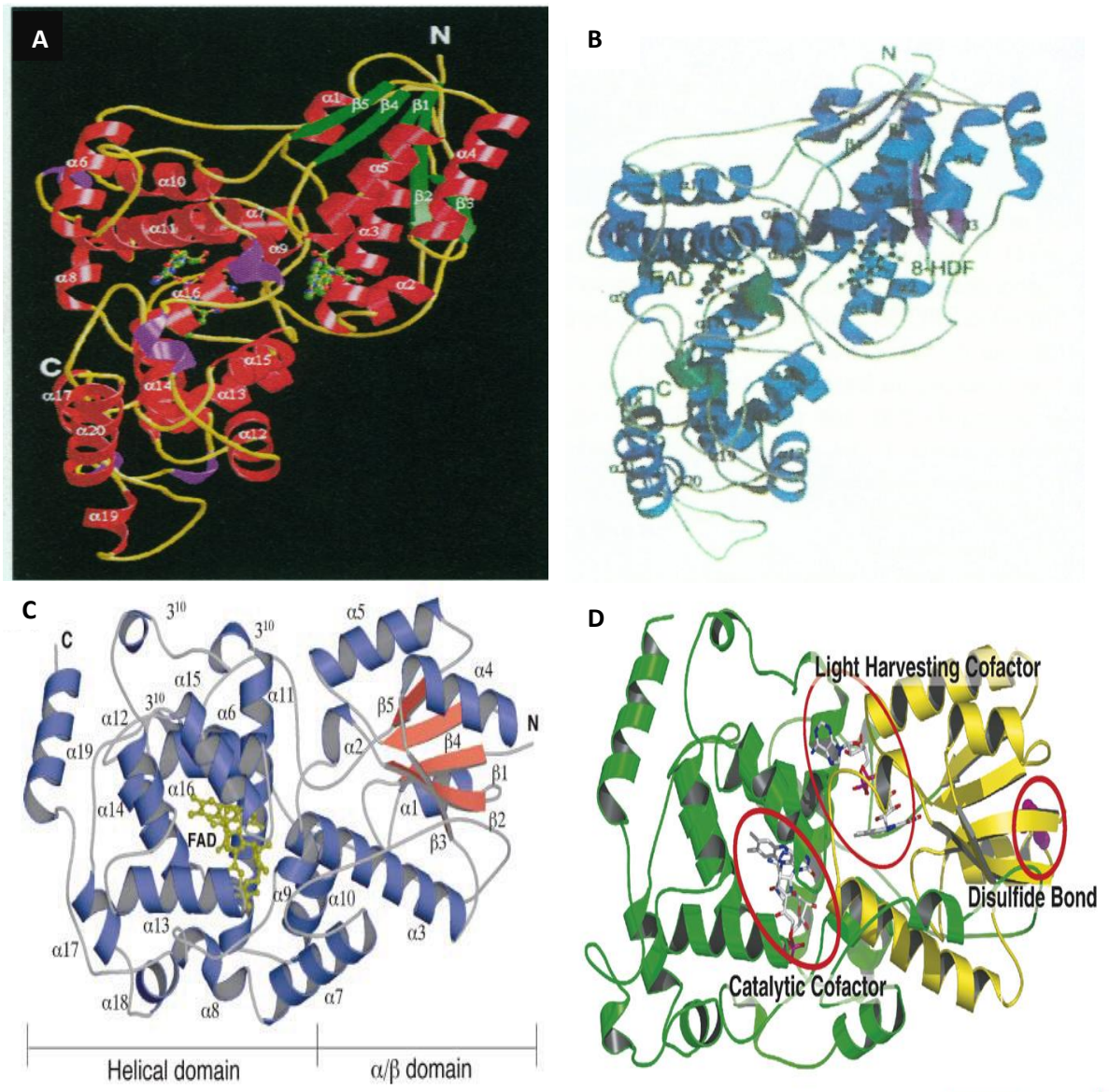

Figure 1.5 Overall view of photolyases crystal structure from different organisms

A) *E. coli* photolyase schematic drawing structure. β strand sheets in green and α helices in red (adapted from Park *et al.* 1995).
B) *A. nidulans* photolyase. β strands in magenta and α helices in blue (adapted from Tamada *et al*. 1997).
C) *T. thermophilus* photolyase. β strand sheets in red, α helices in blue and FAD in yellow (adapted from Komori *et al*. 2001).
D) Green and yellow shows the two domains α-helical and α/β domains, respectively. Two FAD molecules as a catalytic and light harvesting cofactors plus a disulfide bond are shown in the structure (adapted from Fujihashi *et al.* 2007).

The amino acid sequence alignment of these photolyases with *S. solfataricus* photolyase showed some similarity specifically at the C-terminal region of the proteins. This sequence alignment and the GI number for each gene can be found in appendix 9.

All above crystal structures of photolyases from the four species were determined as class I photolyase. However, a recent study resolved the first crystal structure of "class II photolyase from methanogenic archaeon *Methanosarcina mazei* Go1" (Kiontke *et al*. 2011). The overall structure of this methanogenic archaeon (*M. mazei*) photolyase is also similar to the other identified photolyases Fig 1.6. It is composed of α/β domain in the N-terminal and helical domain in the C-terminal of the photolyase structure (Kiontke *et al.* 2011). The C-terminal contain FAD chromophore but the N-terminal lack a light harvesting chromophore (Kiontke *et al.* 2011). There are some distinct features in the structure of this type of photolyase which differs from the other class I photolyases, like the presence of a significant longer linker region that connects both domains as compared with the linker region in class I phtotolyases (Kiontke *et al.* 2011) . Also the C-terminal domain is truncated by approximately 50 residues (Kiontke *et al.* 2011).

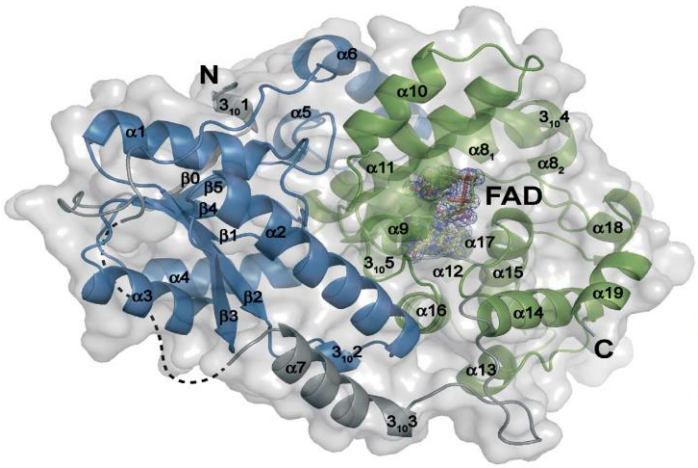

Figure 1.6 crystal structure of class II photolyase

Overall crystal structure of *M. mazei* photolyase. C-terminal domain (green) shows the FAD cofactor binding and N-terminal (blue) without cofactor. Linker region shown in grey color and a dashed grey line represent the undefined part by electron density of the linker region. (adapted from Kiontke *et al*. 2011).

Photoreactivation Mechanism

The overall mechanism of photolyase-catalysed DNA repair is as follows Fig.1.7 a, b. The mechanism starts in a light-independent manner, the enzyme binds to its substrate and either remains bound until induced by photoreactivation light to carry out the repair mechanism, or stimulates the NER mechanism in the dark to repair UV lesions (Thompson and Sancar 2002).

The light-dependent activity of photolyase, called photoreactivation, is well characterized for CPD photolyase by Sancar in 1994 (Sancar 1994). After light-independent binding between the enzyme and its substrate by interactions with the damaged DNA strand, the dimer is 'flipped out' into the cavity of the protein and forms a high affinity ES complex (Thompson and Sancar 2002)

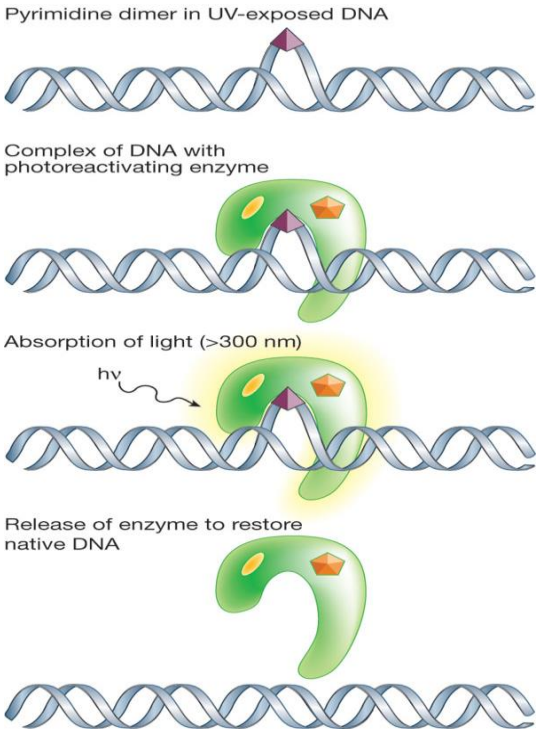

Figure 1.7a Overview of photo-reactivation. The blue strand represents the DNA double helix with the thymine dimer, which is shown as a purple triangle. The photolyase (green shape) with its two chromophores (yellow and orange shape) recognizes and binds to the dimer (Friedberg 2003).

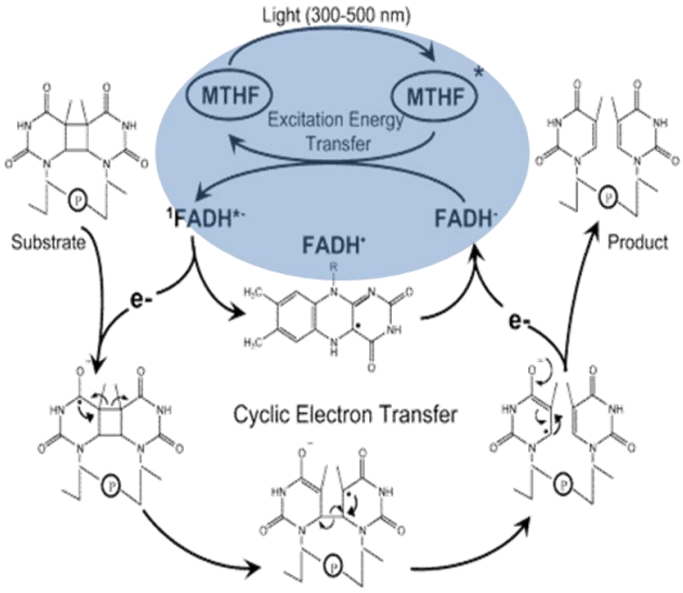

Figure 1.7b Mechanism of action of CPD photolyase. This is initiated by absorption of visible light by the light harvesting chromophore. Following energy transfer to the catalytic cofactor, the damage is repaired and the enzyme is released returning the DNA to its normal confirmation. (electron transfer mechanism in *E.coli* CPD photolyase (Sancar 2008). This mechanism is described in detail in the text.

The second photoantenna chromophore, which is either folate or dezaflavine, absorbs light energy in the form of a photon in the wavelength range of 300-500 nm and becomes excited. This excited energy is then transferred to the reduced flavin adenine dinucleotide ($FADH^-$) cofactor. The excitation of $FADH^-$ is followed by an electron transfer to the CPD lesion. The dimer is split by rearrangement of the bonds of the cyclobutane ring, leading to the conversion of the dimer to its original monomeric form. Finally the electron is back-transferred to the flavin radical resulting in restoration of the pyrimidine and the functional

form of the $FADH^-$ (Song et al. 2007; Thompson and Sancar 2002). The repair mechanism of 6-4 photolyase is believed to be similar to CPD photolyase but only one difference was observed. Once the 6-4 photolyase binds to the dimer, it converts the 6-4pp to an oxetane intermediate, which is similar to cyclobutane ring, and then the electron absorption mediates the ring breakage, restoring the DNA shape (Kim *et al.* 1994; Zhao *et al.* 1997).

Studies on CPD photolyases led to the discovery of plant and animal cryptochromes plus the discovery of 6-4 photolyases, which are less widely distributed than CPD enzymes but are much similar to animal cryptochromes.

6-4 photolyase, which repairs only 6-4pp lesions, was first discovered by (Todo *et al.* 1993) in *Drosophila melanogaster* cell-free extract. (Kim *et al.* 1994) revealed that 6-4 photolyase monomerizes 6-4pp and proposed the formation of an oxetane intermediate for the repair of this lesion by 6-4 photolyase, and so far 6-4 photolyases were found in only some higher eukaryotes (Hitomi *et al.* 2001).

Photolyases and cryptochromes

Photolyases and cryptochromes are flavoprotins, sharing a high similarity in the gene sequence but carrying out distinct functions (Cashmore 2003; Yuan *et al.* 2007). Cryptochromes together with photolyases, make up the superfamily of photolyase/cryptochrome (Partch and Sancar 2005).

Early discovery of cryptochromes was in 1993, when proteins from *Arabidopsis thaliana* (cryptochromes) were found to have a sequence homology with microbial CPD photolyase but with no repair activity (Ahmad and Cashmore 1993). The function of these proteins as blue-light photoreceptors was also reported in the same study (Ahmad and Cashmore 1993). Furthermore in 1996, a report showed that 6-4 and CPD photolyases plus cryptochromes are evolutionarily related (Todo *et al.* 1996). In 1996 cryptochromes were identified in humans (Hsu *et al.* 1996), and it was shown later in 1998 that they are involved in regulating the circadian clock (Thresher *et al.* 1998).

Cryptochromes are blue-light photoreceptors that are responsible for regulating growth and development in plants, plus regulating the circadian clock in animals (Cashmore 2003; Yuan *et al.* 2007). Animal cryptochromes are closely related to the 6-4 photolyases in the protein

sequence, and were first discovered in 1995 as a putative photolyase homologues when the human genome was examined (Cashmore 2003; Adams *et al.* 1995). In all characterized cryptochromes, the presence of both folate and flavin cofactors was reported (Sancar 2003). Cryptochromes and photolyases are not universally distributed; i.e *Drosophila melanogaster* contains both CPD and 6-4 photolyases plus a cryptochrome whereas *Haemophilus influenza* contains neither a photolyase nor a cryptochrome (Worthington *et al.* 2003; Sancar 1994; Thompson and Sancar 2002). Placental mammals have only cryptochromes but not photolyases and therefore UV photoproducts are removed by the sole mechanism which is NER (Sancar 1996a; Wood 1997; Thompson and Sancar 2002). Humans have two cryptochromes known as *hCry1* and *hCry2* which are the representatives of photolyase/cryptochrome family in humans (Hsu *et al.* 1996; Thompson and Sancar 2002).

Photolyases Classification

Photolyases are classified into class I and II depending on the similarity between their amino acid sequence (Yasui *et al.* 1994; Kanai *et al.* 1997; Hitomi *et al.* 2000). Class I photolyases are found in many microbial organisms, whereas most of class II photolyases are found in higher organisms such as *Carassius auratus* (goldfish) (Yasuhira and Yasui 1992), *Drosophila melanogaster* (fruit fly) (Yasui *et al.* 1994), *Cucumis sativus* (cucumber) (Takahashi *et al.* 2002), *Potorous tridactylis* (rat kangaroo) (Yasui *et al.* 1994). Class I photolyases are further sub-classified into folate-or deazaflavin-type, according to the presence of the second light harvesting cofactor; a dezaflavine type has 8-hydroxy-5-dezaflavin (8-HDF) as the light harvesting cofactor whereas a folate type has 5,10-methenyltetrahydrofolate (MTHF) as the second cofactor (Weber 2005). Photolyases of the folate class include *E. coli* (Johnson *et al.* 1988), *Salmonella typhimurium* (Li and Sancar 1991), the yeast *Saccharomyces cerevisiae* (Johnson *et al.* 1988) and *Vibrio cholera* (Worthington *et al.* 2003) whereas the dezaflavin class of photolyases includes *Anacystis nidulans* (Yasui *et al.* 1988), *Streptomyces griseus* (Eker *et al.* 1981), and *Halobacterium halobium* (Iwasa *et al.* 1988).

Photolyase application as a light therapy

Application of photolyases as an active protein delivered into human skin by liposomes could be a potential therapeutic method to repair UV damage and can be an alternative to gene therapy (Kraemer and DiGiovanna 2002; Weber 2005). Theoretically, proteins can be applied directly to the damaged skin cells and their amount can be controlled, plus in case of any adverse effects the treatment can be stopped at any time (Kraemer and DiGiovanna 2002). Stege *et al.* demonstrated the effectiveness of topical application of photolyase from *Anacystis nidulans* delivered by liposomes in UVB irradiated human skin after exposure to photoreactivation light (Stege *et al.* 2000). In this study the UV-induced dimers were decreased by 40-45%. Another recent study in 2012 also demonstrated the effective addition of photolyases from *Anacystis nidulans* into a traditional sunscreen, in which they observed a significant reduction in CPDs and apoptotic cell death in biopsy of ten volunteers (Berardesca *et al.* 2012).

These studies "suggests that the use of protein therapy may have untapped potential for treatment of skin diseases ……and the topical enzyme therapy of skin diseases may soon be a reality" (Kraemer and DiGiovanna 2002).

As stated by Aziz Sancar, there is "No End of History for photolyases" (Sancar 1996b).

1.3 DNA repair mechanisms for different types of DNA damage

1.3.1 Base excision repair (BER)

Is one of the DNA repair mechanisms that operates as a response to a DNA damage in a single base (Friedberg 2001). This change in the base can arises from either endogenous damage such as base hydrolysis and reactive oxygen species or from exogenous damage such as ionizing radiation and alkylating agents (Seeberg and Bjoras 1995). It is initiated by a class of enzymes known as DNA glycosylases, which recognize the altered base and cleaves it at the N-glycosidic bond (Sinha and Hader 2002). Each type of glycosylase removes a specific type of damage (Seeberg and Bjoras 1995). For example, uracil DNA-glycosylase recognizes only uracil as an altered base in the DNA strand Fig 1.8 a (Friedberg 2001). Once the inappropriate base is removed, it generates a purinic/ apyrimidinic (AP) site, which is removed by an AP endonuclease or an AP lyase (Sinha and Hader 2002). This enzyme induce

a nick in the DNA backbone and the deoxyribose phosphate residue is then removed by deoxyribo phosphodiesterases (dRPase) (Sinha and Hader 2002). The resulting gap is then refilled by DNA polymerase and both ends are sealed by DNA ligase (Seeberg and Bjoras 1995, Sakumi 1990).

AP site is " probably the most frequent type of endogenous DNA damage at a frequency of 10000 per human cell per day" (Sinha and Hader 2002). BER proteins exist in organisms ranging from bacteria to humans (Posnick and Samson 2001).

In hyperthermophilic archaea the frequency of mutation in a single base due to hydrolysis, oxidation or methylation is higher as a result of living in high temperature environments (Garrette and Klenk 2007). In archaea specific DNA glycosylaes were found, this include uracil DNA glycosylase (UDG) which was found in different archaeal species including *S. solfataricus* (Blum 2004). Also 8-oxo guanine DNA glycosylase, which removes the oxidized guanine was found in *M. Jannaschii* (Blum 2004).

1.3.2 Mismatch repair (MMR)

Is an excision repair mechanism operated on incorrect or mismatched base that was " added opposite a normal base during replication" (Posnick and Samson 2001). This incorrect base is added by DNA polymerase during DNA replication "because of limitied fidelity of the DNA replicative machinery" (Friedberg 2001). For example, thymine may be added opposite a guanine in the newely synthesized strand of DNA (Posnick and Samson 2001; Friedberg 2001). All cells have the machinery to distinguish between the newely synthesized DNA strand and the parental strand (Friedberg 2001). The first step in *E. coli* is the recognition and binding of a mismatch base in the newely synthesized DNA strand by a complex called MUTSα which is composed of MSH2 and MSH6 Fig 1.8 b (Posnick and Samson 2001; Fiedberg 2001). This complex binds together with the help of another complex (MUTLα), which is also composed of two proteins (MLH1 and PMS2) (Posnick and Samson 2001; Fiedberg 2001). A third protein called MUTSβ composed of MSH2 and MSH3 is also work on damage recognition plus MUTH binds to the above proteins and becomes activated (Posnick and Samson 2001; Fiedberg 2001). MUTH can make an incision in the newely replicated DNA strand that contains the mismatched base (Posnick and Samson 2001). Then other enzymes will work to remove this DNA segment and the gap is repaired by DNA

polymerase and DNA ligase (Posnick and Samson 2001). The MMR "in mammalian cells is not well understood" but it is believed that it involves other protein complexes called MLH1, DMS2 and MLH3 (Friedberg 2001). Defects in genes coding proteins involved in the MMR in humans might predispose to cancer such as colon cancer as well as " uterine, ovarian and gastric cancer" (Friedberg 2001).

In comparison to the MMR in *E. coli* and humans, hyperthermophilic archaea lack certain DNA repair proteins involved in mismatch repair, as no protein homologous of MMR such as MUTS and MUTL was found (Sachadyn 2010).

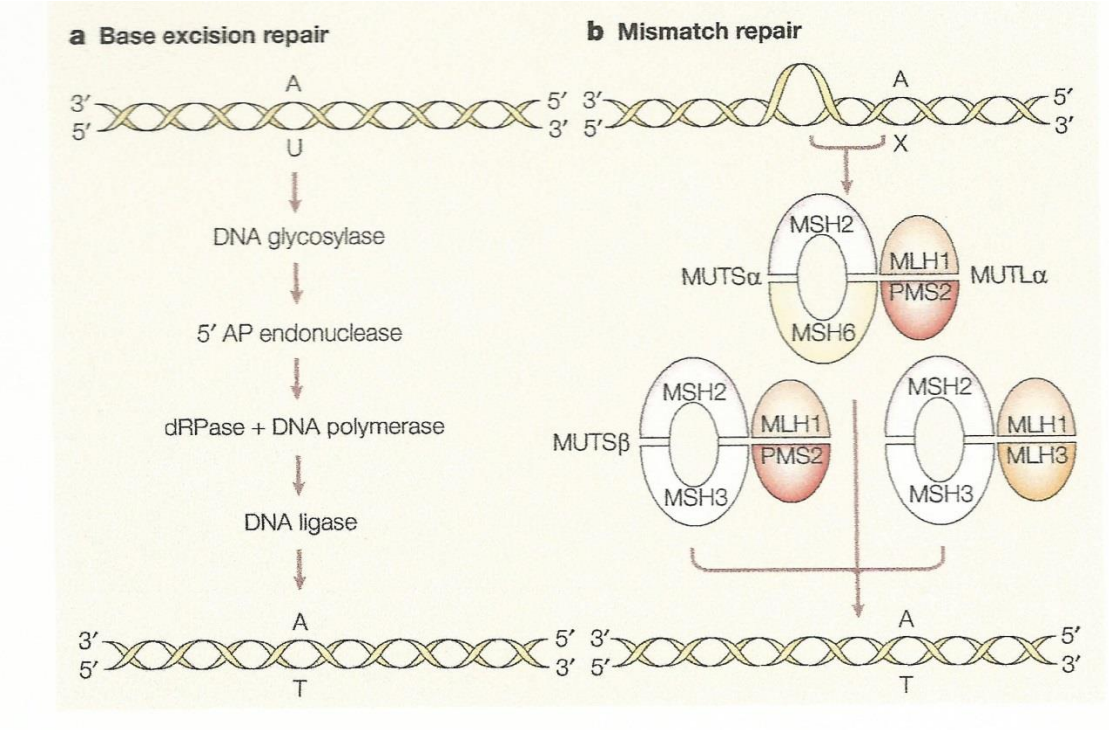

Fig 1.8 Base excision repair and mismatch repair mechanisms

a) BER. A single base damage recognized by DNA glycosylases and excise it, leaving a site in the DNA without a base. AP endonuclease is then cleaves this site and dRPase removes the deoxyribose sugar. The gap is then refilled with DNA polymerase and both ends are ligated by DNA ligase.

b) MMR. Incorrect base pair arises during DNA replication can be repaird with the help of many protins that involves MUTSα, MUTSβ and MUTLα. Each of which is composed of two proteins as illustrated. The equivalent of these proteins in mammalian cells is believed to be MLH1, MLH3 and PMS2.
The details of this mechanism can be found in the text (adapted from Friedberg 2001).

1.3.3 Methyltransferases

These are DNA repair enzymes involved in removing and transferring mutagenic methyl group from oxygens on guanine residue (o^6-methylguanine) and on thymine residue (o^4-methylthymine) (Posnick and Samson 2001). Transferases enzymes are working by " direct reversal of Damage" and are found in " bacteria, yeast and humans" (Posnick and Samson 2001). After transferring the methyle group to a cysteine receptor site, it remains attached to the active site of the enzyme and the protein becomes inactivated (Peeg 2000: Posnick and Samson 2001). Therefore, each enzyme molecule can repair only one lesion (Posnick and Samson 2001). It acts by flipping out the damaged base from DNA douple helix into a pocket in the enzyme (Pegg 2000).

This mechanism is important to protect cells from mutation induced by alkylating agents. It was found that there is a relation between p53 tumour suppressor gene and alkyltransferases (AGT, OGT and MGMT) expression, in which p53 mediates a response to ionizing radiation by stimulating expression of alkyltransferases (Peeg 2000). Studies on transgenic mice proved that changing the levels of alkyltransferases in cells are important in protecting against carcinogenesis (Peeg 2000). Alkyltransferases are conserved among eukarya, prokarya and archaea and these enzymes were found in *S. solfataricus* and are important for thermophilich organisms (Perugino *et al.* 2012). This is because thermophilic organisms are exposed to methylating agents in nature as " by-products of biomass decay" and to "endogenous methylating agents such as S-adenosylmethionine or N-nitroso compounds" which are highly reactive at high temperature environments (Perugino *et al*. 2012).

1.3.4 Homologous recombination (HR)

Two major DNA repair pathways for double strand breaks (DSBs) include: homologous recombination (HR) and non-homologous end joining (NHEJ).

HR is one of the most important DNA repair mechanisms in repairing DSBs and interstrand crosslinks (ISCs) (Sinha and Hader 2002; Li and Heyer 2008). It mediates its action "only during S phase and only if there is sufficient homology" (Lieber 2010). HR involves series of biochemical pathways that result in repairing the damaged strands (Sinha and Hader 2002;

Li and Heyer 2008). Ionizing radiation and oxidative free radicals causes DNA damage such as DSBs and single-strand breaks (Word 1988, lieber 2010). DSBs are major threat to DNA and can cause genome instability and if this damage is left unrepaired it can lead to "chromosome loss, chromosome rearrangements, apoptosis, or carcinogenesis" (Li and Heyer 2008). HR also occurs normally during meiosis and involves at least 20 proteins in *E. coli* (Sinha and Hader 2002). It is believed that the recombination mechanism is a common pathway in a wide variety of organisms (Shinohara 1995). HR is an important "support for DNA replication in the recovery of stalled or brocken replication fork" (Li and Heyer 2008).

The most critical proteins involved in this mechanism are RecA and its homologue in eukaryotes Rad51 (Li and Heyer 2008). The repair mechanism summarized in Fig 1.9 starts when a DSBs or single-strand breaks arises during for example meiosis, the HR mechanism "fills the daughter strand gap by transferring a pre-existing complementary strand from a homologous region of DNA to the site opposite the damage" (Sinha and Hader 2002). The lesion is still unrepaired and the cell enters "another round of replication " which makes the lesion available to be processed by excision repair (Sinha and Hader 2002). RecA proteins search for a homology sequence on the sister chromatide and then DNA strand exchange, is mediated (Li and Heyer 2008). Mutations in recombination genes predispose humans to breast and ovarian cancer (Li and Heyer 2008).

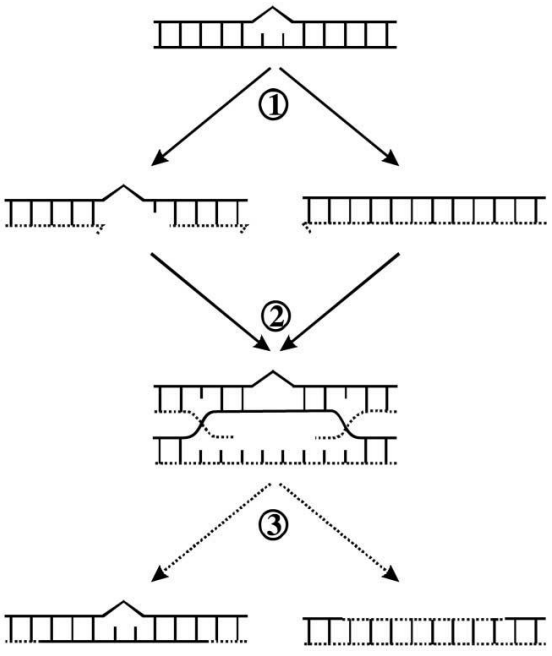

Fig 1.9 schematic diagram for homologous recombination

Homologous region from the other chromosome is used to repair the damaged DNA strand.

More details are in the text (adapted from Sinha and Hadre 2002).

1.3.5 Non-homologous end-joining (NHEJ)

Is the other repair mechanisms for repairing DSBs "at any time during the cell cycle and does not require any homology" (Lieber 2010). The enzymes and proteins involved in NHEJ mechanism in eukaryotes involves "Ku, DNA-PKcs, Artemis, polymerase mu, polymerase lambda, XLF, $XRCC_4$, and DNA ligase IV" (Lieber 2010). This mechanism is present in many prokaryotes and in all eukaryotes (Lieber 2010). Generally, the mechanism starts when DSBs arises and Ku protein binds first to the DSB end and form a Ku:DNA complex Fig 1.10 (Lieber 2010). This binding will improve the binding of nuclease, polymerase and ligase, which will provide mechanistic flexibility for the NHEJ mechanism (Lieber 2010). This flexibility is important to "handle every diverse array of DSB end configuration and to join them" (Lieber 2010). NHEJ is conserved among all domains of life and is "highly efficient in mammalian cells" (Barbat *et al*. 2004).

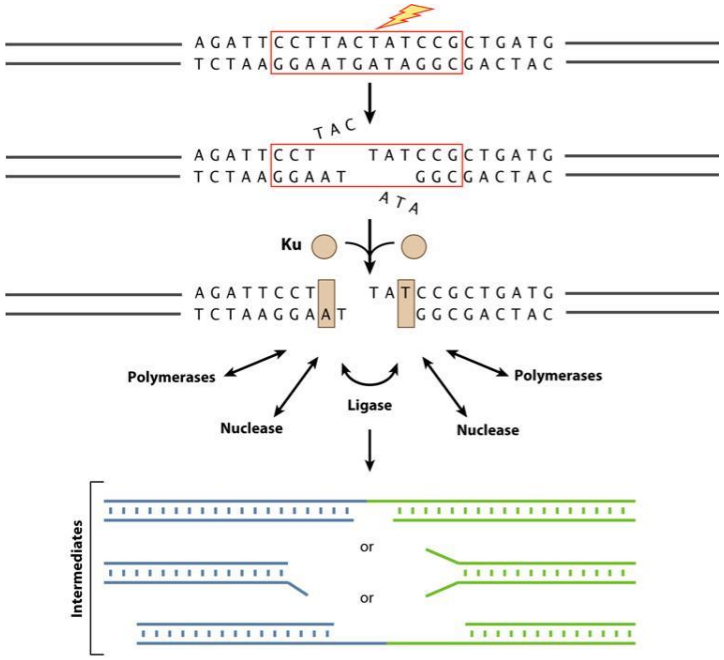

Fig 1.10 schematic diagram for general steps in NHEJ mechanism

The first protein that binds to the DSB in NHEJ mechanism is Ku. This binding will stimulate the binding of other enzymes such as nuclease, polymerase and ligase, which provides a mechanistic flexibility at the ends of DSB. This flexibility will allow the end joining (adapted from Lieber 2010).

1.4 Archaea as a third domain of life

A class of microorganisms was in existence on earth and was not recognised until about 35 years ago. This class of microorganisms was first identified by Carl Woese in 1977, based on the sequence of small-subunit (SSU) ribosomal-RNA and was named as Archaebacteria (Woese and Fox 1977). In a subsequent report, the name was shortened to Archaea and was assigned as a third domain of life in addition to Bacteria and Eukarya (Woese *et al.* 1990). For decades, this class of Archaea was misclassified as bacteria because of the similarity in morphology (Allers and Mevarech 2005). However, the phylogeny of rRNA, which was chosen by Carl Woese, revealed that Archaea share homology between Bacteria and Eukarya.

Thereafter, studies of molecular mechanisms confirmed a similarity between Archaea and eukaryotic systems in DNA replication, transcription and translation (Olsen and Woese 1996; Londei 2005). Archaea are also similar to bacteria in many aspects like the size of the cell, lack of nucleus and chromosome organisation (Gribaldo and Brochier-Armanet 2006). However, archaea have unique cell membrane lipids that are isoprenoid ethers linked to glycerol-1-phosphate (G1P), whereas the membranes of bacteria and eukarya are fatty acid esters linked to glycerol-3-phosphate (G3P) (Kates 1993).

As can be seen from Fig 1.11, the phylogenetic tree of SSU rRNA showed two major archaeal phyla, the Euryarchaeota and the Crenarchaeota as assigned in *Bergey's manual of systematic bacteriology* (Boone and Castenholz 2001). Euryarchaeota are more diverse than Creanarchaeota and include different organisms from halophiles, methanogens, thermoacidophiles and hyperthemophiles, while Creanarchaeota include only hyperthermophiles, such as *Sulfolobus solfataricus*. The first archaeal genome sequence was published for *Methanocaldococcus jannaschii* in 1996, and thereafter the full genome sequences of other archaeal species from different phyla were published (Bult *et al.* 1996). The discovery of new species from measophilic archaea is increasing and these species were affiliated with the creanarchaeota (Muller *et al*. 2010). The measophilic Creanarchaeota showed difference when compared with the hyperthermophilic Creanarchaeota because the former showed a deeper branch in the 16S rRNA phylogenetic tree (Brochier-Armanet 2008). Therefore, mesophilic Creanarchaeota was considered as a new third phylum in the archaea and were named as Thaumarchaeota Fig 1.11 (Brochier-Armanet 2008).

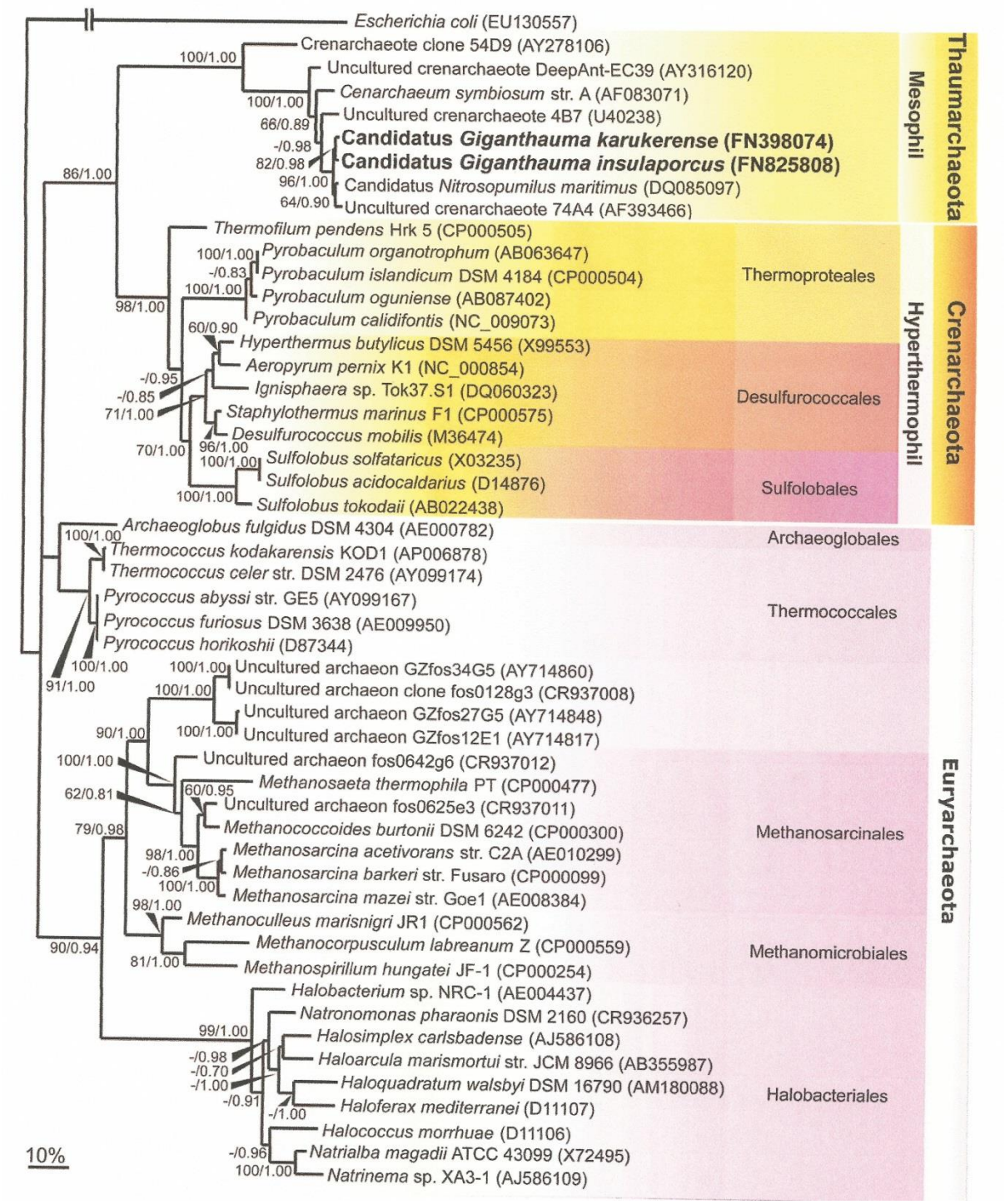

Figure 1.11 phylogenetic tree of the three archaeal phyla

Based on the 16S rRNA sequences, this tree illustrate the archaeal domain with three phyla, Euryarchaeota, Crenarchaeota and Thaumarchaeota. New archaeal species were added to the Thaumarchaeota phylum (in bold) (Adapted from Muller *et al*. 2010).

In addition, new other archaeal species were also classified as Thaumarchaeota because of the deep branching in 16S rRNA gene sequence which include *Candidattus Giganthauma Karukerense* and Candidatus Giganthauma Insulaporcus Fig 1.11 (Muller *et al.* 2010).

Interestingly, another recent archaeal phylum has been discovered in 2013 from a high temperature and highly acidic Yellowstone environment and given a name Geoarchaeota (Kozubal *et al.* 2013). Gene analysis of this new candidate phylum found genes involved in oxygen metabolism, such as heme copper oxidase and unique bacterial-like cofactors and transport genes (Kozubal *et al.* 2013).

Although the majority of studies on UV damage and DNA repair were conducted on bacteria and eukarya, the interest now has been expanded to the archaeal domain (Fröls *et al.* 2009). This is because of the similarity between archaeal and eukaryal systems which involves DNA replication, recombination and transcription (Allers and Mevarech 2005; Kelman and White 2005). Moreover, the homology between them is also found in DNA repair systems (Aravind *et al.* 1999; Kelman and White 2005).

Archaea are very diverse and widespread organisms, which exist not only in extreme environments but also in terrestrial and aquatic environments (Gribaldo and Brochier-Armanet 2006). Many archaea thrive under extreme conditions (including extremes of temperature, salinity, low and high pH, pressure) that would kill other organisms, and aretherefore called extremophiles (Madigan and Marrs 1997). Amazingly, these organisms do not only tolerate these harsh environments but also require them for their growth (Madigan and Marrs 1997). Extremophiles are generally divided into six groups: thermophiles (Temp 60-80 ºC) or hyperthermophiles (Temp 80-105 ºC), acidophiles (pH < 2-3), alkaliphiles (pH > 9), halophiles (2-5 M NaCl), psychrophiles (Temp < 15 ºC) and piezophiles (high pressure up to 130 MPa), depending on the natural habitats used by the microorganisms (van den Burg 2003). In addition to these groups further other groups have been classified due to the increased discoveries of many other species, such as Endolith (organisms live in microscopic spaces within rocks), Hypolith (organisms live inside rocks in cold deserts), Lithoautotroph (organisms whose only source of carbon is carbon dioxide), Metalotolerant (organisms capable of tolerating high levels of heavy metals dissolved in solution such as copper and zink, Osmophile (organisms capable to grow in high sugar concentration environment) and others. However, some organisms fall under multiple groups, i.e organisms that live in

extreme hot springs and in acid environments, such as *Sulfolobus solfataricus,* are both hyperthermophiles and acidophiles and are sometimes described as thermoacidophiles.

In halophilic archaeon (*Halococcus hamelinensis*), exposure to UVlight and the induction of different repair mechanisms as a response to UV damage was investigated (Leuko *et al*. 2011). It was clear from this study that *Hcc. Hamelinensis* was able to tolerate high levels of UVC doses (up to 500 J/m^2) and different DNA repair genes were identified such as UvrA, UvrB, UvrC and phr2 which was found upregulated to repair UV damage (Leuko *et al*. 2011). Theses archaeal species showed ability to completely repair UV damage within 16h following visible light illumination or within 24h following dark incubation (Leuko *et al*. 2011).

Enzymes from extremophiles, Extremozymes, are proteins considered valuable by many biologists because of their ability to function and to be stable at extreme conditions. Also their importance has expanded and reached to an industrial domain, where some of the methanogenic archaea are used to produce biomethane as a fuel (Allers and Mevarech 2005). In fact, enzymes from hyperthermophiles are the most interesting for researchers and among the best studied of extremophiles (Madigan and Marrs 1997).

1.4.1 Hyperthermophiles

Microbes that are heat lovers are called thermophiles and grow optimally at temperatures above 60 ºC, and some of them, known as hyperthermophiles, prefer to grow at temperatures above 80 ºC. These organisms were first discovered by Thomas D. Brock and his colleagues from a large collection of microorganisms from Yellowstone National Park (Madigan and Marrs 1997). In late 1960s, the same group identified the first thermophilic organism able to grow at temperatures above 70 ºC, which is now known as *Thermus aquaticus,* and an enzyme from this species is now widely used in the PCR technique (Madigan and Marrs 1997). The same group also discovered the first hyperthermophile from an extremely acidic and hot spring, which is *Sulfolobus acidocaldarius* (Brock *et al.* 1972). Despite the presence of thermophiles in both Bacteria and Archaea, the latter domain has the vast majority of hyperthermophiles species (Adams 1993).

The first full genome sequence which was published for hyperthermophilic archaea was from *Archaeoglobus fulgidus* in 1997 (Klenk *et al.* 1997). So far, more than 50 species of hyperthermophiles have been discovered and many of them were isolated by Karl O. Stetter and his team (Madigan and Marrs 1997).

Living at high temperature environments has a significant effect on microorganisms (Brock 1985). Hyperthermophiles which are able to survive at very high temperatures were found to have a very stable macromolecules as compared with those of conventional organisms and just small changes in the nucleotide sequence can result in an increase in the thermostability (Brock 1985). Many living organisms are able to live in those hot environments in nature such as volcanic hot springs and hypothermal vents under see water (Brock 1985). " the upper temperature limit for life is somewhere between 110 ºC and 250 ºC " (Brock 1985). It was found that temperature above 250 ºC will destroy the peptides and phosphodiester bonds (White 1984) as well as the amino acids (Brock 1985). High temperatures can cause DNA denaturation and the separation of the two strands of double helix to single strands, as the hydrogen bonds between the bases in the duplex are hydrolysed (Ussery 2001). Studies on DNA structure at high temperatures demonstrated the discovery of reverse gyrase, which is an enzyme known to provide DNA positive supercoiling at 80 ºC (Kikuchi and Asai 1984; Forterre *et al.* 1985). This suggested that this type of DNA structure is the possible reason for providing DNA thermostability at elevated temperatures (duguet 1993).

1.4.2 Sulfolobus solfataricus

Sulfolobus solfataricus is a hyperthermophile and a member of the Crenarchaeota phylum, which includes mainly organisms that grow at high temperatures and low pH. The genus *Sulfolobus* was first identified as a new bacterial genus by T. D. Brock and his colleages in 1972 and many of the isolations were from Yellowstone National Park (Brock *et al.* 1972). It was described as spherical cells with an unusual cell wall, grows on sulfur or on organic compounds with pH optimum of 2-4 and a temperature optimum 65-95 ºC (Cavicchioli 2007).

There are two well-known strains from this genus, *Sulfolobus acidocaldarius* which was first described by T.D.Brock (Brock *et al.* 1972), and *Sulfolobus solfataricus* P2 which was first isolated by Wolfram Zillig in 1980 from the Solfatara (volcano) in Naples, Italy, where its

name *solfataricus* came from (Zillig *et al.* 1980). It is found naturally in volcanic hot springs and typically appears as an oily glimmering layer on water or mud. *Sulfolobus solfataricus* grows aerobically, which makes it easy to grow in the laboratory and therefore it is considered as a model system for many researchers interested in understanding the ability of these organisms to adapt to live in extreme conditions. Furthermore, *Sulfolobus* obtains its energy by oxidizing sulfur to sulphuric acid and hence lowering the pH of the growthmedium.

Sulfolobus solfataricus is a useful organism for the study of genetic integrity and DNA repair among hyperthermophilic organisms, as in their natural environment they survive at very high temperatures and are capable of keeping their genome stable against the harmful effect of UV light (Dorazi *et al.* 2007; Fröls *et al.* 2007).

Hence, this suggests that *S. solfataricus* might have a very efficient DNA repair mechanism and some studies have been conducted to examine the reactions of *S. solfataricus* to UV damage (Fröls *et al.* 2009).

The investigation of DNA repair mechanisms in *S. solfataricus* demonstrated the presence of an active NER mechanism, which repairs the UV photoproducts in the dark (Salerno *et al.* 2003). The same study also demonstrated the presence of CPD after the exposure of *S. solfataricus* to UV light. However, it was found that hyperthermophilic archaea lack the mismatch repair pathway (Grogan 2004).

S. solfataricus exposed to UV damage, showed growth inhibition, cell death and double strand breaks between 2-8h after UV treatment (Fröls *et al.* 2007). It was assumed from this study that the formation of CPD lesions was the reason for the formation of DNA double strand breaks.

In 2007, Dorazi *et al* has shown that *S. solfataricus* can repair the DNA photoproducts with the same efficiency on both transcribed and non-transcribed DNA strands, and also observed very active light repair kinetics in *S. solfataricus* in the presence of visible light, which was consistent with the presence of a photolyase gene in this organism (Dorazi *et al.* 2007). Also in this study, it was proposed that the first mechanism induced after UV radiation is photoreactivation, mediated by photolyase, in repairing CPD lesions (Dorazi *et al.* 2007).

All the above studies suggest the presence of a photolyase gene and an active photoreactivation mechanism in *S. solfataricus*. However, all these studies focused on

examining the response of *S. solfataricus* to UV radiation and looking at the possible DNA mechanisms present in the organism in order to tolerate the effect of UV treatment. These studies proved the presence of active NER and photoreactivation in removing UV lesions, but no attempts were done to identify, express and functionally characterise the photolyase gene from *S. solfataricus*.

In a recent study in another species of *Sulfolobus*, mutations in two genes coding for proteins involved in repairing UV lesions in *S. acidocaldarius* demonstrated that only one gene Saci_1227 encods an active DNA photolyase in repairing UV damage (Sakofsky *et al*. 2011).

1.5 DNA repair in mammalian cells

Reports on the presence of photolyases in mammals are conflicting, and so far homologues of photolyase genes, such as hCRY1 and hCRY2, have been identified in humans (Todo *et al.* 1996; vanderSpek *et al.* 1996; Hsu *et al.* 1996). However, it is generally accepted that placental mammals lack genes encoding an active photolyase for unknown reasons (Chao 1993; Li *et al.* 1993; Ley 1993). UV photoproducts in mammals are removed from the DNA by the more complex and less efficient repair mechanism, NER.

Early studies on mammalian photoreactivation were done on species containing photolyases such as marsupials and this includes *Monodelphis domestica* (Ley 1984) and *Potorous triductylus* (Rat kangaroo) (Harm 1980), because their responses to UV light have beenshown to be similar to placental mammals (Ley *et al.* 1991).

Thereafter, transgenic technology was used to express the photolyases in a variety of mammalian cells that lack this enzyme. This system enabled the researchers to better understand many aspects of this mechanism, which involves the structure of CPD and 6-4pp photolesions plus the interactions between the enzyme and its substrate (Sancar 2000).

Insertion of *E. coli* photolyase into V79 rodent cells after UV treatment, followed by photoreactivating light, monomerizes the pyrimidine dimers (Sutherland and Hausrath 1980).

Furthermore, microinjection of *Anacystis nidulans* and *Saccharomyces cerevisiae* photolyases in human fibroblasts showed a rapid repair of pyrimidine dimers induced after UV treatment followed by visible light administration (Zwetsloot *et al.* 1985). Moreover, it was demonstrated that CPD lesions are the primary responsible lesions for inducing mutations in mammalian cells exposed to UVB radiation (You *et al.* 2001). In addition, expression of marsupial CPD photolyase in XP-A cells (NER-deficient), revealed an increase in UV resistance and decrease in mutational frequency after the removal of CPD lesions (Asahina *et al.* 1999). Chigancas *et al* established the first human cell line derived from HeLa cells that are able to express marsupial photolyase (*Potorous tridactylus*) cloned in pCY4B vector and revealed the repair of pyrimidine dimers by photoreactivation (Chigancas *et al.* 2000). Subsequently, the same group generated a recombinant adenovirus vector containing a gene of marsupial CPD photolyase and demonstrated photorepair of the infected human cells (Chigancas *et al.* 2004).

In line with these findings, another study has been conducted using transgenic mice expressing marsupial CPD photolyase from *Potorous tridactylus*, and showed rapid repair of CPD lesions in both epidermis and dermis (Schul *et al.* 2002). This study also showed that photoreactivation of CPDs in intact skin of mice reduces UV effects such as erythema, hyperplasia and apoptosis. Also, another report found that in transgenic mice that express both CPD and 6-4pp photolyases, the CPD photolyase is more able to confer resistance to UV-induced tumourgenesis than 6-4 photolyase (Jans *et al.* 2005).

The action of photolyases in mammalian cells is not limited to transgenic animals, but also involve the topical application of enzyme-containing liposomes on human skin exposed to UV light. A study done by Stege *et al* in Germany showed a reduction in CPD lessions by 40-45% after application of *Anacystis nidulans* photolyase to UV treated human skin (Stege *et al.* 2000). Another recent study in 2012 also observed an affective application of a sunscreen containing photolyase from *Anacystis nidulans* which showed a significant reduction of CPD lesions and apoptotic cell death (Berardesca *et al.* 2012).

All these results prove that mammalian cells still have the machinery for providing a functional expression of photolyases and further investigation of this system is required which might involve studies on applying these enzymes (as proteins) together with UV sunscreens in order to protect us from the harmful effect of sunlight (Eker *et al.* 2009).

Expression of photolyases from different organismas such as *E. coli*, *A. nidulans* and *P. triductylus* in mammalian cells proved that these enzymes were functionally active in repairing UV lesions after transfection of a recombinant plasmid containing the *phr* genes. This means that the mammalian cell machinery including gene transcription by mRNA, translation by ribosomes with the help of tRNA and rRNA, protein folding and translocation of the protein into the nucleus is suitable for expressing the photolyase gene.

Interestingly, studies on examining the functional expression of archaeal photolyases in mammalian cells have not been done yet, despite the similarity of the two systems in DNA repair. Also photolyases from hyperthermophilic organisms might add advantages when using these enzymes in sunscreens because of their stability at high temperatures.

1.6 Aims of the project:

- To identify and clone a putative photolyase gene(s) from *Sulfolobus solfataricus.*
- To express the photolyase gene(s) in heterologous or homologous systems.
- To characterize the repair activity of the enzyme using *in vivo* and *in vitro* assays.
- To characterize the optimum temperature of *S. solfataricus* photolyase(s).
- To express *S. solfataricus* photolyase gene(s) in mammalian cell lines and to examine the effects of photolyase expression on DNA repair following UV radiation.

Chapter 2 – Cloning, expression and purification of *Sulfolobus solfataricus* photolyase

2.1 Introduction

The use of bacterial systems to express recombinant proteins is a popular technology, because of their rapid cell growth, inexpensive cost, and high productivity. *E. coli* is the commonly used organism to express a heterologous protein and there are many cloning vectors available to produce high levels of the expressed protein (Terpe 2003).

The first trial was to initially express the *Sulfolobus solfataricus* photolyase gene in an *E. coli* system, followed by expression of the enzyme in a homologous system (in *S. solfataricus*), if the first trial was unsuccessful.

The work in this project started in 2008 and one of the aims was to identify a *phr* gene from *S. solfataricus*. The search result in ncbi database website showed no annotation of this *phr* sequence. Therefore, a BLAST search of the full genome sequence of *S. solfataricus* was done with the *phr* gene sequence identified from *S. tokodaii* strain 7 (Fujihashi *et al.* 2007). However, two years later, a search in another gene bank website (http://www.ebi.ac.uk/services) showed the sequence annotation of *phr* gene from *S. solfataricus* P2, which was published in 2001 (She *et al.* 2001). Alignment of the amino acid sequences of the identified *S. solfataricus* photolyase sequence from the BLAST search and the puplished sequence for *S. solfataricus* P2 photolyase by She *et al.* in 2001 showed 100% similarity (see appendix 10 for alignment).

This chapter will cover the successful cloning procedure and the successful heterologous expression of *S. solfataricus* photolyase.

2.2 Materials and Methods

Materials:

All laboratories reagents used in this project were obtained from Sigma-Aldrich, Poole, UK, Fisher Scientific, Loughborough, UK or Melford Laboratories, Suffolk, UK unless specified otherwise.

DNA template of *S. solfataricus* P2 was obtained from the Centre for Extremophile Research (CER) lab, University of Bath. Oligonucleotide primers were supplied by Invitrogen, Paisley, UK. Restriction enzymes (NheI, SacI), dATP, and Phusion High Fidelity DNA polymerase kit were obtained from New England Biolabs (NEB), Hitchin, UK. PCR cleanup system, Gel extraction kit, Wizard SV miniprep kit, pGEM-T Easy Vector system, JM109 cells, T4 ligase, and 1Kb plus 100 bp DNA ladders were all obtained from Promega, Southampton, UK. *E. coli* BL21 (DE3) cells and *E. coli* Rosetta cells plus pET-28a vector were supplied by Novagen Merck Biosciences, Nottingham, UK. Shrimp Alkaline Phosphatase and Complete EDTA-Free Protease Inhibitor Cocktail Tablets were from Roche, Mannheim, Germany. Lysozyme from Fluka, Switzerland. SDS-PAGE protein standard, 30% acrylamide/bis solution, ammonium persulphate (APS) were all obtained from Bio Rad Laboratories Ltd, Hemel Hampstead, UK. Metal chelating cellulose was obtained from Bioline, London, UK.

Methods:

1. Identifying the putative sequence of *S. solfataricus phr* gene:

Sulfolobus solfataricus putative photolyase gene sequence was identified by a BLAST search of the whole genome sequence of *S. solfataricus* P2 (obtained from archaeal genome browser, http://archaea.ucsc.edu/) with *Sulfolobus tokodaii strain 7* photolyase gene (obtained from NCBI, http://www.ncbi.nlm.nih.gov/).

2. Cloning of *S. solfataricus phr* gene:

Primers for the putative *phr* gene of *S. solfataricus* were designed in which they were sharing homology at the start and the end of *phr* gene sequence. Both primers were designed with specific restriction sites (SSforNheI, SSrevSacI) for cloning into the pGEM-T vector. The forward and reverse primers contain NheI, and SacI restriction sites respectively. These two restriction enzymes were selected because they do not induce any internal cut within the gene (according to the restriction mapper website, http://www.restrictionmapper.org/). Both primers were checked for their melting temperatures (T_m) and GC content using this website http://www6.appliedbiosystems.com/support/techtools/calc/. In the forward primer 1 base had to changed in order to incorporate the ATG as a start codon.

3. Amplification of *phr* gene using PCR:

In order to amplify the gene, 100µM solutions from both primers (SSforNheI, SSrevSacI) were made and 0.5µl from each solution was used for PCR reaction. Also 10X dilution of 1µl *S. solfataricus* DNA was made and 0.5µl was used for PCR.

The primer sets used were listed in Table 2.1a.

The reaction volumes for 50 µl PCR reaction were as follows Table 2.1b: Two PCR reactions were made one in Phusion HF buffer and the other in Phusion GC buffer

Table 2.1a Primers for cloning *S. solfataricus phr* gene in pGEM-T vector

Primer name	**Sequence 5' to 3'**	**Tm ºC**	**Amplicon size**
SSforNheI	CTAG*CTAGCATGCTCTGCCTATTTATA	56	1300bp
SSrevSacI	CGAGCT*CCTATTTTATTTTAGATTTCCTACA	55	

Red sequences indicate the incorporated restriction sites

The thermocycling conditions were carried out as described in Table 2.1c.

Table 2.1b Reaction volumes for PCR (Added in the following order)

Component	**50 µl reaction**	**Component**	**50 µl reaction**
H_2O	Add to 50 µl	SSrevSacI primer (100 µM)	0.5 µl
5x Phusion HF/GC buffer	10 µl	Template DNA purified from miniprep kit	0.5 µl
dNTPs (10 mM)	1 µl	DMSO (3%)	1.5 µl
SSforNheI primer (100 µM)	0.5 µl	Phusion DNA polymerase (2U/ µl)	0.5 µl

Table 2.1c PCR cycling conditions:

Cycle step	**Temp**	**Time**	**Cycles**
Initial denaturation	98°C	30s	1
Denaturation Annealing Extension	98°C 50°C 72°C	10s 30s 2 min	40
Final extension	72°C 4°C	10 min hold	1

Agarose gel extraction:

The two PCR products in the two different buffers were visualized on a 1% (w/v) agarose gel using 1x TAE buffer (40Mm Tris acetate, pH 8.2, 1 Mm EDTA) and supplemented with 2µl of 10mg/ml ethidium bromide. 10 µl of 6x DNA loading dye (50 mM EDTA, 50% (v/v) glycerol, pH 8.0, 0.05% (w/v) bromophenol blue) was added to both samples and 15 µl samples plus 6 µl DNA ladder (1kb) were loaded into the gel wells. The gel was run at 80V for about 1.5 h and the bands were visualized on an UV illuminator. The band in GC buffer

that contained the gene was excised (because the yield was better in this buffer) using a sterile razor blade and placed into a 1.5ml microcentrifuge tube. The extraction of DNA from the gel was performed using Promega gel extraction protocol. The protocol instructions were followed exactly as stated except the DNA was eluted in 30 µl Milliq water.

A-Tailing of PCR product:

In order to facilitate the ligation of PCR fragments into pGEM-T vector, adenine nucleotides were added to both ends of the PCR products. The following components in Table. 2.2 were added and incubated at 70°C for 30 minutes.

Table 2.2 A-tailing reaction component

Component	**Amount**
Taq polymerase (5U/µl)	1µl
10X reaction buffer	1 µl
2 mM dATP	1 µl
PCR product	7 µl
Total volume	10 µl

Ligation:

The pGEM-T Easy vector (vector map is in Appendix 4) was used for the cloning of the A-tailed DNA. The following components Table 2.3 were added for the ligation reaction and incubated at 4°C overnight.

Table 2.3 Ligation reaction

Component	**Amount**
pGEM-T Easy vector (50ng/µl)	1µl
2X rapid ligation buffer	5 µl
A-tailed DNA	3 µl
T4 DNA ligase (100U)	1 µl
Total volume	10 µl

Ethanol precipitation of ligation reaction:

In order to precipitate the ligation reaction to remove all salts that might affect the transformation, the following components were added as shown in Table 2.4.

Table 2.4 Ethanol precipitation reaction

Component	**Amount**	**Component**	**Amount**
Ligation reaction	10µl	Dextran blue	1 µl
3M Na acetate pH 5.2	1 µl	Ethanol	20 µl

The above components were incubated at -20°C for 30 min and then centrifuged for 5 min at 4°C. The supernatant was discarded and the pellet was washed with 50 µl of 70% ethanol. The centrifugation and washing with ethanol was repeated twice more and the pellet was air dried. Dried pellet was resuspended in 5 µl Milliq water.

Transformation of *E. coli* competent cells:

JM109 electrocompetent cells were used for the transformation of the cloned insert. Cells were thawed on ice and a 0.1 cm path length electroporation cuvette was pre incubated on ice. In a 1.5 microcentrifuge tube, 0.5 µl of ligation reaction was added to 50 µl JM109 cells, mixed and incubated on ice for 2 min. Cells were then transferred to cold electroporation cuvette and electroporated on Ec1 (1.8 kV and 5.4 ms electrical pulse). 1 ml Lysogeny Broth (LB) medium (10 g/L tryptone, 10 g/L NaCl and 5 g/L yeast extract) was added quickly into the cuvette, mixed and cells were transferred to a 15 ml Falcon tube. Cells were then placed in a shaker incubator (230 rpm) at 37°C for 1 h. 100 µl of transformants were plated on carbenicillin (50µg/ml) LB plates [2% (w/v) agar + LB]. These plates were previously spread with 100 µl of 100 Mm isopropyl-β-D-thiogalactopyranosid (IPTG) and 20 µl of 50 mg/ml of bromo-chloro-indolyl-galactopyranoside (X-Gal) and left to dry (to allow for blue/white selection). Plates were placed in an incubator at 37°C overnight.

Extraction of plasmid DNA:

Seven white colonies and one blue colony (control) were selected for analysis of the transformants. Cell cultures were prepared in 50 ml Falcon tubes. Each tube, containing 10 ml LB media and 10 µl of 50 mg/ml carbenicillin, was inoculated with a single colony. Tubes were then placed in a shaker incubator (230 rpm) at 37°C overnight. In order to purify the plasmid DNA, all 10 ml overnight cultures were harvested by centrifugation for 15 min at 8000 rpm. Promega wizard miniprep protocol was followed and the DNA was eluted in 50 µl MilliQ water.

Restriction digests of the cloned pGEM-T:

The purified plasmid was digested using two restriction enzymes to check if the insert of the right size is present. The digestion was performed as follows in Table 2.5:

Table 2.5 Digestion reaction

Component	**amount**	**Component**	**Amount**
Miniprep DNA	5 µl	100X BSA (10 mg/ml)	0.2 µl
10X buffer (1)	2 µl	Milliq water	11.8 µl
NheI restriction enzyme (20,000 U/ml)	0.5 µl	SacI restriction enzyme (20,000 U/ml)	0.5 µl

The mixture was then incubated at 37°C for 2 h and the DNA digests were checked by electrophoresis using 1% agarose gel with 1Kb marker (6 µl).

Sequencing:

After visualizing the gel to determine which digested plasmid gives the correct insert size, the selected plasmids were sent for sequencing using T7F and SP6 primers. The plasmids were sequenced using GeneServices, Cambridge. The alignment of the sequencing results was done using GeneDoc. software.

Gel extraction and purification of the insert:

The band that has the correct insert sequence was selected, excised from the gel and purified as described before.

Restriction digests of pET28a vector:

Digestion reaction of the pET28a expression vector was done exactly the same as the digestion of pGEM-T vector. Alkaline phosphatase was added just 30 minutes before the end of incubation time to prevent the annealing of both ends of the vector. The plasmid was then purified as described previously.

Ligation:

To ligate the gel extracted DNA (the correct insert sequence) into the digested expression vector; the reaction was performed as in Table 2.6 and was incubated at 4°C overnight:

Table 2.6 Ligation reaction of pet28a

Component	**Amount**
digested pET28a	1µl
2X rapid ligation buffer	5 µl
Gel extracted DNA	3 µl
T4 DNA ligase (100U)	1 µl
Total volume	10 µl

Ethanol precipitation of ligation reaction was performed as described previously.

Transformation of *phr*-pET28a into JM109 *E.coli* cells:

Ligated pET28a vector with *phr* insert was first transformed into JM109 cloning strain to be able to purify the plasmid and to digest it using restriction enzymes. The transformants were checked by visualizing the digests on 1% agarose gel. The transformation, cell culture and miniprep were done as described before except that the cells were plated on Kanamycin (final concentration 50µg/ml) LB plates.

Transformation of *phr*-pET28a into BL21 *E. coli* cells:

After the digested plasmid was checked on agarose gel and confirmed to have the right size of both digestion products (inserted gene and vector), transformation into expression strain like BL21 cells was done. The transformation of BL21 *E.coli* chemical competent cells was performed by heat shock. 100 µl of BL21 cells were thawed on ice and 5 µl of the plasmid

was added. The mixture was incubated on ice for 10 min and then heat shocked at 42°C for 45 s. Cells were then placed on ice for 2 minutes and about 1 ml LB media was added. This mixture was placed in a shaking incubator at 37°C for 1 hour. 20 µl cells were then plated on Kanamycin LB plates and incubated at 37°C overnight.

Protein expression:

Ten ml overnight culture of BL21 cells was prepared in 50 ml Falcon tube. Rosetta cells were also tested for expressing the photolyase protein using chloramphenicol antibiotic (final concentration 50µg/ml). 10 ml LB media with 10 µl Kanamycin for BL21 cells or 10 µl chloramphenicol for Rosetta cells (final concentration 50µg/ml) was inoculated with one colony of the transformed cells. The culture was left in the shaker incubator at 37°C overnight.

A larger culture was then prepared in 2L flask with 500ml LB media and 500 µl Kanamycin or chloramphenicol (final concentration 50µg/ml) plus a 1 ml inoculum from the small overnight cell culture. The culture was left in the shaker incubator (230 rpm) at 37°C for nearly 4 hours until the right OD at 600 nm was reached. The cells were then induced with IPTG (final concentration 0.4mM) and incubated at 24°C in a shaker incubator (230rpm) overnight.

To check the photolyase protein expression, samples were collected after induction with IPTG. Five ml of cell culture was collected at 0 hour, 4 hour, and overnight and all samples were kept at -20 °C freezer. Samples were then resuspended in a 1.5 ml His bind buffer (50 mM Tris buffer pH 8.0, 300 mM NaCl and 20 mM imidazole) and sonicated (20 s x5 with intervals by keeping the cells on ice for 20 s). All samples were centrifuged at 13000 rpm for 5 minutes at 5°C. The supernatant was collected and this contains the soluble proteins. For the insoluble fractions, the pellet was resuspended in a 0.5 ml of 8M urea and centrifuged at 13000 rpm for 5 minutes at room temperature. The supernatant was collected and this contains the insoluble fractions. Both soluble and insoluble proteins of both cells at 0h, 4h, and overnight expression were run on 10% SDS-PAGE gel (components in Table 2.7) to check the expression.

In a 1.5 ml microcentrifuge tube, 12µl of each fraction was added with 4 µl of SDS loading buffer (4 ml 0.5 M Tris/HCl, pH 6.8, 2 ml 10% (w/v) SDS, 4 ml glycerol, 100 µl β-mercaptoethanol, 8 mg bromophenol blue). The tubes were then placed in a heat block at

100°C for 3-5 minutes. Seven µl of each sample was loaded alongside with SDS protein marker and the SDS gel was run at 200 Volt for 45 minutes in Tris/glycine buffer (144 g glycine, 30 g Tris and 100 ml of 10% (w/v) SDS made up to 1 L with MilliQ water). The gel was then stained with Coomassie brilliant blue and then de-stained by appropriate solution.

Purification of *phr* protein:

The purification of a his-tagged *phr* protein was done on a His-bind column. Cells were harvested by centrifugation at 6000 rpm for 10 minutes at 5°C and then resuspended in 10 ml fresh his-bind buffer. Lysozyme (1ml, 1mg/ml) and 100 µl of protease inhibitor cocktail (1 pellet was dissolve in 1 ml MilliQ water) were added to cells and the mixture was placed on ice for 30 minutes. Cells were sonicated for 20 s 5 times with intervals (were kept on ice for 20 s). They were then centrifuged at 10,000 rpm for 10 minutes and the supernatant was removed. This supernatant was filtered through a 0.45 µm syringe filter and then was applied to the His bind column. This column was prepared by adding metal chelating cellulose (the resin) and charged with $NiSO_4$ (2 ml of 400 mM solution). Flow through was applied and then reapplied on this column. This was followed by two times wash with 5 ml his-bind buffer and 2 times wash with 5ml of 5% his-elute in his-bind buffer. phr protein was then eluted four times with 0.5 ml his-elute buffer (50 mM Tris buffer pH 8.0, 300 mM NaCl, 1 M imidazole).

Table 2.7 SDS-PAGE gel components.

Separating gel		Stacking gel	
Component	Volume	Component	Volume
MilliQ water	4 ml	MilliQ water	1.1 ml
1.5 M Tris/HCl pH 8.8	2.5 ml	0.5 M Tris/HCl pH 6.8	500 µl
30% acrylamide	3.3 ml	30% acrylamide	330 µl
10% SDS	100 µl	10% SDS	20 µl
10% APS	100 µl	10% APS	20 µl
TEMED	10 µl	TEMED	5 µl

SDS-PAGE:

The different fractions that were obtained from the purification in His-bind column (flow through, W1 his-bind, W2 his-bind, W1 5% his elute in His bind, W2 5% his elute in His bind, elute1, elute2, elute3, elute4) were all run on 10% SDS-PAGE gel to check the purity and to determine in which fraction the protein was mainly eluted. The fractions were run on a SDS gel exactly the same as described previously.

Dialysis of the purified protein:

Imidizole was removed from the purified protein by dialysis against Tris buffer (200 mM NaCl, 50 mM Tris/ HCl pH 8). Phr protein was placed in a dialysis tube and left overnight at 4°C in 1L Tris buffer.

Spectroscopic analysis of the purified protein:

A Varian Cary 50 Bio UV/visible light spectrophotometer was used to scan the purified sample in the range of 260- 600 nm. This was done to calculate the concentration of the purified protein, using Beer-Lambert law, and to check whether there are two peaks, one for the protein and the other for FAD cofactor, at 280 and 455 nm, respectively. In addition the ratio between *phr* protein and FAD was also calculated.

High-resolution Mass Spectrometry analysis of the purified protein:

In order to obtain an accurate M_r measurement of the photolyase protein and a conformation of its size, a purified protein sample (200 µl) was sent to the University of Reading to be analyzed on a High-resolution Mass Spectrometry (HRMS). The dialyzed protein was sent after centrifugation at 14000 rpm for 5 minutes.

2.3 Results

Bioinformatics results:

A BLAST search of the whole genome sequence of *S. solfataricus* P2 with the photolyase gene sequence of *S. tokodaii strain 7*(from the websites that were outlined in section 1.2) revealed that *S. solfataricus phr* gene had a similarity, gene size, and GC content of 73%, 1302 bp, and 34% respectively. Both gene and protein sequences can be found in the Appendix 1 and 2.

Amplification and purification of *phr* gene:

S. solfataricus phr gene was amplified using the two primers as described previously. The primer sequences and the name of the incorporated restriction sites are found in Appendix 3.

PCR amplification of the *phr* gene was done using Phusion DNA polymerase and two primers specifically designed to anneal to phr gene in *S. solfataricus*. Two different buffers (GC and HF) in the PCR reaction were tested to determine which one gives the best yields. Two PCR products were run on a 1.0 % agarose gel and the bands were visualized on an UV illuminator. As shown in figure 2.1, both bands in lane 1 and 4 were of the right size of *phr* gene (1300 bp), but the yield in GC buffer was higher than in HF buffer. Therefore, the PCR product in GC buffer was selected to be excised from the gel and was purified using Promega gel extraction protocol as outlined before.

A-tailing and cloning into pGEM-T Easy vector:

The isolated fragment of *phr* gene from the gel was A-tailed to facilitate the ligation into pGEM-T vector. The ligated plasmids were then transferred into JM109 electrocompetent cells and plated, as described previously, on carbenicillin LB plates (with IPTG and X-gal) for blue / white screening.

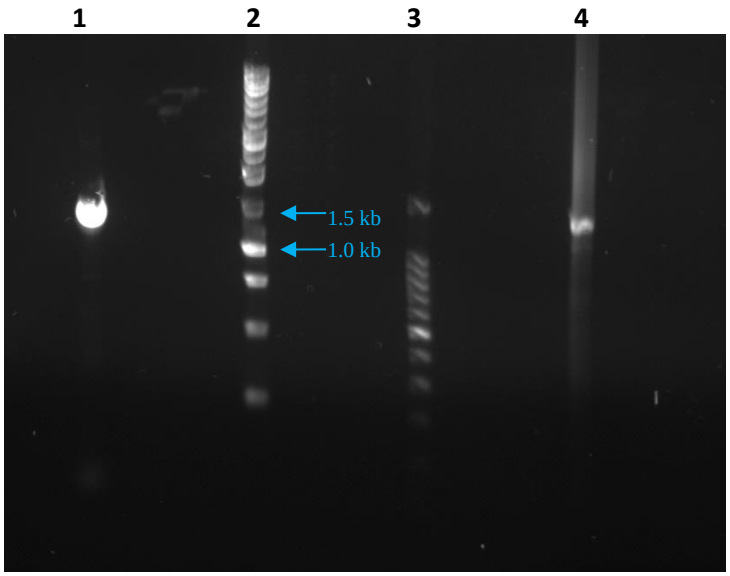

Figure 2.1: PCR amplified products in GC and HF buffers

Lanes from left to right: 1- PCR product in GC buffer; 2- 1kb DNA ladder; 3- 100 bp DNA ladder; 4- PCR product in HF buffer;

Blue arrows indicate the size of the bands in 100 bp ladder

Transformation results:

Cells grown on carbenicillin LB plates showed a high proportion of white colonies comparing with the blue colonies. This means that high percentage of cells were successful transformants. To check these transformants, 7 white colonies and 1 blue colony were selected and grown in a liquid culture overnight. The plasmids from these selected cells were then purified using Promega wizard miniprep protocol

Restriction digest:

Double digestion of the purified plasmids was performed using two restriction enzymes (NheI and SacI) (Fig 2.2), lanes 1-7 represent the double digested plasmids from the 7 selected white colonies. The lower bands in lane 1, 3, 4, and 6 give a possibility that one of these bands is the correct size (1.3 Kb) of the *phr* gene insert.

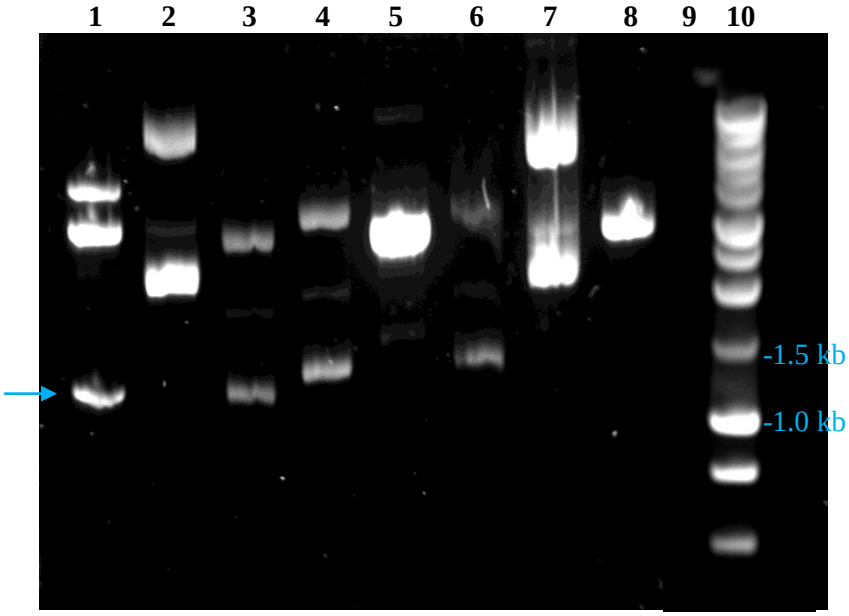

Figure 2.2: Double digests of *phr*-pGEM-T vector

Lanes from left to right:
1-7 double digested plasmids of 7 white colonies;
8- Double digested plasmid of a blue colony;
9- Blank;
10- 1kb DNA ladder;
Blue arrow indicates the right *phr* gene insert of 1.3 Kb.

Sequencing:

Plasmids with the correct insert size after double digestion (lanes 1, 3, 4, and 6 in Fig 2.2) were sent to be sequenced. The resulting sequences were checked and aligned using the Gene doc Program. Only one plasmid that represent lane 1 in Fig 2.2 had the right insert sequence and therefore was used for insertion into an expression vector.

Double digests of pET28a and ligation of the purified *phr* gene:

In order to ligate the correct *phr* gene into pET28a vector, the lower band in lane 1 Fig 2.2 that was confirmed to have the correct gene sequence was first excised from the gel and then purified as described previously in section 2. The expression vector pET28a was digested using two restriction enzymes (NheI and SacI) and the purified *phr* gene was ligated into this vector.

Transformation of *phr*-pET28a into JM109 *E.coli* cells:

The ligated pET28a vector with *phr* gene was transformed into JM109 cloning strain and the cells were plated on a kanamycin LB plate. 18 colonies were observed and 3 colonies were selected. Each single colony was inoculated in a liquid cell culture in order to purify and digest the plasmids to check the transformants. The purified plasmids were digested by double cut using two restriction enzymes (NheI and SacI). The digestion was checked and visualized on an agarose gel (Figure 2.3). The upper bands in lane 1, 2, and 3 represent the digested pET28a vector whereas the lower bands in the three lanes represent the *phr* gene insert. The digestion of *phr*-pET28a had the right size of both expression vector (5000 bp) and the phr gene (1300 bp).

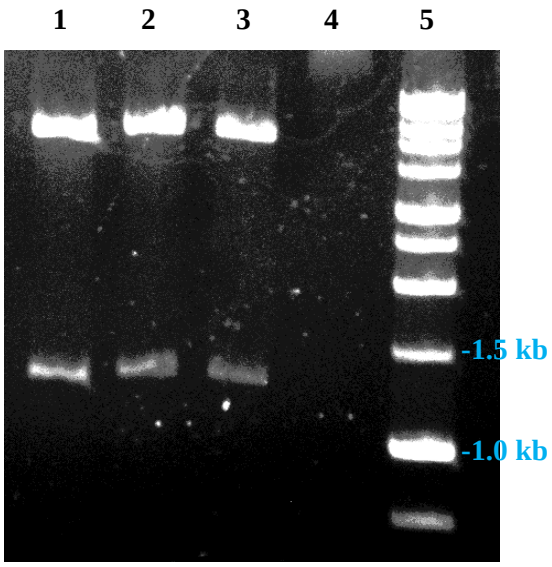

Figure 2.3: Double digests of *phr*-pET28a vector

Lanes from left to right:
1-3 double digested plasmids of 3 colonies;
4- Blank;
5- 1kb DNA ladder.

Transformation of *phr*-pET28a into expression cells (BL21 cells):

Since all the three purified plasmids from JM109 cells were confirmed to have the right size of both digests, transformation of *phr*-pET28a (colony 1 plasmid was selected) into two selected expression strains BL21 cells and Rosetta cells was done. Many colonies were observed on the kanamycin LB plate and a single colony was selected to be inoculated in a liquid cell culture in order to prepare a small overnight culture (as outlined in section 2.2).

Protein expression:

BL21 cells and Rosetta cells in two flasks of 500 ml LB were grown for 4 hours to an optical density of 1.12 and 0.81 at 600 nm respectively, then they were induced with 0.4 mM IPTG (as a final concentration).

Samples were collected at 0h, 4h, and overnight after induction with IPTG. Cells were lysed and the soluble plus insoluble fractions were run on an SDS-PAGE gel. Fig 2.4 shows the soluble and insoluble proteins that were expressed in both BL21 and Rosetta cells. Lanes (2, 3, 4) and (8, 9, 10) in this figure represent the expressed soluble and insoluble proteins of Rosetta cells respectively. Lanes 2 and 8 are the zero hour which represent the expressed proteins at zero hour after induction with IPTG. Lanes 3 and 9 represent the expressed proteins after 4 hours from induction with IPTG, whereas lanes 4 and 10 are the overnight expressed proteins of Rosetta cells.

Lanes (5, 6, 7) and (11, 12, 13) represent the soluble and insoluble expressed proteins in BL21 cells respectively. Lanes 5 and 11, 6 and 12, 7 and 13 represent the expressed proteins at 0h, 4h, and overnight respectively. From Fig 2.4 it seems that between 66 and 45 kD marker band size there was a single over expressed protein shown as a dark band of approximately 54 kD size, which corresponds to the predicted size of the photolyase protein (54 kD). It was also obvious that the photolyase protein was expressed gradually and at 4 hour samples the expression was low as compared with the overnight samples, which was highly expressed. The trend of photolyase expression was similar in both BL21 and Rosetta cells and in both soluble and insoluble fractions.

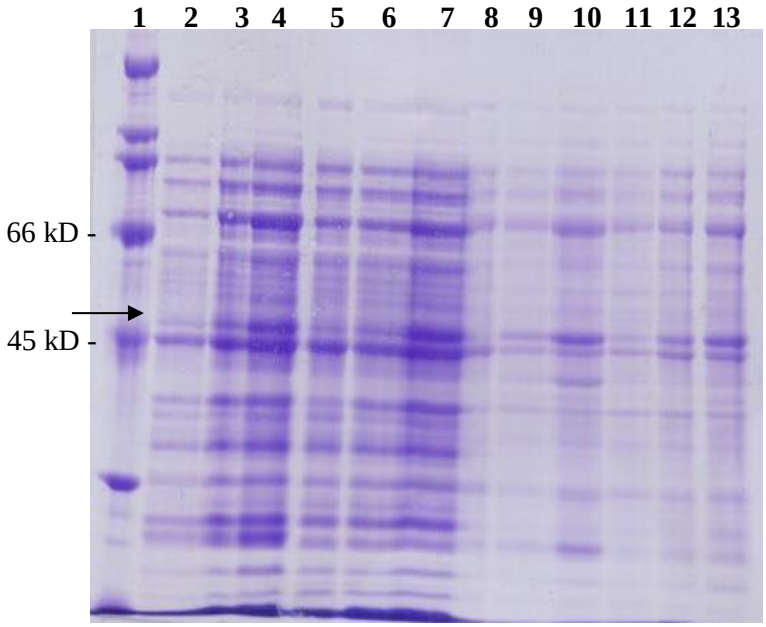

Figure 2.4: Protein expression of both Rosetta and BL21cells

Lanes from left to right:
1- SDS marker;
2- Rosetta Soluble proteins at 0 h;
3- Rosetta soluble proteins at 4 h;
4- Rosetta soluble proteins overnight;
5- BL21 soluble proteins at 0 h;
6- BL21 soluble proteins at 4 h;
7- BL21 soluble proteins overnight;
8-Rosetta insoluble proteins at 0 h;
9- Rosetta insoluble proteins at 4 h;
10- Rosetta insoluble proteins overnight;
11- BL21 insoluble proteins at 0 h;
12- BL21 insoluble proteins at 4 h;
13- BL21 insoluble proteins overnight;
Black arrow indicates the right phr protein size of 54 kD;

Both BL21 and Rosetta cells transformed with *phr*-pET28a vector were grown in two large LB cultures. From these large overnight cultures, cells were harvested and lysed in order to apply the His-tagged proteins to the His bind column. Figure 2.5 shows the purification results of the His-tagged proteins from BL21cells. Lanes 1 and 2 represent the flow through whereas lanes 3-6 represent the washes in his bind buffer (lane 3 and 4) and the washes in 5% his elute in his bind buffer (lane 5 and 7). Lanes 8-12 represent the eluted proteins in 0.5 ml his elute buffer. It was clear that a His-tagged protein of approximately correct size was eluted. The photolyase protein was eluted mainly in elute 2 and elute 3. Although there was contamination with other proteins in elute 2 and 3, it was of a low percentage and therefore was ignored.

Purification of his-tagged proteins from Rosetta cells was also done. However, the amount of the purified photolyase protein from BL21 cells was obviously higher than from Rosetta cells and this was clearly shown on a SDS gel (The image is not added here). Therefore, BL21 cells were selected for expressing the His-tagged photolyase protein.

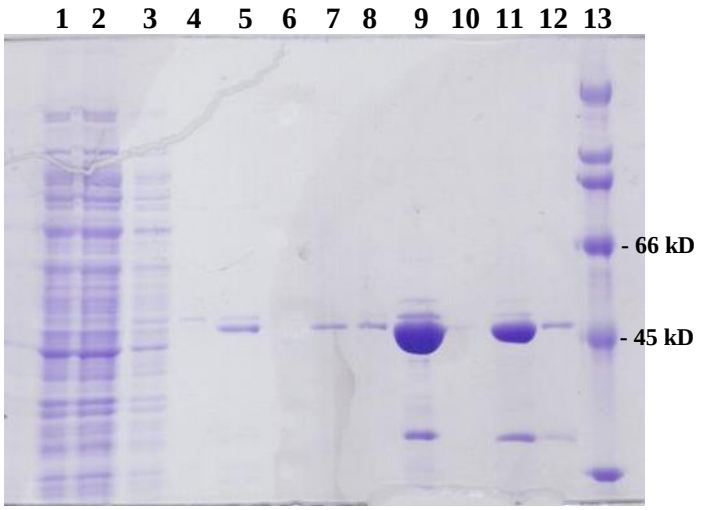

Figure 2.5: protein purification of photolyase from BL21 cells

Lanes from left to right:
1 and 2- the flow through;
3- Wash 1 in His bind buffer;
4- Wash 2 in His bind buffer;
5- Wash 1 in 5% His elute in His bind buffer;
6- Blank;
7- Wash 2 in 5% His elute in His bind buffer;
8- Elute 1; 9- Elute 2; 10- Blank; 11- Elute 3; 12- Elute 4;
13- SDS marker;

Spectroscopic analysis of the purified protein:

Since the purified protein was eluted mainly in elute 2 and 3 by his elute buffer, this buffer contains imidizole which can absorbs the light at the wave length of 280 nm. As a result, it could interfere with the absorption of the protein at the same wave length. Therefore, these two fractions were combined together and dialyzed overnight in 1L Tris buffer (200mM NaCl, 50 mM Tris/HCl pH 8) in order to remove the imidizole. This dialyzed protein was then scanned by spectrophotometer in a range of (260-600 nm). The purified protein was of a yellow greenish colour which indicates the presence of an FAD cofactor. This was confirmed by the scan results that showed two peaks Fig 2.6 A, one at 280 nm and another peak at 455 nm which represent the photolyase protein and possibly FAD respectively. Furthermore, the absorption spectrum of *S. tokodaii* photolyase, which was taken directly after purification (Fujihashi *et al.* 2007) Fig 2.6 B, was very similar to the spectrum that we obtained for *S. solfataricus* photolyase under the same conditions Fig 2.6 A.

By using Beer-Lambert law ($A= \varepsilon C L$), the concentration of the photolyase and FAD was determined. The average absorbance values and predicted molar extinction coefficient of the photolyase protein at 280nm were 0.61 and 95940 $M^{-1}cm^{-1}$ respectively, whereas for the FAD the values at 455nm were 0.15 and 11300 $M^{-1}cm^{-1}$ respectively. The ratio of *phr* molecule to FAD molecule was also determined and it was 1 *phr* to 2 FAD molecules.

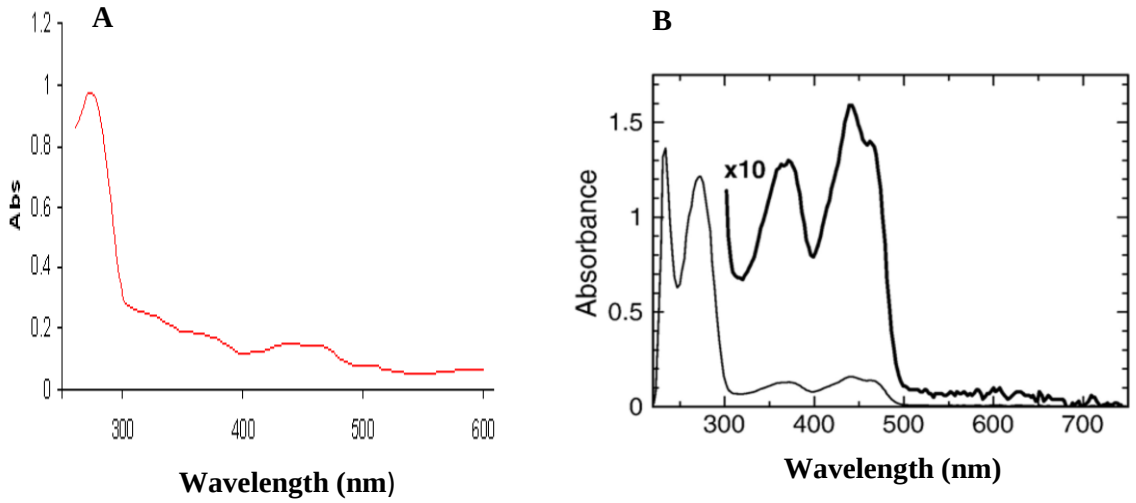

Figure 2.6 Spectral analysis of the purified proteins

A) Spectral analysis of the diluted (1:6) and purified *S. solfataricus* photolyase showing two peaks at 280 and 455 nm.
B) Spectral analysis of the purified *S. tokodaii* photolyase showing the same two peaks with the diluted version (Adapted from Fujihashi *et al.* 2007).

HRMS analysis result of the purified photolyase protein:

The phr protein was run on the mass spectrometry (MS) at University of Reading and the results of the electrospray spectrum and the deconvolution report are in figure 2.7 and 2.8. The sample appears to be a mixture of several components but one of the major components, component B, is probably the *phr* protein and mass measures at 54435. This is about 0.0006% of the calculated protein mass with a predicted size of 54470.1 and 54338.9 with and without the start methionine respectively, and is within the specification of the instrument for this type of measurement.

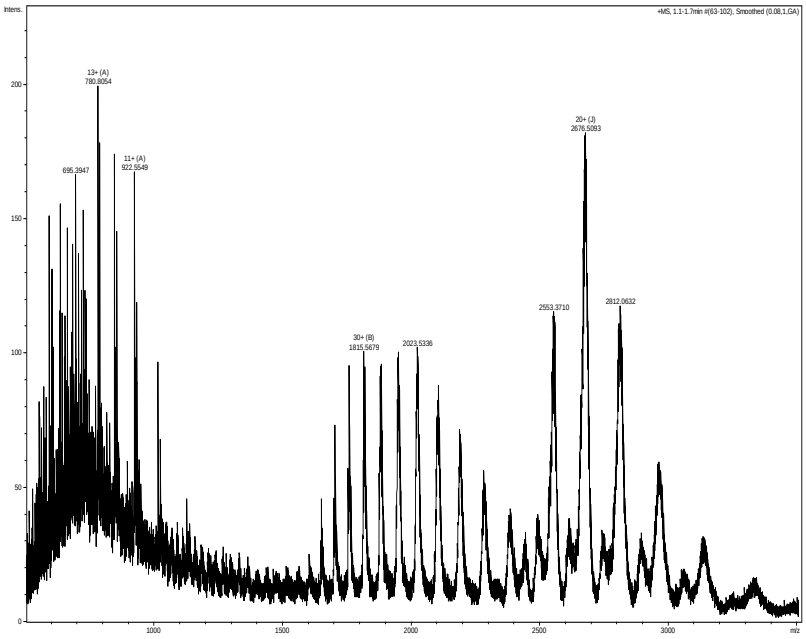

Figure 2.7: ESI spectrum of phr:

Analysis of the phr protein in the MS showed many peaks that represent the protonated value of the protein and also many adducts that was formed in the MS. These can be a mixture of protons, sodium or potassium cations in any combination. Above each peak there is a number e.g 30^{+} which indicates the number of charges on that particular cluster.

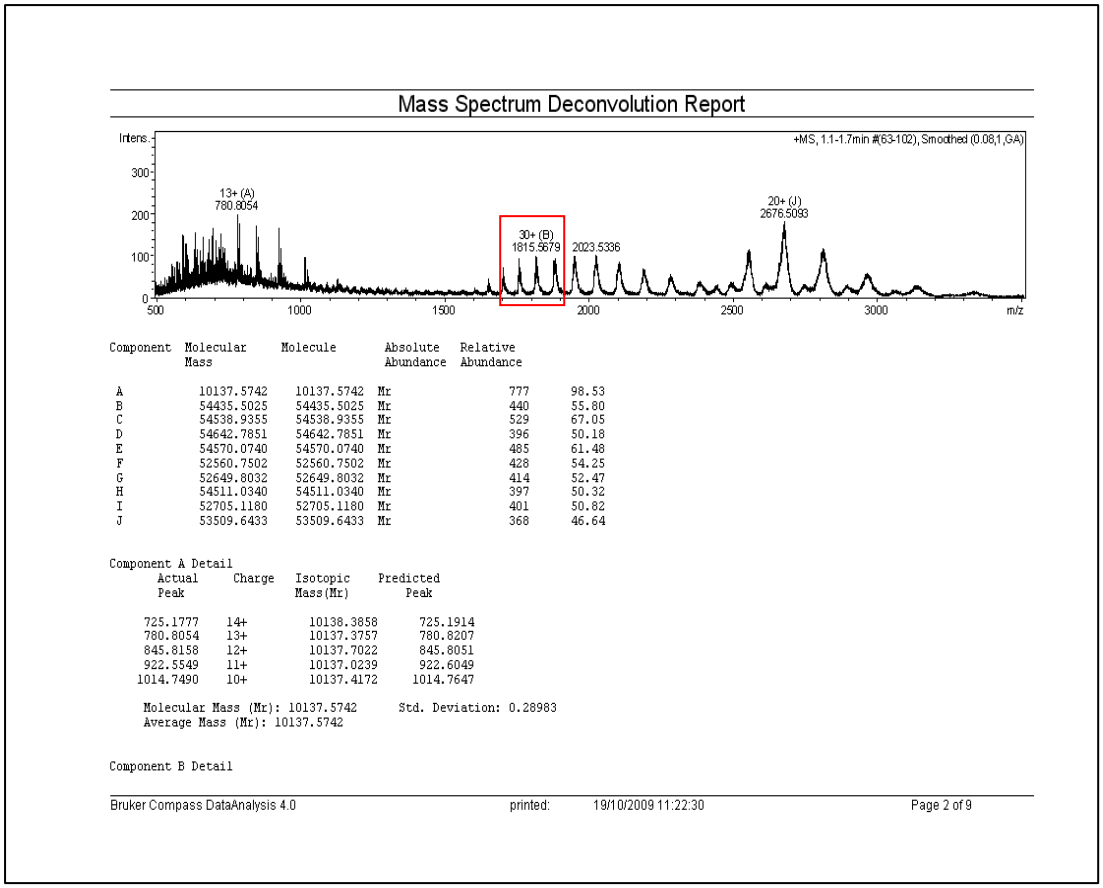

Mass Spectrum Deconvolution Report

Component	Molecular Mass	Molecule		Absolute Abundance	Relative Abundance
A	10137.5742	10137.5742	Mr	777	98.53
B	54435.5025	54435.5025	Mr	440	55.80
C	54538.9355	54538.9355	Mr	529	67.05
D	54642.7851	54642.7851	Mr	396	50.18
E	54570.0740	54570.0740	Mr	485	61.48
F	52560.7502	52560.7502	Mr	428	54.25
G	52649.8032	52649.8032	Mr	414	52.47
H	54511.0340	54511.0340	Mr	397	50.32
I	52705.1180	52705.1180	Mr	401	50.82
J	53509.6433	53509.6433	Mr	368	46.64

Component A Detail

Actual Peak	Charge	Isotopic Mass(Mr)	Predicted Peak
725.1777	14+	10138.3858	725.1914
780.8054	13+	10137.3757	780.8207
845.8158	12+	10137.7022	845.8051
922.5549	11+	10137.0239	922.6049
1014.7490	10+	10137.4172	1014.7647

Molecular Mass (Mr): 10137.5742 Std. Deviation: 0.28983
Average Mass (Mr): 10137.5742

Component B Detail

Figure 2.8: mass spectrum deconvolution report of phr:

This report shows closely related proteins that are present in the sample.
Component B (red box) has a mass very close to the fully protonated phr protein.

2.4 Discussion

In this chapter, the initial aim was to identify the sequence of *S. solfataricus* photolyase and to express the protein. After choosing the *S. tokodaii* photolyase gene sequence for BLAST search with the full genome sequence of *S. solfataricus,* the amino acid sequence alignment for *S. solfataricus* photolyase identified by BLAST search was 100% identical (Appendix 10) and in agreement with the published gene sequence of *S.solfataricus* P2 photolyase (She *et al.* 2001). Although, the gene sequence of *S. solfataricus* photolyase was identified from the annotation of the genome sequence in 2001, the function of the enzyme as a photoreactivating enzyme has not been characterized yet.

Since the start and the end of the phr gene were determined, the amplification of this gene was possible from the *S. solfataricus* DNA by using two nucleotide primers. Following amplification, the *phr* gene was cloned initially into pGEM-T Easy Vector to give high clones yield in order to send it for sequencing and to sequence the full gene located between the two vector primers (T7F and SP6). After confirming the right phr gene sequence, the gene was then cloned into pET28a for expression.

The gene was predicted to encode a polypeptide of 433 amino acid residues and has a predicted M_r of 52,017. Although, the calculated molecular weight of the cloned *S. solfataricus* photolyase was 54470, this is because several amino acids had to be added at the N-terminus of the protein in order to add a his-tag to the protein. The photolyase protein was his tagged using pET28a vetor since this vector carry two his tag sequences, one at the N-terminal and the other at the C-terminal. We chose to His tag the photolyase protein at the N-terminal region for no specific reason, because proteins can be tagged at either terminal.

The *S. solfataricus* photolyase protein was purified using his bind column as it is a his-tagged protein. The apparent molecular weight of the purified protein was 54 kD as determined by SDS-polyacrylamide gel electrophoresis and the exact protein size was confirmed by HRMS analysis. This result was similar to a previously reported photolyase molecular weight of 54,000 in *Salmonella typhimurium* (Li and Sancar 1991) and close to 53,994, 51,555 molecular weights of *E. coli* (Sancar *et al.* 1984) and *S. tokodaii* (Fujihashi *et al.* 2007) photolyases respectively.

This purified protein was in the soluble fraction and of a yellow-greenish coloured solution which indicates the presence of flavins. The ratio of the purified protein to FAD molecules

was calculated as 1 to 2 respectively. This suggests that both chromophores of *S.solfataricus* photolyase are FAD molecules and in fact this result was expected and in agreement with another study that demonstrated the presence of two FADs chromophores in *Sulfolobus tokodaii* photolyase (Fujihashi *et al.* 2007).

The average calculated concentration of the final purified photolyase protein prepared from 500 mL of IPTG induced overnight culture was 43 µM, and this concentration is sufficient for detecting the activity of the enzyme *in vitro*.

To full understand this photoreactivation system in *S.solfataricus* and to examine the activity of the purified photolyase, the *in vivo* and *in vitro* assays were developed.

Chapter 3 – Characterization of functional activity of *Sulfolobus solfataricus* photolyase *in vivo* and *in vitro*

3.1 Introduction

In order to demonstrate the photoreactivation activity of *S. solfataricus* photolyase *in vivo*, *E. coli* cells were used. The UV sensitivity of *E. coli* cells expressing the recombinent *S. solfataricus* photolyase was examined in the dark or under white illumination.

To study the *in vitro* characteristics of this enzyme as a photoreactive enzyme in repairing UV lesions, *S. solfataricus* photolyase was overexpressed and purified from *E. coli* cells.

A new method was developed in the lab to detect the functional activity of The photolyase *in vitro.* The principle of this method depends on tow forms of the DNA, the relaxed open form and the supercoiled form as their movement on the agarose gel is different. Its principle according to TREVIGEN product data for *E.coli* photolyase is that the "Repair of UV-induced DNA damage is demonstrated by a loss in conversion of the supercoiled plasmid to relaxed, open circle form following treatment with the CPD-specific endonuclease T4-PDG (T4-Endonuclease V)" Fig 3.1'. This T4 endonuclease has both DNA glycosylase and AP lyase activity. It recognizes the CPD dimers and cleaves the 5' end of the glycosyl bond and the phosphodiester bond at the AP site of the dimer. This difference between supercoiled and relaxed plasmid was visualized on 1%.

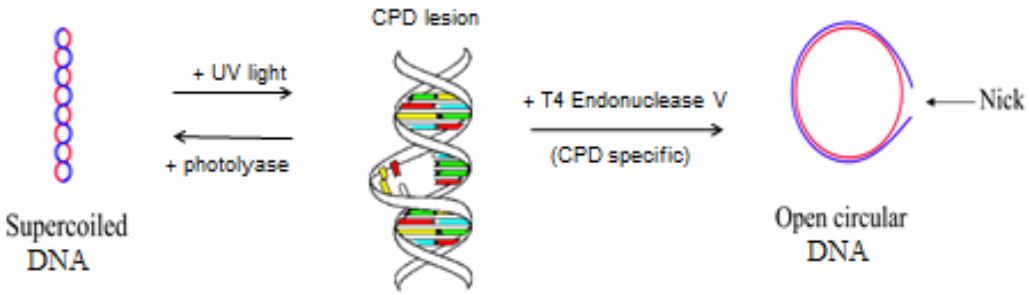

Fig 3.1' technique principle for characterising functional activity of photolyase *in vitro*

Photolyase repair of UV damage was measured *in vitro* as a loss in conversion of the supercoiled plasmid to relaxed, open circle form following treatment with the CPD-specific endonuclease T4-PDG (T4-Endonuclease V).

When the DNA is exposed to UV damage, UV photoproducts such as CPD lesions are induced. The addition of T4-Endonuclease V (CPD-specific enzyme) will recognize the CPD lesions only and induced a nick in the supercoiled plasmid. As a result the supercoiled plasmid will be converted to a relaxed open circular form. However, when a functional active photolyase is added to a UV treated supercoiled DNA, it will repair most of the damaged lesions and after the addition of the T4-Endonuclease V, only what was left unrepaired from the UV lesions will be detected and cleaved by the endonuclease. Therefore, the amount of the relaxed open form of the DNA will reduce. The difference in the amount of the two forms of the plasmids will be seen on agarose gel as the supercoiled plasmids move faster than the relaxed form.

Pyrimidine dimers from supercoiled plasmids were induced by irradiation with UV light and the repair of this UV damage by *S. solfataricus* photolyase was detected *in vitro*.

This chapter will cover the *in vivo* and *in vitro* functional characteristics of *S. solfataricus* photolyase activity.

3.2 Materials and Methods

Materials:

BL21 cells and pET-28a vector were supplied by Novagen Merck Biosciences, Nottingham, UK. *E. coli* photolyase, 10X reaction buffer 14 and DDT were all obtained from Trevigen distributor in UK, AMS Biotechnology (Europ), Abingdon, UK.

T4-PDG (T4-Endonuclease V) and 10X reaction buffer 11 were obtained from New England Biolabs (NEB), Hitchin, UK. pGEM-T Easy Vector system was obtained from Promega, Southampton, UK.

Methods:

Characterisation of photoreactivation activity of *S. solfataricus* photolyase in *E. coli* cells (*in vivo*):

The *S. solfataricus* photolyase was expressed in BL21 cells exactly the same as described in section 2.2. *Aeropyrum pernix* E2 gene expressed in BL21 cells was used as a control (donated by Karl Payne, Lab 1.33). The E2 gene was cloned into pET28a vector and transformed into BL21 cells. Both transformed cells with different genes were grown in LB medium at 37°C until the OD at 600 nm reached 0.94 and 0.89 in BL21 cells expressing *phr* and BL21 cells expressing E2 respectively. Cultures were then induced with IPTG at a final concentration of 0.4 mM in cells expressing *phr* and 1mM in cells expressing E2. Both cultures were then incubated at 24 °C for 4 hours. Eight Kanamycin plates were prepared and divided by pen to six equal sectors Fig 3.1''. In order to get a uniform distribution of cells in each plate, glass beads were used to spread 200 µl of cell culture onto each plate. 4 plates were used to spread cells expressing *phr* and out of them two plates were used as a dark and light control. The other two plates were illuminated with UV light (254 nm, 6W at a distance of 25 cm) (cover removed) and each part of the six divisions was exposed to UV light at different time intervals. Of these two plates, one was kept in the dark and the other was illuminated with white light (using light box, 2 fluorescent tube, 2 X 8w, the cover was removed) for 30 minutes. In the control with cells expressing E2, the distribution of cells unto 4 plates and their exposure to UV and white light is exactly the same as in the cells expressing *phr*. All eight plates were then placed in the incubator at 37°C and left overnight. The results were scored based on a visual inspection of colonies from each sector in each plate.

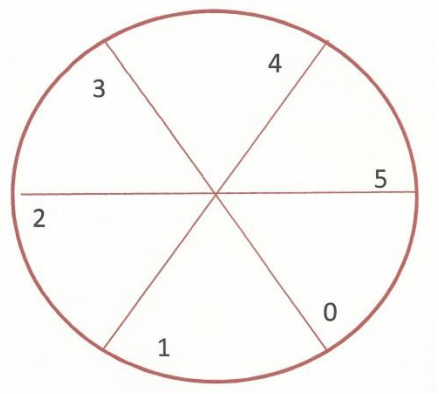

Fig 3.1'' Schematic diagram for the LB plates used for functional characterization of *E. coli* cells expressing *S. solfataricus* and E2

Kanamycine LB plates were plated with *E.coli* cells and divided by pen into six equal sectors. Each sector was exposed to UV light (254 nm, distance 25 cm) at different time intervals. Numbers inside each sector indicates the UV exposure time in min.

Characterisation of photoreactivation activity of *S. solfataricus* photolyase *in vitro*:

Photolyase repair of UV damage was measured *in vitro* according to a method described in TREVIGEN product data for *E.coli* photolyase. "Repair of UV-induced DNA damage is demonstrated by a loss in conversion of the supercoiled plasmid to relaxed, open circle form following treatment with the CPD-specific endonuclease T4-PDG (T4-Endonuclease V)". This T4 endonuclease has both DNA glycosylase and APlyase activity. It recognizes the CPD dimers and cleaves the 5' end of the glycosyl bond and the phosphodiester bond at the AP site of the dimer. This difference between supercoiled and relaxed plasmid was visualized on 1% agarose gel.

pGEM-T vector with an insert (Methanol dehydrogenase gene) was used as a supercoiled plasmid (donated by Philippe Mozzanega, Lab 1.33). Using a 96 well plate, 50 µl of the purified MDH-pGEM-T plasmid was placed in one well and irradiated with UV light for 2 minutes (This time was optimized previously). In a 1.5 ml microcentrifuge tube, the following reactions, Table 3.1, were prepared according to the protocol that was provided with the *E. coli* photolyase:

Table 3.1 *In vitro* photolyase functional activity reaction.

Component	**Reaction 1 (untreated DNA)**	**Reaction 2 (UV treated DNA)**
MDH-pGEM-T plasmid	20 µl	20 µl
10X reaction buffer 14	10 µl	10 µl
100 mM DTT	10 µl	10 µl
Milliq H_2O	55 µl	55 µl

19 µl of reaction 2 was aliquoted into two 1.5 ml microcentrifuge tubes (A, B) and 1 µl of (5.38 mg/ml *E.coli* photolyase or 26 µM of purified *S. solfataricus* photolyase) was added to tube B only. Tubes were incubated at room temperature (30 ºC) in the dark for 5 minutes and then tube B was illuminated under white light for 1h (tube was opened) using light box. In

order to add T4 endonuclease, 14 µl of 1X reaction buffer 11 was aliquoted into 4 tubes (A^-, B^-, C, D) 5 µl of reaction 1 was added to two tubes (C and D, as untreated controls). In the other two tubes (A^- and $B^{-)}$, 5 µl of reaction 2 from tube A and B were dded respecteively to each tube. 1 µl of 10 units/µl T4 endonuclease V was added to only 3 tubes (A^-, B^-, D) and the reaction was incubated in the incubator at 37°C for 1h. 1% agarose gel was prepared in 1X TAE buffer with 2 µl of 10mg/ml ethidium bromide. 6x DNA loading dye of 10 µl was added to each sample and 12 µl was loaded onto gel. The gel was run on 90 volts for 1h and 30 min and the bands were visualized on an UV illuminator. The intensity of the bands was measured using LabWorks Image Acquisition and Analysis Software from UVP.

3.3 Results

Demonstration of functional activity of *S.solfataricus* photolyase in *E.coli* cells (*in vivo*):

Cells expressing the E2 component of the PDH complex which has no role in photoreactivation, were used as a control for detecting the activity of *S. solfataricus* photolyase *in vivo*. E2 expressing cells were plated on two control plates, one was then kept in the dark and used a dark control whereas the other was illuminated with white light for 30 minutes and used as a light control. After these two plates were incubated at 37 ºC overnight, cells were able to grow and the plates were full of colonies that were distributed uniformly around the whole plate Fig 3.1A: c and d. On the other hand, the two control plates (expressing an E2 enzyme not involved in DNA repair) that were exposed to UV light at different time intervals (from 1-5 min) in each sector (one was kept in the dark and the other was exposed to white light for 30 min) showed no growth of any single colony except in the sector that was non UV irradiated Fig 3.1A: a and b. This means that exposure to UV light induced damage to DNA molecules and therefore the cells died because they were unable to repair this damage.

Cells expressing the *S. solfataricus phr* gene were plated onto two control plates without UV treatment, one was used as a dark control and the other was used as a light control (exposed

to white light for 30 minutes). Both sets of plates, showed a uniform distribution of colonies around the plate Fig 3.1B: g and h. Plates 3.1 e & f however, expressing *phr* gene, where

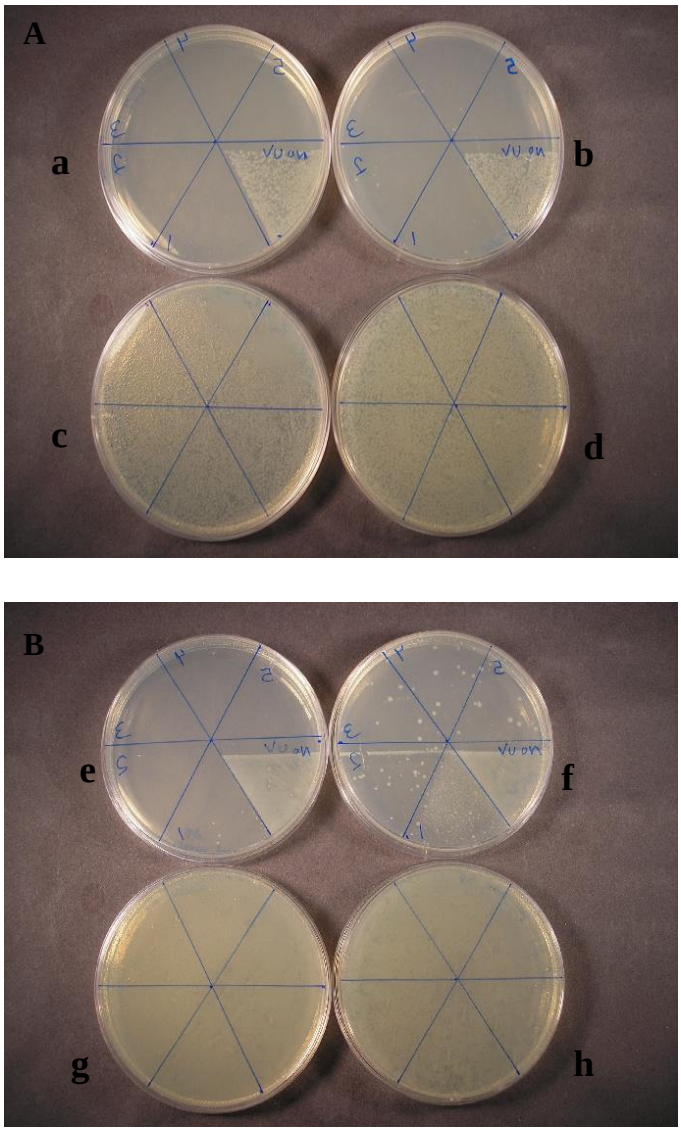

Figure 3.1: Functional activity of *S.solfataricus* photolyase *in vivo* (representative image based on 3 independent experiments)

Figure 3.1A: *E. coli* cells expressing E2 gene (controls) on kanamycin LB plates;
a – UV irradiated plate at five sectors for different time intervals from 1-5 min (25 cm distance) (kept in the dark);
b- UV irradiated plate at five sectors for different time intervals from 1-5 min (exposed to 30 min white light);
c- Control non UV irradiated (kept in the dark);
d- Control non UV irradiated (exposed to 30 minwhite light);

Figure 3.1B: *E. coli* cells expressing *S. solfataricus phr* gene on kanamycin LB plates;
e– UV irradiated plate at five sectors for different time intervals from 1-5 min (25 cm distance) (kept in the dark);
f- UV irradiated plate at five sectors for different time intervals from 1-5 min (exposed to 30 min white light);
g- Control non UV irradiated (kept in the dark);
h- Control non UV irradiated (exposed to 30 minwhite light);

cells were exposed to UV light at different time intervals in each sector, showed different results. In the plate (Fig 3.1B: e) that was exposed to UV light and kept in the dark, only three colonies were observed in the sector that was exposed to 1 minute UV light. This suggests that these cells were able to survive because of the nucleotide excision repair mechanism that works in the dark and was able to repair the damage at only lower dose of UV light. However, this mechanism in the dark was unable to repair the UV damage in cells that were exposed to higher UV dose. The other plate, Fig 3.1B: f, where cells were exposed to UV radiation and then illuminated with white light for 30 minutes, showed interesting results.

Colonies were observed in all five sectors that were exposed to UV light at different times, indicating tolerance up to 5min of UV radiation. This survival rate was decreasing with increasing UV light dose. In the sector that was exposed to 1 minute UV light, many colonies were observed but their number was lower than the grown cells in the non UV radiated sector. Since colonies were observed in all sectors of the white light exposed plate, this suggests that these cells have an active photolyase which uses the visible light to repair the UV damage and therefore the cells were able to survive. This experiment was repeated 3 times and the result was consistent.

Demonstration of functional activity of *S. solfataricus* photolyse (*In vitro*):

A new method was optimized to detect the activity of the photolyase *in vitro* as outlined in section 3.2. Commercial *E.coli* photolyase was initially used to optimise assay conditions. In Fig 3.2 A the activity of *E.coli* photolyase was detected and all upper bands represent the relaxed open plasmids whereas the lower bands represent the supercoiled plasmids. Lanes 1 and 2 are the control non UV irradiated plasmids. In lane 2, CPD-specific T4 endonuclease was added to check for any endogenous DNA damage. In both lanes, the results were similar and most of the plasmids were supercoiled (shown as two large lower bands). Moreover, this result was confirmed by measuring the intensity of the bands using LabWorks Image Acquisition and Analysis Software from UVP. In lanes 1 and 2, the ratio of the percentage intensity of the upper band to the lower band was 9 to 91 % and 10 to 90 % respectively. On the other hand, the plasmid in lane 3 was UV irradiated for 2 minutes and this irradiation induced the formation of pyrimidine dimers that, after addition of T4 endonuclease V, were recognized by the endonuclease resulting in cleavage of the plasmids at the site of damage.

Therefore, most of the damaged supercoiled plasmids were converted to a relaxed open form and this was clearly seen on the gel in lane 3 as a large upper band. This was also confirmed by measuring the percentage intensity of upper band to lower band which was 54 to 46 % respectively. However, in lane 4 the plasmid was UV irradiated for 2 minutes and 1µl E. coli photolyase (5.38 mg/ml) was added. As a consequence of addition of an active photolyase, most of the dimers induced by UV light were repaired following irradiation with white light. Therefore, most of the damaged plasmids were repaired before the addition of T4 endonuclease and once the endonuclease was added, only the remaining unrepaired damaged

plasmids (only few plasmids) were detected and cleaved. As a result of this cleavage, the few damaged plasmids converted to a relaxed open forms and this was clearly seen in lane 4. In this lane the upper band was smaller when compared with the upper damaged band in lane 3 indicating the repair by photolyase. In addition the percentage intensity of the upper band compared to the lower band in lane 4 was determined as 17 to 83 % respectively.

To get a confirmation of this result, this experiment was repeated 3 times and the results are represented in Fig 3.2 B.

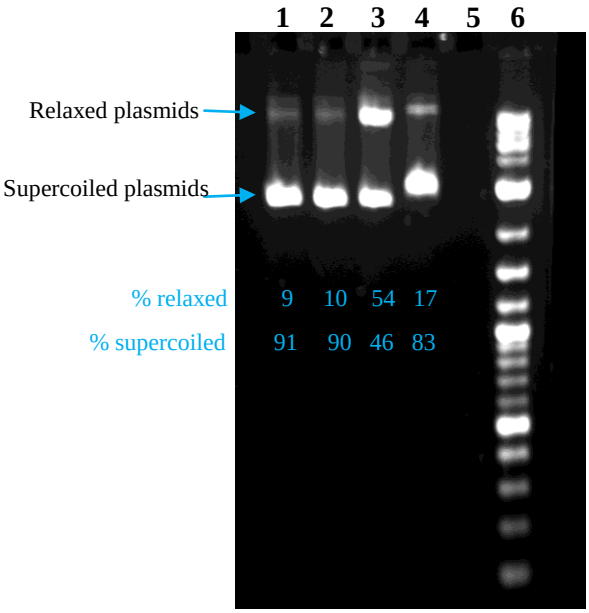

Figure 3.2 A: *E.coli* photolyase activity *in vitro* (representative image)

Lanes from left to right:
1-Non UV irrradiated plasmid;
2-Non UV irraradiated plasmid plus 1µl of 10U/µl T4- endonuclease V;
3- UV irradiated plasmid (2 min, 25 cm) plus 1µl of 10U/µl T4 endonuclease V (dark);
4- UV irradiated plasmid (2 min, 25 cm) plus 100 µM *E.coli* photolyase and 1h light exposure plus 1µl of 10U/µl T4 endonuclease V;
5- Blank;
6- 1kb DNA ladder;
Top arrow indicates relaxed open plasmid (damaged) and bottom arrow indicates supercoiled plasmid (un damaged).

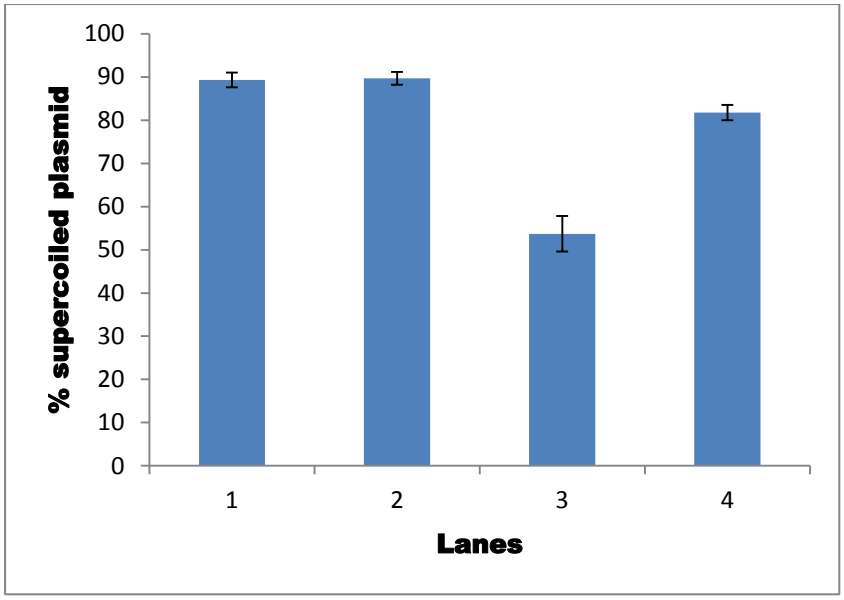

Figure 3.2B: *E.coli* photolyase activity *in vitro*

Lanes from left to right:
1- Non UV irradiated plasmid;
2- Non UV irradiated plasmid plus1µl of 10U/µl T4- endonuclease V;
3- UV irradiated plasmid (2 min, 25 cm) plus 1µl of 10U/µl T4 endonuclease V (dark);
4- UV irradiated plasmid (2 min, 25 cm) plus 100 µM *E.coli* photolyase and 1h light exposure plus 1µl of 10U/µl T4 endonuclease V;
Data represent Mean +/- SEM for 3 independent experiments.

It was observed from Fig 3.2 A, a different migration of the bottom band in lane 4, which represent the supercoiled plasmid. This difference in the migration of the supercoiled plasmids in lane 4 as compared with the migration of the supercoiled plasmids in the other lanes (1-3) was examined. A possibility that the binding of the enzyme to the DNA might be the reason, was tested and proved in Fig 3.2C. Different concentrations from *E. coli* photolyase was tested for their migration on the gel. Lanes 4-7 showed different migration of the bottom bands and it was oserved that the higher enzyme concentration (2-200 µM) the slower migration of the bands

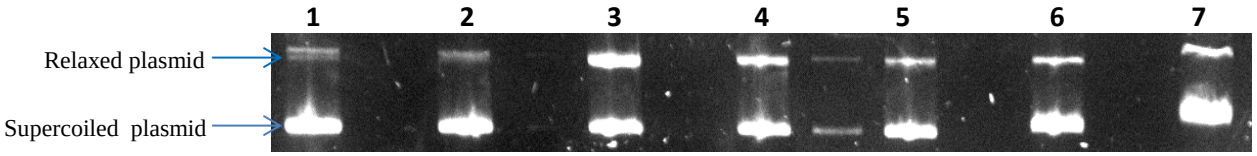

	1	2	3	4	5	6	7
% relaxed	14	13	44	41	22	24	26
% supercoiled	86	87	56	59	78	76	74

Figure 3.2C: *E. coli* photolyase activity *in vitro* troubleshooting

Lanes from left to right:
1- Non UV irradiated plasmid;
2- Non UV irradiated plasmid plus 1µl of 10U/µl T4- endonuclease V;
3- UV irradiated plasmid (2 min, 25 cm) plus 1µl of 10U/µl T4 endonuclease V;
4- UV irradiated plasmid (2 min, 25 cm) plus 2 µM *E.coli* photolyase and 1h light exposure plus 1µl of 10U/µl T4 endonuclease V;
5- UV irradiated plasmid (2 min, 25 cm) plus 20 µM *E.coli* photolyase and 1h light exposure plus 1µl of 10U/µl T4 endonuclease V;
6- UV irradiated plasmid (2 min, 25 cm) plus 100 µM *E.coli* photolyase and 1h light exposure plus 1µl of 10U/µl T4 endonuclease V;
7- UV irradiated plasmid (2 min, 25 cm) plus 200 µM *E.coli* photolyase and 1h light exposure plus 1µl of 10U/µl T4 endonuclease V;
Top arrow indicates relaxed open circular plasmid (damaged) and bottom arrow indicates supercoiled plasmid (un damaged).

Since the activity of *E.coli* photolyase was detected, this enzyme was used as a positive control for detecting the activity of *S. solfataricus* photolyase. In Figure 3.3, the first two lanes (from the left) were the control non UV irradiated plasmids, whereas the third lane represents the UV damaged plasmids (upper band). The intensity percentage of the upper bands to the lower bands in these three lanes was 9 to 91% in lane 1, 8 to 92% in lane 2, 40 to 60% in lane 3 respectively. Lane 4 represents the control *E.coli* photolyase which was added to the UV irradiated plasmid (40 µM). After the addition of T4 endonuclease V to the reactions represented in lane 2, 3, and 4, it was clear that the upper band in lane 4 was less intense than the upper band in lane 3 (which represents the UV damaged plasmids). This was confirmed by measuring the intensity percentage of the upper band in lane 4 which was 16% and that was clearly lower than the intensity percentage of the upper band in lane 3 (40%). This means that the *E.coli* photolyase was active and therefore was able to repair the damage. Lanes 5, 6, and 7 represent three different concentrations of the purified *S.solfataricus* photolyase (low, medium, and high respectively) which were added to the UV irradiated plasmids. The purified *S. solfataricus* photolyase concentration of 26 µM was used as a high concentration, whereas 20 µM and 10X dilution of that concentration (2 µM) were used as medium and low concentrations respectively. These different concentrations were used to test

which photolyase concentration is sufficient to detect the repair. After the addition of T4 endonuclease V to the reactions that are represented in lanes 5, 6 and 7, it was obvious from the figure that the lower concentration of *S. solfatarius* photolyase (lane 5) was unable to repair the UV damage. This was clear as the upper band in lane 5 (which represent the damage and has an intensity percentage of 56%) was not reduced as compared with the upper band in lane 3. However, both upper bands in lane 6 and 7 that represent medium and high concentrations of *S.solfatarius* photolyase respectively, showed smaller bands as compared with the upper band in lane 3. This was confirmed as the percentage of the intensity of these two upper bands was 20% and 16% respectively and these percentages were clearly lower when compared with the 40% damaged plasmids in lane 3. This indicates that at these concentrations of photolyase we were able to detect the repair in UV damaged plasmids. This experiment was repeated also 3 times and the average data is shown in Fig 3.4.

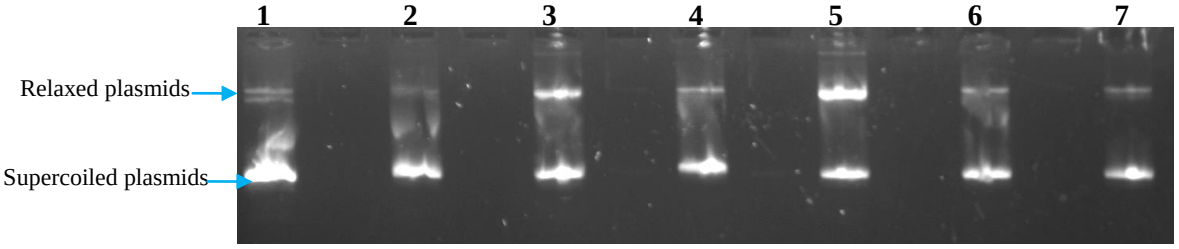

% relaxed	9	8	40	16	56	20	16
% supercoiled	91	92	60	84	44	80	84

Figure 3.3: *S.solfatarticus* photolyase activity *in vitro* (representative image)

Lanes from left to right:
1- Non UV irradiated plasmid;
2- Non UV irradiated plasmid plus 1µl of 10U/µl T4- endonuclease V;
3- UV irradiated plasmid (2 min, 25 cm) plus 1µl of 10U/µl T4 endonuclease V;
4- UV irradiated plasmid (2 min, 25 cm) plus 40 µM *E.coli* photolyase and 1h light exposure plus 1µl of 10U/µl T4 endonuclease V;
5- UV irradiated plasmid (2 min, 25 cm) plus low concentration of *S.solfataricus* photolyase (2µM) and 1h light exposure plus 1µl of 10U/µl T4 endonuclease V;
6- UV irradiated plasmid (2 min, 25 cm) plus medium concentration of *S.solfataricus* photolyase (20µM) and 1h light exposure plus 1µl of 10U/µl T4 endonuclease V;
7- UV irradiated plasmid (2 min, 25 cm) plus high concentration of *S.solfataricus* photolyase (26µM) and 1h light exposure plus 1µl of 10U/µl T4 endonuclease V;
Top arrow indicates relaxed open circular plasmid (damaged) and bottom arrow indicates supercoiled plasmid (un damaged).

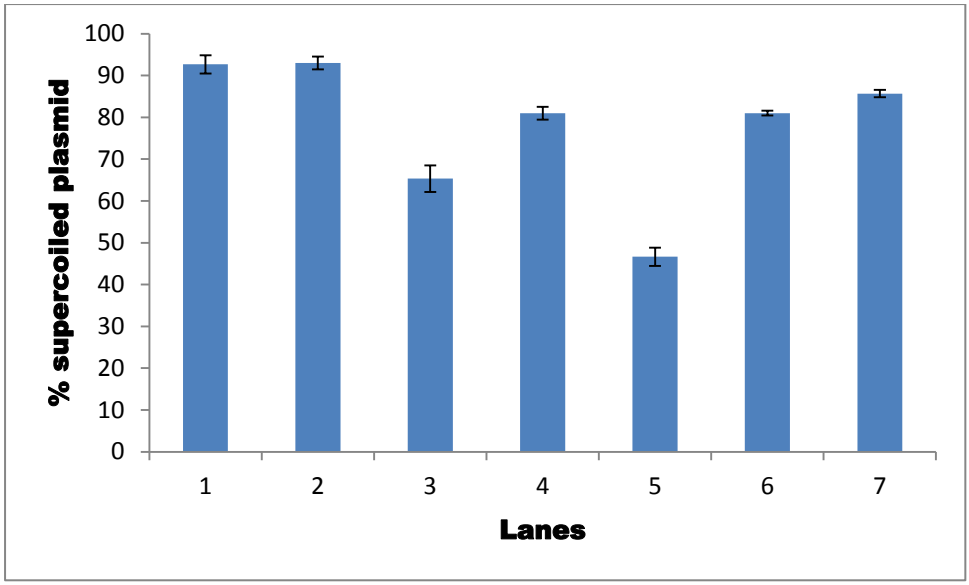

Figure 3.4: *S.solfatarticus* photolyase activity *in vitro* (3 independent experiments)

Lanes from left to right:

1- Non UV irradiated plasmid;
2- Non UV irradiated plasmid plus 1µl of 10U/µl T4 endonuclease V;
3- UV irradiated plasmid (2 min, 25 cm) plus 1µl of 10U/µl T4 endonuclease V;
4- UV irradiated plasmid (2 min, 25 cm) plus 40 µM *E.coli* photolyase and 1h light exposure plus 1µl of 10U/µl T4 endonuclease V;
5- UV irradiated plasmid (2 min, 25 cm) plus low concentration of *S.solfataricus* photolyase (2µM) and 1h light exposure plus 1µl of 10U/µl T4 endonuclease V;
6- UV irradiated plasmid (2 min, 25 cm) plus medium concentration of *S.solfataricus* photolyase (20µM) and 1h light exposure plus 1µl of 10U/µl T4 endonuclease V;
7- UV irradiated plasmid (2 min, 25 cm) plus high concentration of *S.solfataricus* photolyase (26µM) plus 1µl of 10U/µl T4 endonuclease V;
Data represent Mean +/- SEM for 3 independent experiments.

3.4 Discussion

In this chapter, the *S. solfataricus* photolyase has been shown to be active as a photoreactive enzyme in repairing UV- induced DNA lesions. This photoreactivity was detected using both *in vivo* and *in vitro* assays, as the activity was only seen when the enzyme was exposed to visible light.

The measurement of the intensity of UV lamp output in J/m^2 was difficult to achieve because the instrument required to measure it was not available. Therefore we decided to depend on a time scale (min) as the UV dose measurement. It is known that this is not accurate because the UV lamp output is changing overtime. However, there was no other option and thus the measurement of UV dose was rely on the period of UV treatment (min). At this stage of my study, it is too difficult to give an estimate of the UV intensity (J/m^2) used in this project as no one in the lab has measured that before and therefore, no value can be use to build up an estimate of UV intensity.

In vivo detection of *S. solfataricus* photolyase activity has proved the photoreactivation activity of this enzyme. As shown in Fig 3.1B (f), cells illuminated with white light were found to be more UV resistant and were able to survive as compared with those in the dark. This finding was similar to a study done by Kato *et al* on a thermophilic bacterium (Kato *et al.* 1997), in which a photoreactivation activity of *Thermus thermophilus* photolyase was detected *in vivo*. In their study, they used a wild type of *T.thermophilus* strain and found that the UV survival rate of this strain was higher in the illuminated cells with visible light as compared with the cells kept in the dark.

At lower UV doses of 1 min in the dark plate, a small percentage of transformed *E.coli* cells with *phr* gene survived Fig 3.1 B plate (e), suggesting that at lower UV doses, the amount of UV lesions induced was low and therefore it was possible to be repaired by NER mechanism. It also suggests that NER mechanism was stimulated in repairing the UV lesions in the dark. However, this finding was not observed in plate (a) from figure 3.1A, in which the cells were transformed with E2 gene and treated similarly. From these findings, a question raises: why was the NER stimulated in the dark in repairing UV lesions in cells expressing *phr* gene but not from the cells expressing E2 gene.

The answer to this question was reported in other studies (Yamamoto *et al.* 1983; Sancar and Smith 1989; Ozer *et al.* 1995), where it was shown that photolyase can participate in the

stimulation of NER in the absence of light. These studies were done based upon the fact that photolyase binds to pyrimidine dimers even in the absence of photoreactivation light. Therefore, they suggested that there might be another role for photolyase in addition to photoreactivation and their study proved the other function of the enzyme.

In addition, an *in vitro* assay was developed and carried out in the lab to clarify whether the purified *S. solfataricus* photolyase has a photoreactivation activity. The assay was first established and validated using commercially-available *E. coli* photolyase. It was then used to demonstrate photolyase activity of the expressed *S. solfataricus* enzyme. This method depends on measuring the intensity of the agarose gel bands for both supercoiled undamaged plasmids and for relaxed open damaged plasmids, as their movement on the gel is different. By measuring the percentage of the damaged to undamaged plasmids, the photoreactivation activity of photolyase was detected.

In Fig 3.2 A, the functional activity of *E. coli* photolyase as a photoreactive enzyme in repairing UV lesions was detected and it was also observed a different migration of the band that represent the supercoiled plasmid when the *E. coli* enzyme was added (lane 4). It was speculated that the enzyme might bond to the DNA molecules and therefore makes The DNA more heavier and as a result, its migration on the gel became more slower. This hypothesis was tested and the troubleshooting that was done in Fig 3.2C proved that this hypothesis was correct. The addition of different enzyme concentrations (2, 20, 100 and 200 μM) to the DNA showed different migration of the bands (lanes 4-7, respectively). With increasing concentration of the enzyme, the bands movement on the gel became slower and that was observed as the bands were shifted up gradualy with increasing the concentration.

Two studies by Jiang *et al.* and Thoma have proved the success of this method in detecting the repair mechanism of other photolyases (Jiang *et al.* 2007; Thoma 1999).

These results confirm the photoreactivation activity of both *E.coli* and *S. solfataricus* photolyases in repairing UV lesions. The next question was which photolyase is more active in repairing UV damage, the *E.coli* or *S.solfataricus* photolyase? It was planned to do an experiment using the same concentrations of the enzymes from both organisms and compare the repair percentage after white light illumination. However, at this stage in the project the *E.coli* photolyase was no longer available commercially thereby halting any further investigation into this question.

However, it seems that *S.solfataricus* photolyase is more active in repairing pyrimidine dimers as compared with *E.coli* photolyase. This conclusion was based on the result that was shown in figure 3.4, lane 4 and lane 6 which represent the repair by *E. coli* and *S. solfataricus* photolyases respectively. Using 40 µM and 20 µM concentrations from both *E. coli* and *S. solfataricus* photolyases respectively, shows the same repair percentage. This means that just 1/2 of *S.solfataricus* photolyase was able to show the repair of UV damage as compared with *E. coli* photolyase.

The activity of *S. tokodaii* photolyase was demonstrated *in vitro* by using oligo $(dT)_{18}$ to measure the difference in the absorption between thymine dimers (T<>T) and monomers (T-T) at 265 nm ($A\varepsilon=[\varepsilon(T-T)- \varepsilon(T<>T)]=19{,}000\ M^{-1}\ cm^{-1}$ (Fujihashi *et al*. 2007). 46 µM oligo $(dT)_{18}$ was UV-irradiated and was mixed with 20nM of *S. tokodaii* photolyase (Fujihashi *et al*. 2007). This mixture was incubated at room temperature in the dark and under whitle light illumination (Fujihashi *et al*. 2007). The result demonstrated that photolyase was able to repair the (T<>T) after exposure to white light and was compared with the mixture in the dark as well as a non-photolyase containing mixture (Fujihashi *et al*. 2007).

Chapter 4: Characterisation of optimum temperature of *S. solfataricus* photolyase

4.1 Introduction

After demonstrating a functional activity of *S. solfataricus* photolyase in repairing UV lesions both *in vivo* and *in vitro*, enzyme optimum temperature and some other properties were investigated.

Enzymes from *E.coli* tend to have an optimum temperature around 37 ºC, while enzymes from hyperthermophiles like some microorganisms that able to live in volcanic hot springs and hydrothermal vents have higher optimal temperatures above 80 ºC. this variation in optimal temperatures from both organisms corresponds to their growth temperatures in nature.

The higher the temperature the higher the kinetic energy of the reactants. This will allow the reactants to collide to each other and invrease the chance for the reaction to occur. Therefore, with increasing temperature the reaction rate will increase until it reaches to a point where the enzyme denature and loss its activity.

In this chapter, the temperature dependence on the activity of the enzyme was examined to see if it has any significant influence on the total repair efficiency. This was done by comparing the percentage of photoreactivation repair of this enzyme at each specific temperature. Therefore, by measuring the percentage enzyme repair at different temperatures, it was possible to characterise the optimum temperature for the activity of the enzyme.

4.2 Materials and Methods

Materials:

All materials used in this chapter were the same materials described in Chapter 3 section 3.2, plus 3-[4-(2-Hydroxyethyl)-1-piperazinyl]propanesulfonic acid **(**EPPS) that was obtained from Sigma-Aldrich, Poole, UK. Ethylene diamine tetra acetic acid (EDTA) was obtained from Acros Organics (Geel, Belgium). Sodium dihydrogen orthophosphate (NaH_2PO_4) and di-sodium hydrogen orthophosphate (Na_2HPO_4) were obtained from Fisher Scientific (Loughborough, UK). White light exposure was conducted using a LightCraft, twin daylight fluorescent tube, 2 X 15w of 45cm)

Methods

a. Optimise the concentration of *S. solfataricus* photolyase that shows highest repair

S. solfataricus photolyase was expressed, purified and dialyzed exactly as described in chapter 2.

The method used here and its principle were described previously in section 3.2 in the *in vitro* characterisation of photoreactivation activity of *S. solfataricus* photolyase. However, 1 µl of *S. solfataricus* photolyase was added at different concentrations from 1.2 µM -20 µM.

b. Optimise the white light dose

Following the *in vitro* protocol of detecting the activity of *S. solfataricus* photolyase, the exposure to white light was for 1h. In order to characterise the optimum temperatur of this enzyme, the enzyme had to be treated at different temperatures in the PCR and simultaneously exposed to white light. This was difficult to achieve, since placing the tubes in the PCR at different temperatures and exposing to white light at the same time while the tube lid was opened, might cause some evaporation. Therefore, it was planned to reduce white light exposure time and an optimisation of exposure time was done.

The protocol was followed exactly the same, but with different doses of white light (2, 3, 5, 10, 30 and 60 min).

c. Optimise the right buffer for the temperature dependent assays

Since the *E. coli* buffer that was supplied by TREVIGEN was 10X reaction buffer 14, this buffer was Tris buffer and according to the protocol, the enzyme was diluted in this buffer (1X reaction buffer 14). Hovever, this buffer is not suitable to use in the optimum temperature assay because it has very high degree of temperature sensitivity. Therefore, the pH value of Tris buffer will change as a result of temperature change.

Hence, other buffers like phosphate buffer and EPPS buffer were tried using two different recipes. Phosphate buffer a (12.5 mM Na_2HPO_4, 12.5 mM NaH_2PO_4, 1mM EDTA, 0.1mM DTT and 100 mM NaCl, pH 7.8) and phosphate buffer b (10 mM Na_2HPO_4, 10 mM NaH_2PO_4, 1mM EDTA, 1mM DTT and 50 mM NaCl, pH 7.8). For EPPS buffer, also two recipes were used and both EPPS buffers a and b were made exactly the same as phosphate buffer a and b respectively. However, the phosphates in phosphate buffer were replaced with 25 and 20 mM EPPS in buffer a and b respectively. The *S.solfataricus* photolyase was diluted in these buffers and the reaction mixture 2 was also prepared using these two buffers.

d. Optimum temperature assay for *S. solfataricus* photolyase

The protocol followed was the same as described previously in section 3.2 in the *in vitro* detection of *Sulfolobus* photolyase activity. However, the *S.solfataricus* photolyase was diluted to 7.7 µM in phosphate buffer b and 20 µl of the diluted enzyme was preheated at 80 ºC for 3 min. 19 µl of reaction mixture 2 was added into 0.2 ml PCR tube using phosphate buffer b and placed in the PCR at different tested temperatures ranging from 40-99 ºC, and then 1 µl from the preheated enzyme was added to each PCR tube at specific temperature. The addition of the enzyme to all tubes were done simultaneously with white light illumination and (tubes lid was off). All tubes were covered with cling film to prevent evaporation and to allow the illumination with white light at the same time. The incubation was done for 2 min at each specific temperature. Then T4 endonuclease V was added and tubes were incubated in the incubator at 37 ºC for 1h.

4.3 Results

a. Concentration of *S. solfataricus* photolyase that shows highest repair

Different concentrations of the purified *S. solfataricus* photolyase were tested in order to determine the optimum concentration of the enzyme that showed efficient repair.

Several dilutions of the purified enzyme were made in 1X reaction buffer 14 from 1.2 - 20 µM. In Figure 4.1 (a), all upper bands represent the relaxed open plasmids whereas the lower bands represent the supercoiled plasmids. Lanes 1 and 2 are the control non UV irradiated plasmids. In lane 2, CPD-specific T4 endonuclease V was added to check if there is any endogenous DNA damage. In both lanes, the results were nearly similar and most of the plasmids were supercoiled (shown as two large lower bands). Moreover, this visual result was confirmed by measuring the intensity of the bands using LabWorks Image Acquisition and Analysis Software from UVP. In lanes 1 and 2, the ratio of the percentage intensity of the upper band to the lower band was 12 to 88 % and 10 to 90 % respectively. On the other hand, the plasmid in lane 4 was UV irradiated for 2 minutes and this irradiation induced the formation of pyrimidine dimers that, after addition of T4 endonuclease V, were recognized by the endonuclease resulting in cleavage of the plasmids at the site of damage.

Therefore, most of the damaged supercoiled plasmids were converted to a relaxed open form and this was clearly seen on the gel in lane 4 as a large upper band. This was also confirmed by measuring the percentage intensity of upper band to lower band which was 50 % to 50 %. However, in lanes 6-11 the plasmid was UV irradiated for 2 minutes and different concentrations of the purified photolyase were added (1.2, 1.5, 3, 6, 12 and 20 µM) respectively.

As shown in Fig 4.1 (a), highest repair was detected in Lanes 10 and 11, because it showed lower intensity as compared with the intensity of other upper bands (6-9). Moreover, the comparison was also made between the upper band in lane 4 (which represent the total damaged plasmids without photolyase) and the rest of upper bands in lanes (6-11) which represent the repair of UV damage using different enzyme concentrations. The percentage intensity of the upper bands in lane 10 and 11 is 30 % and 29 % respectively which is the lowest as compared with the percentage intensity of the upper bands in lanes (4, 6, 7, 8 and

9). This indicates that using 12 or 20 µM from the enzyme is showing the highest repair in this experiment.

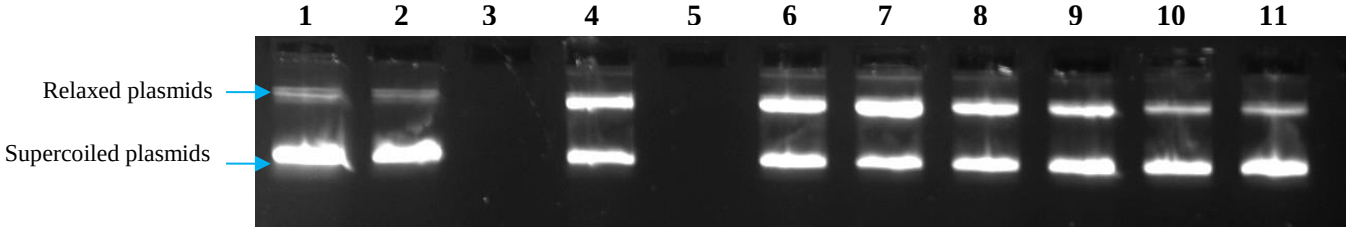

	1	2	3	4	5	6	7	8	9	10	11
% relaxed	12	10		50		51	56	48	46	30	29
% supercoiled	88	90		50		49	44	52	54	70	71

Figure 4.1 (a): Optimise the concentration of *S. solfataricus* photolyase

Lanes from left to right:
1- Non UV radiated plasmid;
2- Non UV radiated plasmid plus T4- endonuclease V;
3- Empty;
4- UV radiated plasmid plus T4 endonuclease V;
5- Empty;
6- UV radiated plasmid plus 1.2 µM of *S.solfataricus* photolyase plus T4 endonuclease V;
7- UV radiated plasmid plus 1.5 µM of *S.solfataricus* photolyase plus T4 endonuclease V;
8- UV radiated plasmid plus 3 µM of *S.solfataricus* photolyase plus T4 endonuclease V;
9- UV radiated plasmid plus 6 µM of *S.solfataricus* photolyase plus T4 endonuclease V;
10- UV radiated plasmid plus 12 µM of *S.solfataricus* photolyase plus T4 endonuclease V;
11- UV radiated plasmid plus 20 µM of *S.solfataricus* photolyase plus T4 endonuclease V;

In figure 4.1 (b), further dilutions from the *S. solfataricus* photolyase were made below 12 µM (6.6, 7.7, 8.8 and 10 µM represented in lanes 7, 9, 11 and 13, respectively). Lanes 1, 3 and 5 were the controls as described previously in figure 4.1 (a). Figure 4.1 (b) also shows that the last 3 lanes, which represents the repair of UV damage by different enzyme concentrations 7.7, 8.8 and 10 µM, showed a similar repair. The percentage intensity of the upper bands in these three lanes were 31, 30 and 32 % respectively and these percentages are lower than the same bands in lanes 5 and 7.

Therefore, based on these results the *S. solfataricus* photolyase concentration that was used in the optimum temperature assay was 7.7 µM.

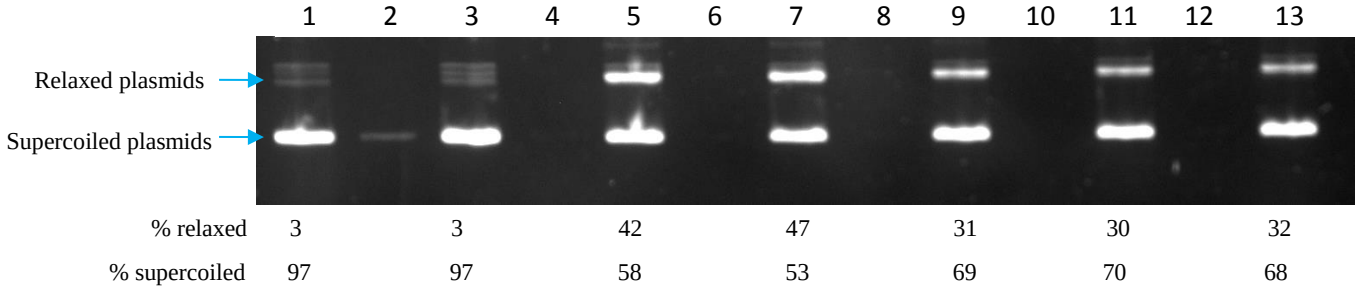

Figure 4.1 (b): Optimise the right concentration of *S. solfataricus* photolyase

Lanes from left to right:
1- Non UV radiated plasmid;
2- Empty
3- Non UV radiated plasmid plus T4- endonuclease V;
4- Empty;
5- UV radiated plasmid plus T4 endonuclease V;
6- Empty;
7- UV radiated plasmid plus 6.6 µM of *S.solfataricus* photolyase plus T4 endonuclease V;
8- Empty;
9- UV radiated plasmid plus 7.7 µM of *S.solfataricus* photolyase plus T4 endonuclease V;
10- Empty;
11- UV radiated plasmid plus 8.8 µM of *S.solfataricus* photolyase plus T4 endonuclease V;
12-Empty;
13- UV radiated plasmid plus 10 µM of *S.solfataricus* photolyase plus T4 endonuclease V;

b. Optimal white light exposure time

In order to reduce the white light exposure time in this *in vitro* assay to reduce the evaporation, this experiment was done using different times of white light illumination.

In Figure 4.2, the first 3 lanes were the controls as described previously in section 4.3 (a). Lanes 4-9 represent the repair by *S. solfataricus* photolyase using 7.7 µM at different white light exposure time (2, 3, 5, 10, 30 and 60 min) respectively. The repair by photolyase was seen in all tested time points and as low as 2 min. This was clear as the percentage intensity of the upper bands in all tested lanes (4-9) was lower than the upper band in lane 3 (which represent the total damage without photolyase repair). Therefore, 2 min white light exposure was used in the optimum temperature and thermostability assays.

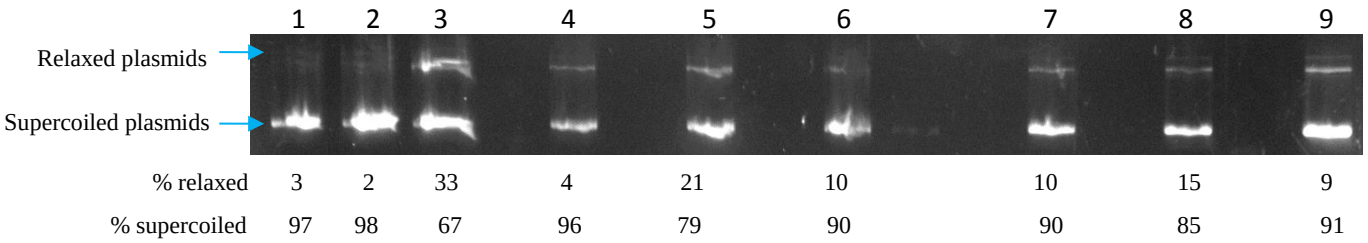

Figure 4.2: Optimise the white light exposure time

Lanes from left to right:
1- Non UV radiated plasmid;
2- Non UV radiated plasmid plus T4- endonuclease V;
3- UV radiated plasmid plus T4 endonuclease V;
4- UV radiated plasmid plus 7.7 µM of *S.solfataricus* photolyase plus T4 endonuclease V plus 2 min white light exposure;
5- UV radiated plasmid plus 7.7 µM of *S.solfataricus* photolyase plus T4 endonuclease V plus 3 min white light exposure;
6- UV radiated plasmid plus 7.7 µM of *S.solfataricus* photolyase plus T4 endonuclease V plus 5 min white light exposure;
7- UV radiated plasmid plus 7.7 µM of *S.solfataricus* photolyase plus T4 endonuclease V plus 10 min white light exposure;
8- UV radiated plasmid plus 7.7 µM of *S.solfataricus* photolyase plus T4 endonuclease V plus 30 min white light exposure;
9- UV radiated plasmid plus 7.7 µM of *S.solfataricus* photolyase plus T4 endonuclease V plus 60 min white light exposure;

c. Optimal buffer for the temperature dependent assays

Different buffers were tested to identify buffers that showed a high enzyme repair as compared with the recommended Tris buffer (according to TREVIGEN) that was used in this assay. In Figure 4.3, the first three lanes (1, 2 and 4) were the same controls as described in section 4.3 (a). Lanes 5 and 6 shows the repair of UV damage when the enzyme was diluted to 7.7 µM in two different EPPS buffer preparations (a and b) respectively. The percentage intensity of the upper bands in lanes 5 and 6 was 40 and 42 % respectively. This percentage represents the relaxed damaged plasmids and was almost close to the percentage intensity of the upper band in lane 4 (41 %) which represents the actual UV damage without photolyase. This means that EPPS buffer was not suitable to detect the functional activity of the enzyme *in vitro*.

However, lanes 7 and 8 represent the repair of UV damage using diluted enzyme in 1X Tris buffer and in Milliq H_2O respectively. The result in Fig 4.3 indicate that the repair of UV

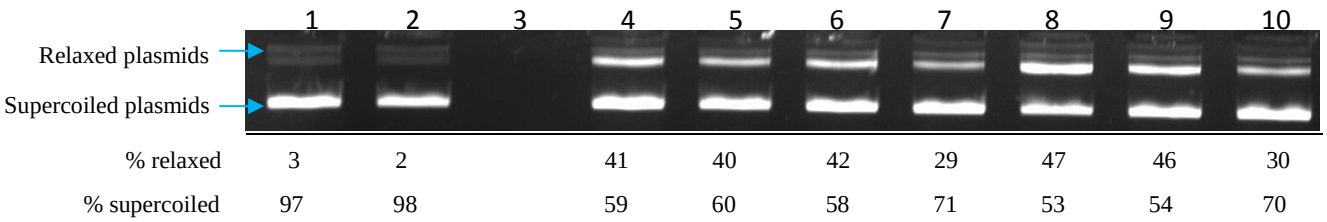

Figure 4.3: Optimise the right buffer

Lanes from left to right:
1- Non UV radiated plasmid;
2- Non UV radiated plasmid plus T4- endonuclease V;
3- Empty
4- UV radiated plasmid plus T4 endonuclease V;
5- UV radiated plasmid plus 7.7 µM of *S.solfataricus* photolyase diluted in EPPS buffer (a) plus T4 endonuclease V;
6- UV radiated plasmid plus 7.7 µM of *S.solfataricus* photolyase diluted in EPPS buffer (b) plus T4 endonuclease V;
7- UV radiated plasmid plus 7.7 µM of *S.solfataricus* photolyase diluted in 1X Tris buffer plus T4 endonuclease V;
8- UV radiated plasmid plus 7.7 µM of *S.solfataricus* photolyase diluted in Milliq H_2O plus T4 endonuclease V;
9- UV radiated plasmid plus 7.7 µM of *S.solfataricus* photolyase diluted in phosphate buffer (a) plus T4 endonuclease V;
10- UV radiated plasmid plus 7.7 µM of *S.solfataricus* photolyase diluted in phosphate buffer (b) plus T4 endonuclease V;

damage by phr was highest in lane 7 (the enzyme diluted in 1X Tris buffer), as the percentage intensity of the upper band was 29 %. This comparison was made with the upper band in lane 4 that represent the actual UV damage without photolyase and its percentage intensity was 41 %. This was expected as the photolyase in lane 7 was diluted in 1X Tris buffer which was the recommended buffer for photolyase. However, dilution of the enzyme in H_2O as represented in lane 8 was not showing any functional activity as the percentage intensity of the upper band in this lane was 47 % which was higher than 41 % (the total represented damage in lane 4 without photolyase).

The UV damage repair by diluted photolyase in phosphate buffer a and b are shown in lanes 9 and 10 respectively. It was obvious from Fig 4.3 that the highest repair was seen when the enzyme was diluted in 1X Tris buffer (lane 7) and phosphate buffer b (lane 10), as the

percentage intensity of the upper bands in these two lanes was nearly similar (29% and 30% respectively). Therefore, based on this results it was clear that phosphate buffer b was suitable for this *in vitro* assay as a replacement for Tris buffer in order to characterise the optimum temperature assay for *S. solfataricus* photolyase.

d. Optimal temperature for *S. solfataricus* photolyase

In order to characterize the optimum temperature for the activity of *S. solfataricus* photolyase, the enzyme (7.7 µM) was assayed at different temperatures from 40-99 ºC. Initially, the enzyme was showing two optimum temperatures that gives the highest activity of the enzyme in repairing UV damage, one at 50 ºC and the other was at 90 ºC. This result was observed from three independent experiments Fig 4.4A. However, after pre-heating the enzyme at 80 ºC for 3 min followed by assays at different temperatures, only one optimum temperature was observed and this showed the highest enzyme activity of *S. solfataricus* photolyase was at 90 ºC. This was expected as this temperature corresponds to optimum growth temperature for *S. solfataricus*. Fig 4.4B shows the optimum temperature curve from the average of three experiments.

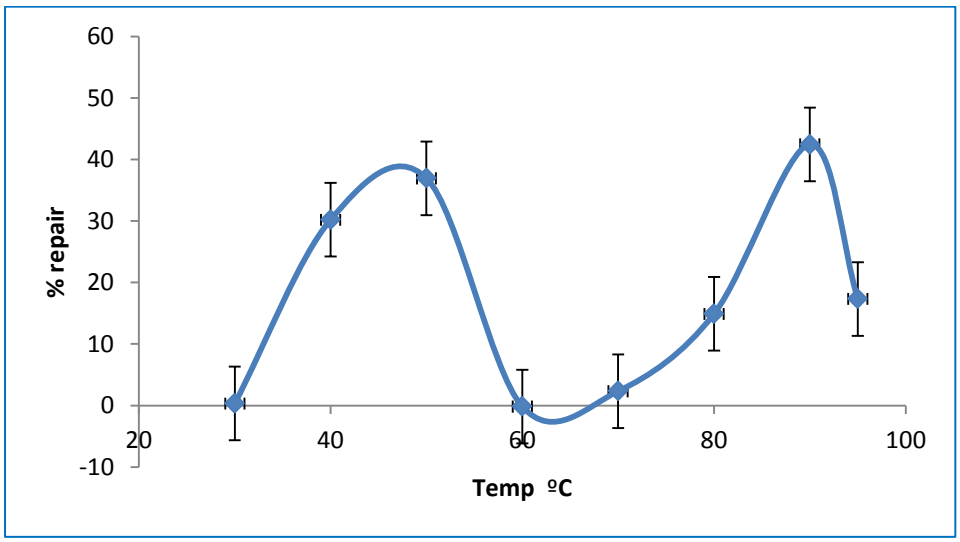

Fig 4.4A Two optimum temperature peaks were observed initially

7.7 µM of *S.solfataricus* photolyase was assayed at different temperatures from 30-95 ºC for 2 min simultaneously with white light illumination. It showed two peakes at 50 ºC and at 90 ºC.

Data repreaents mean +/- SEM from 3 independent experiments.

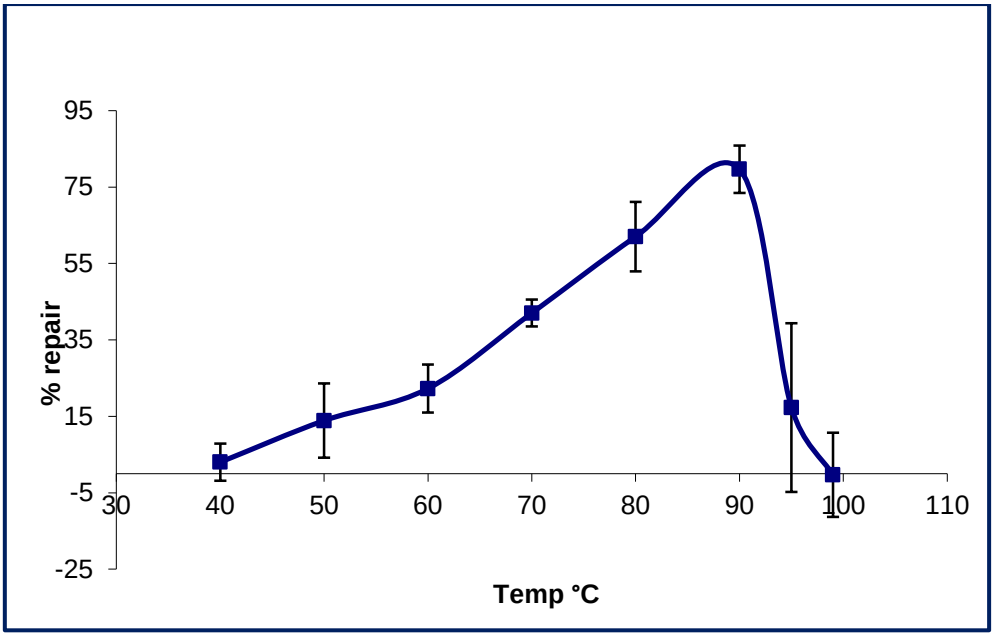

Figure 4.4 B: Characterisation of optimum temperature for the activity of *S. solfataricus* photolyase

7.7 µM of *S.solfataricus* photolyase was preheated at 80 ºC for 3 min and then the enzyme was assayed at different temperatures from 40-99 ºC for 2 min simultaneously with white light illumination.

Data repreaents mean +/- SEM from 3 independent experiments.

The percentage repair of UV damage by *S. solfataricus* photolyase was calculated as:

$$\% \text{ repair} = \frac{\% \text{ intensity of S.P at each temperature} - \% \text{ intensity of S.P of total damage}}{\% \text{ intensity of S.P for undamaged} - \% \text{ intensity of S.P of total damage}}$$

S.P = supercoiled plasmid

The intensity of the bands (determined by *in vitro* assay) which was measured by LabWorks Image Acquisition and Analysis Software, was used to calculate the percent repaie of *S. solfataricus* photolyase at each temperature and these values were used to plot the graph for the photolyase optimum temperature.

4.4 Discussion

S. solfataricus is a hyperthermophilic archaea and therefore it can grow at very high temperature environments in a range of 55-90°C. Hence, enzymes from this organism are thermostable and can function at very high temperatures. In this chapter, the effect of temperature on the functional activity of *S. solfataricus* photolyase was investigated.

In order to characterise the optimum temperature for the activity of *S. solfataricus* photolyase, several points were taken into consideration.

Firstly, the exact enzyme concentration that showed highest repair efficiency had to be specified. This is because any extra units from the enzyme have no additional effect on enzyme activity. From the results, 7.7 µM of *S.solfataricus* photolyase was specified as the right enzyme concentration that showed efficient repair.

Secondly, the white light exposure time had to be optimised and reduced, because according to the protocol that was supplied by TREVIGEN on characterizing the activity of *E. coli* photolyase *in vitro,* the illumination with white light was for 1h. This was difficult to apply on the temperature dependent assays because the tubes lid had to be opened for heat treatments and white light illumination simultaneously. This will cause evaporation of the reaction and changes the concentration of the enzyme. Therefore, several time points (less than 1h) of white light illumination were tested for efficient photorepair.

According to the results in Fig 4.2, all tested time points showed photorepair as compared with the total damage without photolyase. Hence, 2 min white light exposure was enough for the *in vitro* photorepair assay. In fact, this result was consistenct with one reported study (Saxena *et al.* 2004), in which they found the repair by photolyase was ultrafast and can occur in femtosecond.

Thirdly, the buffer was optimised for determination of the optimum temperature of *S. solfataricus* photolyase. Tris buffer that was originally used in this *in vitro* assay was not suitable to be used in these temperature dependent assays; because the pH of this buffer changes with temperature change and this could affect the activity of the enzyme. This is because any changes in the pH could induce changes in the enzyme active site and can lead to activity loss and or enzyme denaturation.

From the results in Fig 4.3 we found phosphate buffer (b) was suitable to be used in this *in vitro* assay as the highest photolyase activity was seen when the enzyme was diluted in this buffer. In addition, this finding was similar to the study that was done on *S. tokodaii* photolyase (Fujihashi *et al.* 2007), in which the buffer that they used for the purified enzyme was sodium phosphate (pH 8.0).

The results in Fig 4.4A, showed to optimum temperature peaks for the activity of the purified photolyase enzyme one at 50 ºC and the other at 90 ºC when the enzyme was assayed at different temperatures from 30-95 ºC. The explanation of this initial observation of the optimal temperature for *S. solfataricus* photolyase was the possibility of the presence of two forms from the purified enzyme. One form was not folded correctly and was the reason for the peak at 50 ºC and another form that was folded correctly and gave the peak at 90 ºC. Therefore, in order to get rid of the non-correct form of the enzyme, the photolyase from *S. solfataricus* was preheated at 80 ºC for 3 min and as a result of that only one optimum temperature peak at 90 ºC was observed.

Previous reports found that photorepair of CPDs was temperature sensitive in cucumber cotyledons (Takeuchi *et al.* 1996) and in Arabidopsis (Pang and Hays 1991). In the present study, the result is in agreement with these previous studies, in which the repair of pyrimidine dimers by *S. solfataricus* photolyase was temperature dependent and was increasing with increasing temperature from 40-90^{o}C, then after 90^{o}C the activity of the enzyme dropped down and the enzyme started to denature. As seen in Fig 4.4B, the optimum temperature for the activity of *S. solfataricus* photolyase was 90^{o}C which corresponds to the growth temperature of *S. solfataricus* in nature.

Chapter 5: Transfection and expression of *S. solfataricus* photolyase in mammalian cells

5.1 Introduction

Photolyases have been found in all species ranging from bacteria to non-placental mammals. However, the genes encoding photolyases have been lost through evolution among all placental mammals, including humans. The role of photolyases in repairing UV-induced DNA damage makes it an interesting target for expression in human skin fibroblasts. Previous studies have attempted to express photolyases from different organisms in mammalian cells and investigated their functional activity in repairing UV-induced DNA damage. This includes the expression of photolyases from *Potorous tridactylus* (Rat kangaroo) (Chigancas *et al.* 2000), *E. coli* (Sutherland and Hausrath 1980), *Anacystis nidulans* (Stege *et al.* 2000) and yeast (*Saccharomyces cerevisiae*) (Roza *et al.* 1990).

All above studies demonstrated an effective repair of UV-induced DNA damage after the expression of photolyases followed by illumination with white light.

To our knowledge, this is the first study conducted to investigate the expression of an archaeal photolyase (*S. solfataricus*) in human cells. Eukaryotic and archaeal systems share DNA information pathways (DNA replication, recombination and transcription) and DNA repair systems (Olsen and Woese 1996; Londei 2005; Aravind *et al.* 1999; Kelman and White 2005). *S. solfataricus* is a hyperthermophilic archaea that grows at very high temperatures, from 55-90 ºC. The expression of *S. solfataricus* photolyase at 37 ºC in *E. coli* cells showed a functionally expressed enzyme which repaired UV-induced DNA damage. This chapter discusses the expression of *S. solfataricus* photolyase in human cervical carcinoma cells (HeLa) that are deficient in photolyase expression. A recombinant mammalian expression vector containing a photolyase-DsRed fusion protein was generated. pDsRed-Monomer-N1 is a mammalian expression vector (Appendix 5) that encodes DsRed-Monomer, a red fluorescent protein containing forty-five amino acids, that can be detected by fluorescent microscopy when expressed in mammalian cells.

In this study, transient transfection was chosen because in this type of transfection, the transfected DNA's will not be integrated into the nuclear genome permanently and therefore

the effects of the introduced DNA will last for only a short period of time. Hence, it was sufficient for the photorepair assay as the introduced DNA's were tested for protein expression after 24-72h and then the photoreactivation assay was done. Moreover, transient transfection is simpler and takes less time to obtain results plus gives higher efficiency.

There are many types of transfection methods and each method has its own advantages and disadvantages. Lipofection is the most common chemical method used in research (Schenborn and Goiffon 2000). Its principle is simple; it involves the delivery of liposome-based gene by interaction between the positively charged chemicals (i.g cationic lipids, calcium phosphate etc.) and negatively charged DNA. This complex then binds to the cell membrane and delivers the genetic material inside the cell by endocytosis or phagocytosis. Lipofection transfection method was chosen to deliver the recombinant photolyase-pDsRed-Monomer because it is an easy method and gives high transfection efficiency as well.

To evaluate the functional expression of photolyases, photorepair assay was conducted on the transfected HeLa cells with the recombinant plasmids and the viability of UV-treated cells following white light illumination was estimated using MTT viability test. The MTT assay is one of the simplest methods used as an indicator of cell damage and cell viability. It uses 3-[4, 5-dimethylthiazol-2-y]-2, 5-diphenyltetrazolium bromide, which is a water soluble yellow dye that is taken up by viable cells only and reduced by active mitochondrial dehydrogenases. The product formed by this active enzyme is a water-insoluble blue formazan, which is then dissolved by ethanol or propanol to produce a blue colour that can be used for colourimetric measurement.

This chapter will cover the cloning of photolyases from three different organisms, *S. solfataricus, Potorus triductylus* (Rat Kangaroo) and *E. coli* in a mammalian expression vector and our attempt in transfection of these constructs into HeLa cells. Rat kangaroo and *E.coli* photolyases were used as controls for expression of *S. solfataricus* photolyase because it was reported that these two enzymes can be expressed in mammalian cells (Chigancas *et al.* 2000; Sutherland and Hausrath 1980). Functional expression of these enzymes was evaluated using a photorepair assay.

5.2 Materials & Methods

Materials:

All materials used for cloning of *phr* genes were obtained as outlined previously in chapter 2. pDsRed-Monomer was purchased from Clontech, USA.

1X TrypLE Express, advanced DMEM/F12 with reduced serum medium (1:1), 100X Glutamine and penicillin streptomycin (P/S) were all obtained from GIBCO, Paisley, UK. Isopropanol was purchased from Fisher Scientific, Loughborough, UK.

HeLa cells were kindly donated by Dr. Jim Caunt, University of Bath, UK. The plasmid pcDNA3.1 with GFP tag was kindly donated by Prof. David Tosh, University of Bath, UK.

CRL 1360 cell line was obtained from ATCC, Middlesex, UK.

(3-[4, 5-dimethylthiazol-2-y]-2, 5-diphenyltetrazolium bromide) MTT, Trypan Blue and fetal bovine serum (FBS) were all purchased from Sigma Chemical Company, Poole, UK. DreamFect (DF) transfection reagent and pVectOZ-GFP plasmid were obtained from OZ Biosciences (Marseille cedex, France)

Methods:

Cloning of *S. solfataricus,* Rat Kangaroo and *E. coli phr* into a mammalian expression vector.

Two controls were used for this purpose and were cloned exactly the same as the cloning of *S. solfataricus phr*. These two controls were Rat kangaroo (*Potorous triductylus*) *phr* and *E. coli phr*.

The cloning of the three *phr* constructs were following the same procedure that was explained previously in chapter 2 section 2.2 for the cloning of *S. solfataricus* photolyase.

Briefly, the three genes were PCR amplified using specifically designed primers that were sharing homology at the start and the end of each gene. The primers were designed with a restriction site incorporated in both forward and revers primers. The restriction sites were chosen according to the Restriction Mapper website based on choosing the non-cutter enzymes for the whole gene.

A nuclear localization sequence (NLS) was also added upstream in the forward primer for each gene. This is because this sequence is important to translocate the protein inside the nucleus as it is a DNA binding protein and therefore the protein will be expressed in its target location. The sequence of this NLS that was added upstream of each gene was determined according to a previous reported study (Gassman *et al.* 2011). This study was on identifying a three amino acid NLS sequence at the N-terminal region of human mismatch repair proteins (MSH6) which was found to be conserved in higher eukaryotic species (Gassman *et al.* 2011).

The shortest identified NLS sequence from that previous study was chosen to be added upstream of *phr* genes in the forward primers and this sequence is KRK. The names and primer sequences for each gene can be found in the appendix 7.

Moreover, the reverse primers were designed with sharing homology at the end of each gene and upstream of the stop codon that was present at the end of the genes. The exclusion of the stop codons when the reverse primers were designed was very important because the plan was to clone the three *phr* genes into the mammalian expression vector (pDsRed-Monomer-N1) as fusions to the N-terminus of DsRed-Monomer protein. DsRed-Monomer in this vector is used as a fusion tag. Genes cloned into the multiple cloning site (MCS) are expressed as fusions to the N-terminus of DsRed-Monomer if they are in the same reading frame and there are no intervening stop codons. The expression of the fusion protein is derived by CMV promoter. The recombinant vector can be transfected into mammalian cells using any standard transfection method.

DNA templates used for the amplification of those three *phr* genes were *S. sofataricuse phr*-pET28a, Rat kangaroo *phr*-PCY4B (kindly donated from Prof. Carlos Menck, University of São Paulo) and *E. coli* K12 plasmid for *S. solfataricus*, Rat kangaroo (RK) and *E. coli* respectively. Cycling instructions for PCR, gel purifications of the bands, A-tailing, ligation into pGEM-T, ethanol precipitation and transformation into JM109 was similar as described in chapter 2. Also plasmids miniprep, digestion of the *phr* genes from pGEM-T vector, digestion of the pDsRed-Monomer-N1, ligation and checking the genes sequence was followed as described previously in chapter 2.

The three constructs of *phr* genes from the three organisms were cloned successfully into the mammalian expression vector (pDsRed-Monomer-N1) and were ready for transfection into human cells. The sequence of these genes with the addition of NLS upstream of each gene

and the elimination of stop codons at the end of each gene was verified in both pGEM-T and pDsRed- Monomer vectors.

Characterisation of UV sensitivity in HeLa cells

HeLa cells were grown in 90cm tissue culture petriplates (Fisher Scientific, UK) in a humidified 37°C multigas incubator with 5% CO_2/95% air in DMEM/F12 (Reduced Serum) medium supplemented with 2% FBS, 1% glutamine and 1% penicillin/streptomycin. When the cells reached to about 80% confluence, they were trypsnized first for 2-5 minutes at 37ºC until cells were detached from the plate. Then 10 ml of fresh medium was added to the cells in the plate to deactivate the trypsin and cells were harvested by centrifugation at 1500 rpm for 5 min. Supernatant was removed and cells were resuspended in fresh 5 ml medium. In order to characterize the UV sensitivity of HeLa cells, Cells were plated at a density of $5x10^4$/well in 4 flat bottom 96 well Costar plates, tissue culture treated (Sigma Company, Poole, UK) and left over night for cell adhesion in the humidified 37°C multigas incubator with 5% CO_2/95% air. The medium used was DMEM/F12 serum-free medium with 1% Glutamine and 1% P/S.

Next day cells were exposed to UV light (254 nm, 6 W at a distance of 25cm.) at room temperature (18-20 ºC) for different time intervals (0.5, 1, 2, 3, 4, 5, 6, 8, and 12 min).

A positive control was used by adding 10% dimethyl sulfoxide (DMSO) to one column (11) (because DMSO is a very well-known cytotoxic reagent if used at higher concentration like 10%) and negative control was cells only without UV light (column 12).

After UV irradiation the four plates were kept in the same incubator at 37°C and each plate was left for different recovery times of 19, 24, 48 and 72h before the cell viability test (MTT assay) was done. Figure 5.2 shows the different doses of UV light which HeLa cells were exposed to in each column of the 96 well plate.

MTT (1mg/ml) in DMEM/F12 medium was prepared fresh. 50ul MTT was added to cells in each well and the four plates were placed in the incubator at 37°C for 60 min. When the cells turned blue under microscope, MTT was removed and 50ul isopropanol was added to each well in the plates and the absorbance was measured at 560 nm using a plate reader. This

experiment was repeated 4 times and the absorbance average for each condition was calculated.

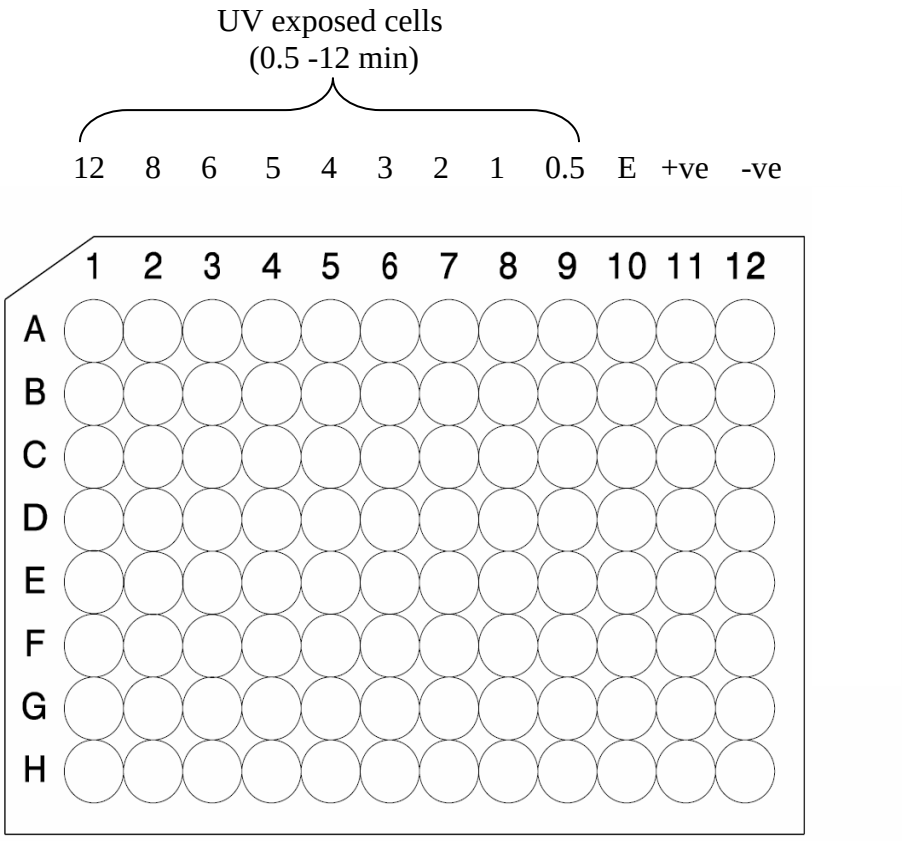

Figure 5.2 Characterisation of UV sensitivity in HeLa cells

Different UV exposure time in HeLa cells illustrated in each column of 96 well plate (1-9 column), each exposure time is indicated above each column. E is empty column, +ve is the positive control (DMSO) and –ve is the negative control (no UV radiation).

Transfection of *phr* constructs into HeLa cells

Cells were split into a Costar 96 well plate at a density of $2x10^4$ cell/well in DMEM/F12 medium supplemented with 1% Glutamine and 1% FBS but without antibiotic. The exclusion of antibiotics from the medium during transfection has been reported to enhance the levels of gene expression (DreamFect instruction manual). Cells were left overnight in the humidified multigas incubator with 5% CO_2/95% air at 37°C. Next day, and before transfection, the medium was changed to serum free medium with glutamine only (to increase the efficiency of transfection). Medium was warmed (without serum and antibiotic) first and the DF reagent plus the DNA were left out in room temperatures for 30 min before the transfection. Medium was added first to all 1.5 ml microcentrifuge tubes and then DF plus DNA stock solutions

were aliquoted directly into the medium. DNA solutions were prepared in which 0.4 µg of each plasmid (RKphr, S.Sphr and Ecoliphr constructs plus pDsRed-Monomer vector only) was diluted in 25 µl of culture medium without serum and antibiotics. DF solutions were prepared in which 0.8 µl of DF was diluted in 25 µl of culture medium without serum and antibiotics. The two solutions were combined together within 5 min and incubated at room temperature for 15-20 min. 50 µl/well of the complex (DNA plus DF) was added to cells in the 96-well plate and incubated at 37 °C in the humidified multigas incubator with 5% CO_2/95% air. Medium was changed after 3-4h to serum free medium (toxicity was observed when the complex was left 24h post-transfection). Cells were placed again in the same incubator and the protein expression (red fluorescence) was monitored after 24 and 48h.

Trypan Blue exclusion test

50 µl of 1% Trypan Blue was added to 500 µl medium/well in 24 well plate and incubated for 5 min at room temperature. Cells were screened under a light microscope at a lens magnification of 20X and 40X.

Photorepair assay in HeLa cells

The transfection of the three *phr* constructs in HeLa cells was done as described previously in two 96 well plates (dark and light plates) and the expression of the proteins was checked after 48h. Cell medium in both plates was changed before UV radiation Two sets of transfection were prepared in each plate (UV radiated and non UV radiated sets). Each set includes the transfection of the three *phr* constructs and the pDsRed-Monomer (vector only) plus the un transfected cells. UV irradiation was done for 4 min in uncovered sets from both plates (half of the plates and the other half was covered). After UV radiation, one plate was exposed to white light for 30 min (cover on to prevent any extra exposure of UV light from white light exposure (Chu 1965) and the distance was 25 cm. The other dark plate was covered with foil and the two plates were then incubated in the humidified incubator at 37 °C.

After 24h UV recovery, viability of the cells was measured using the MTT assay (50 µl MTT at 1mg/ml in medium). After approximately 45 min incubation at 37ºC, the MTT solution was removed completely and 50 µl isopropanol was added to solubilise the formazan crystals and the absorbance was measured at 560nm in plate reader.

5.3 Results

Cloning of the three *phr* genes in mammalian expression vector

S. solfataricus phr gene was amplified for cloning into pGEM-T vector (initially) using two primers. The forward primer (SSphr-stopforNheI) has a NheI restriction site (G*CTAGC) and a melting temperature of 73.54°C, whereas the reverse primer (SSphr-stoprevKpnI) has a KpnI restriction site (GGTAC*C) with a melting temperature of 70.11°C.

Rat kangaroo and *E. coli phr* genes were also amplified (controls) for cloning into pGEM-T vector using two primers for each gene. The forward primers were (RK-stopforNheI) and (Ecoli-stopforSacI) with NheI and SacI (GAGCT*C) restriction sites plus melting temperatures of 75.06°C and 76.47°C for the Rat kangaroo and *E. coli phr* genes respectively.

The reverse primers for the above two genes were (RK-stoprevSacI) and (Ecoli-stoprevKpnI) with SacI and KpnI restriction sites respectively. Both revers primers had 75.78°C and 76.06°C melting temperatures for the Rat kangaroo and *E. coli phr* genes respectively.

All the six primer sequences for the three genes are found in the Appendix 7.

The PCR amplification and the cycling instructions for all three genes were exactly the same as described previously in chapter 2 section 2. As seen in Fig 5.3 from the PCR products, lanes 2 and 4 are showing a single band that represent the amplification of Rat kangaroo and *S. solfataricus phr* genes respectively. The sizes of these single bands corresponds to the right gene size of both Rat kangaroo and *S. solfataricus phr* genes, which is 1.59 kb and 1.3 kb, respectively.

On the other hand, the amplification of the *E. coli phr* gene (lane 3) showed multiple bands. Optimisation of PCR cycling was not successful. The second band in lane 3 representing the correct amplicon size for *E.coli phr* (1.4 kb.) was excised and all three bands for the *phr* genes of three different organisms were excised from the gel and purified as outlined before in chapter 2.

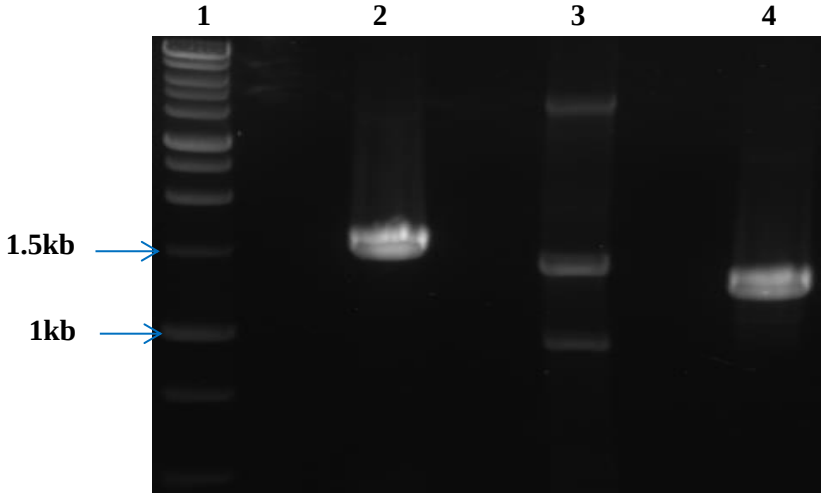

Figure 5.3: PCR amplified products for the three *phr* genes in GC buffer

Lanes from left to right: 1- 1kb DNA ladder; 2- RK *phr* gene amplicon;3- *E. coli phr* gene amplicon; 4- *S. solfataricus phr* gene amplicon;
Blue arrows indicate two band sizes of 1 kb DNA ladder;

After gel purification of these three *phr* genes, A-tailing, cloning into pGEM-T vector, transformation into JM109 electrocompetent cells and plating the cells on carbenicillin LB plates were carried out as described previously in chapter 2 section 2.

The results of transformation of the three *phr* gene constructs in pGEM-T vector showed many white and blue colonies of nearly similar proportion. White colonies represent successful transformants and were checked for having the right gene inserts by double digests of the purified miniprep plasmids from overnight cultures as outlined before. Figure 5.4a shows the result of double digests of three constructs of RK *phr*- pGEM-T using NheI and SacI restrictions enzymes. It was obvious from this result that the digestion of two constructs in lane 2 and 3 gave the right size of the RK *phr* gene insert which is 1.59Kb (lower bands), but the digestion of the construct in lane 4 showed no inserted gene. Therefore, the lower bands that represent the RK *phr* genes in lane 2 and 3 were excised from the gel and purified as outlined previously. The minipreps that represent these two purified *phr* genes were then sent for sequencing.

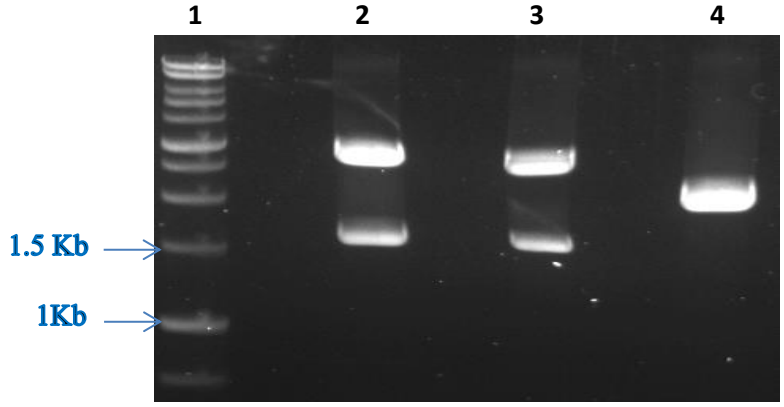

Figure 5.4a: Double digests of RK*phr*-pGEM-T vector

Lanes from left to right:
1- 1Kb DNA ladder;
2-4 Double digested plasmids of 3 white colonies;
Blue arrows indicate two band sizes of 1 kb DNA ladder;

The result of double digests of *S. solfataricus* and *E. coli phr* constructs in pGEM-T are shown in fig 5.4b. As seen from this figure, the digestion of 5 white colonies from *E. coli phr* constructs in pGEM-T gave the right gene insert from only two digested plasmids represented in the lower bands of lane 4 and 5 with the right gene size of 1.4 Kb. However, the digestion of *S. solfataricus phr* from 5 white colonies showed the right size of gene insert from all plasmids (lower bands in lanes 7-11) with the *phr* gene size of 1.3 Kb. Upper bands represent the digestion of pGEM-T vector (3 Kb). The digestion of these two *phr* genes from the vector were done using (NheI and KpnI, SacI and KpnI) for *S. solfataaricus* and *E. coli phr* constructs in pGEM-T respectively. Therefore, the lower bands in lane 4 and 5 plus 7 and 8 were excised from the gel and purified in order to send them for sequencing. The sequence of these selected purified bands was checked, aligned (as outlined previously in chapter 2) and confirmed as having the right *phr* gene sequence for all three organisms.

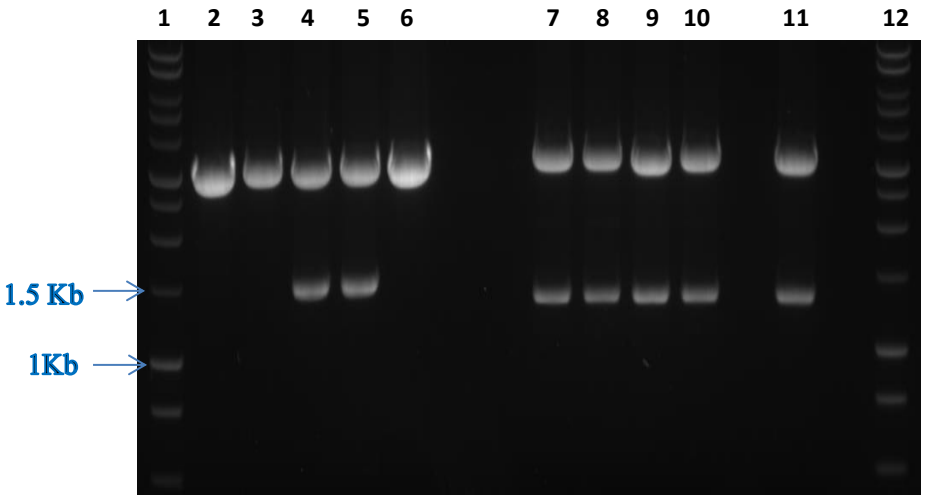

Figure 5.4b: Double digests of *E.coliphr*-pGEM-T and *S.s phr*-pGEM-T vectors

Lanes from left to right:
1- 1Kb DNA ladder;
2-6 Double digested plasmids of 5 white colonies of *E. coli-phr*-pGEM-T;
7-11 Double digested plasmids of 5 white colonies of *S.s-phr*-pGEM-T;
12-1Kb DNA ladder;
Blue arrows indicate two band sizes of 1 kb DNA ladder;

The purified bands that gave the correct gene sequence from each *phr* gene of the three organisms was used for insertion into a mammalian expression vector, pDsRed-Monomer. Digestion of this vector was done using restriction enzymes that corresponded to the original incorporated restriction sites during primers design for each *phr* gene. The three *phr* genes from the three different organisms were digested from pGEM-T vector and then ligated into a digested pDsRed-Monomer for each specific gene. Digestions and ligations were done exactly as described previously in chapter 2. The ligated *phr* genes in pDsRed-Monomer were transformed into JM109 cloning strain to be able to digest the constructs and check the presence of right gene size and sequence. After the transformation, cells were plated on kanamycin LB plates and colonies were observed. 4 colonies from each *phr* construct were

selected for plasmid digestion in order to check the presence of the right inserted *phr* gene for S.s, RK and *E. coli*.

Figure 5.5a shows the result of digestion of RK-pDsRed-Monomer and S.s-pDsRed-Monomer. Lanes from 2-5 represent the digestion of 4 miniprep colonies of RK-pDsRed-Monomer and it was clear from this result that all lower bands in these lanes showed the presence of RK *phr* insert with the right gene size of 1.59 Kb. However, the digestion of 4 colonies from S.s-pDsRed-Monomer (lanes 6-9) showed only two lower bands with the correct gene size (1.3 Kb) in lane 7and 9. All upper bands in this figure represent the digested pDsRed-Monomer (4.7 Kb).

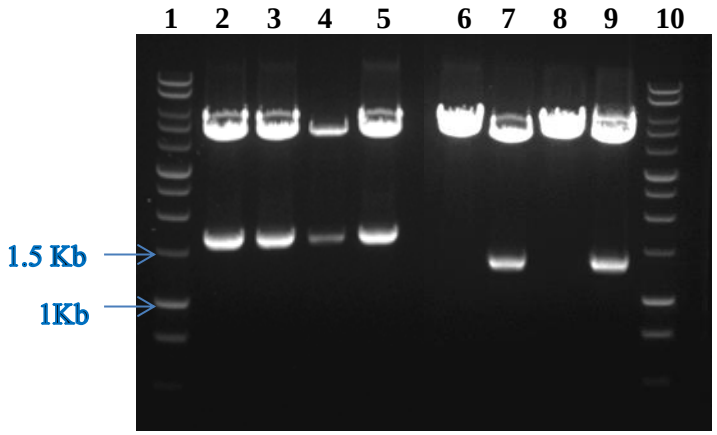

Figure 5.5a: Double digests of RK*phr*-pDsRed and S.s*phr*-pDsRed Monomers

Lanes from left to right:

1- 1 Kb DNA ladder;
2-5 Double digested plasmids from 4 colonies of RK*phr*-pDsRed-Monomer;
6-9 Double digested plasmids from 4 colonies of S.s*phr*-pDsRed-Monomer;
10- 1 Kb DNA ladder;
Blue arrows indicate two band sizes of 1 kb DNA ladder;

The result in Fig 5.5b shows the digestion of *E. coli phr*-pDsRed-Monomer from also 4 miniprep colonies (lanes 2-5) and was obvious that the *E.coli phr* insert was found in the lower bands of 3 constructs (lanes 2-4) because it gave the right gene size of 1.4 Kb. All upper bands in this figure represent the digested pDsRed-Monomer.

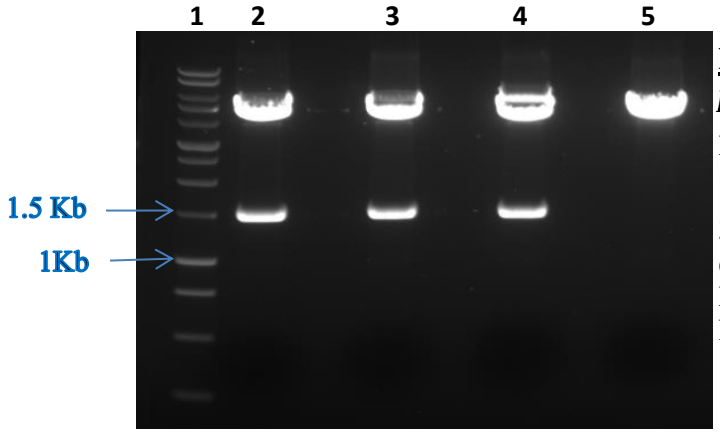

Figure 5.5b: Double digests of *E. coli phr*-pDsRed-Monomer

Lanes from left to right:

1- 1 Kb DNA ladder;
2-5 Double digested plasmids from 4 colonies of E. coli *phr*-pDsRed-Monomer;
Blue arrows indicate two band sizes of 1 kb DNA ladder;

The sequence of these digested *phr* gene inserts from the three organisms was checked again and confirmed for having the right gene sequence using CMV IE primer for single read. This confirmed the addition of NLS sequence upstream the *phr* genes

Also the reverse primers for each gene were used to sequence the end of *phr* genes and to confirm the removal of the stop codon from each gene.

The three *phr* genes from the three organisms were cloned successfully in a mammalian expression vector and were ready to use for transfection in human cells.

Characterisation of UV sensitivity in HeLa cells

HeLa cells were split into four 96 well plates and exposed to different doses of UV light. Each plate was left in the incubator for different UV recovery times (19-72h). Cell viability was measured using MTT assay and the percentage viability of the cells at each UV dose was calculated against non-UV radiated controls. Figure 5.6a shows the average percent viability of HeLa cells at different UV doses (1-12 min) from 3 independent experiments 48h post-UV radiation. Recovery from UV light (19, 24, 48 and 72h) did not vary and hence the 48hr recovery time is shown in Fig 5.6a. Hela cells showed a high sensitivity to UV at all tested UV doses with the percent viability dropping down to 45% (data not shown) and below, after 1 min UV dose and remained below that percentage viability at all higher UV doses. Also, the sensitivity was nearly similar in all tested UV recovery times.

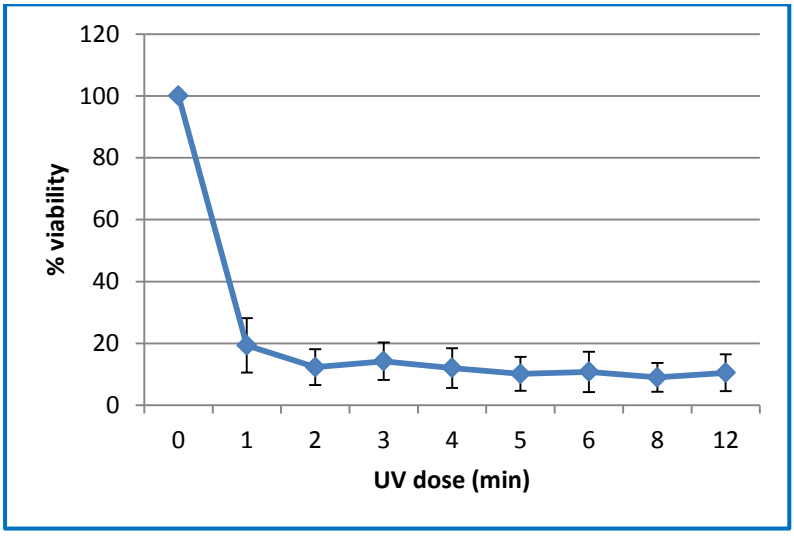

Figure 5.6a: UV sensitivity in HeLa cells at different UV doses

Percent viability of HeLa cells 48h post-UV radiation was plotted vs. different UV doses (1-12min). Data represents the mean +/-SEM from 3 independent experiments, with each experiment containing 4 replicates.

Figure 5.6b shows the effect of varying recovery times (19-72h). After two UV doses of 4 and 8 min on sensitivity to UV radiation in HeLa cells, the percent viability of the cells with both UV doses did not vary significantly at all the recovery times.

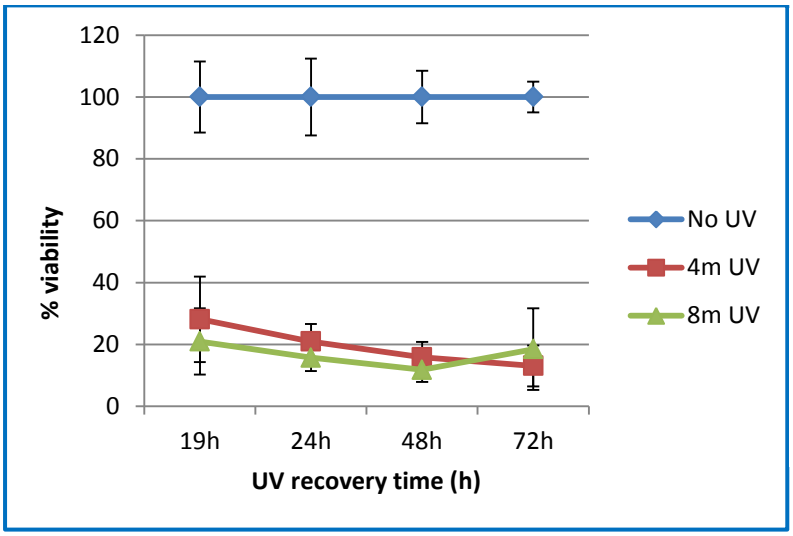

Figure 5.6b: UV sensitivity in HeLa cells at different UV recovery time

Percent viability of HeLa cells was plotted vs. different UV recovery time (19-72h). Data represents Mean +/- SEM from 3 independent experiments, each containing 4 replicates

Therefore, 4 min UV dose and 24h UV recovery time were chosen in performing the photorepair assay in HeLa cells.

Another cell line (CRL1360), which is NER deficient cells from Xeroderma pigmentosum patiants, was also tested for their UV sensitivity Fig 5.6c, because they lack both NER and photoreactivation repair mechanisms. It was obvious from Fig 5.6c that the CRL 1360 cells were not UV sensitive as expexted, because their cell viability remained high, 24 post-UV treatment at all tested UV doses (2-16 min).

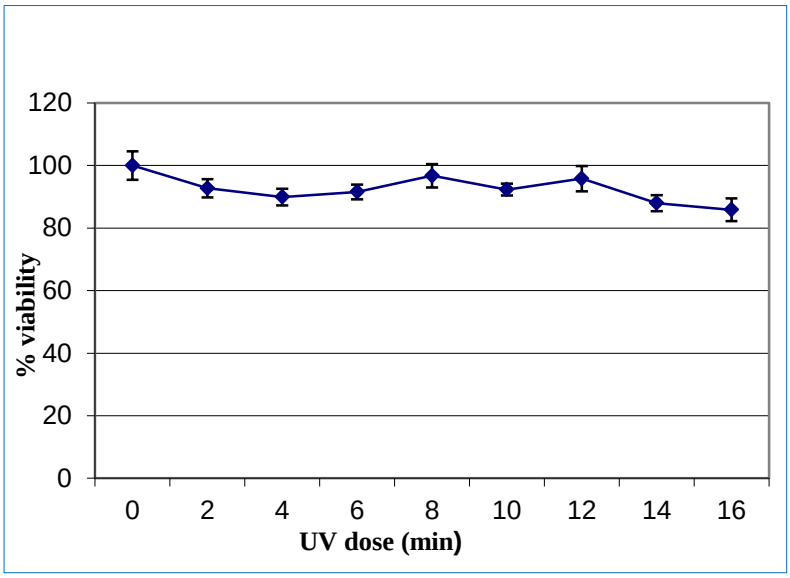

Fig 5.6c UV sensitivity for CRL1360 cells at different UV doses

Percent viability of CRL 1360 cells 24h post-UV radiation was plotted vs. different UV doses (2-16 min). Data represents the mean +/-SEM from 3 independent experiments, with each experiment containing 4 replicates

Transfection of 3 *phr* constructs into HeLa cells

The first trial on optimisation of high transfection efficiency was done in Costar 96 well plates using pcDNA1.3-GFP and pDsRed-Monomer vector only controls.

The cells were split at a density of 2 x 10^4 (DreamFect instruction manual) in DMEM/F12 supplemented with 2% FBS and 1% of glutamine without P/S. The expression of these two plasmids was very low as the green and red fluorescent from pcDNA1.3 and pDsRed-Monomer respectively was seen in only few cells (1-2). Figure 5.7a shows low transfection efficiency in HeLa cells for both above plasmids after 48h.

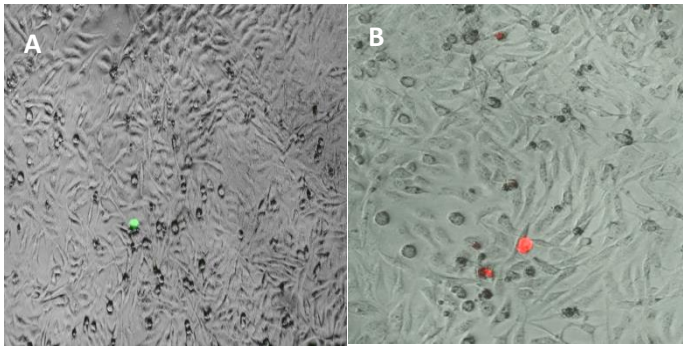

Figure 5.7a: Expression of pcDNA1.3-GFP and pDsRed-Monomer vectors in HeLa cells

Overlay images from florescent microscope at 4x magnification 48h post transfection;

A- GFP expression from pcDNA3.1;
B- RFP expression from pDsRed-Monomer;

This low transfection efficiency in Hela cells was unexpected because according to DreamFect manual instruction, the transfection efficiency in HeLa cells using DreamFect reagent was 70-80%. Dreamfect company plasmid (pVect-OZ) with GFP tag was then used as a control and the reagent was left to reach to the ambient temperature. In addition, two ratios of DF (µl)/DNA (µg) (recommended 2/1 or 4/1 respectively) with different DNA concentrations from (0.125- 2µg) and different DF volumes from (0.25-8µl) were used, resulting in an increased transfection efficiency of 40-45 %. Figure 5.7b shows that the expression of pDsRed-Monomer increased with increasing DNA concentration and DF volume. The highest transfection efficiency was seen in the highest DNA concentration and highest DF volume from both ratios (2µg DNA with 4 or 8µl DF).

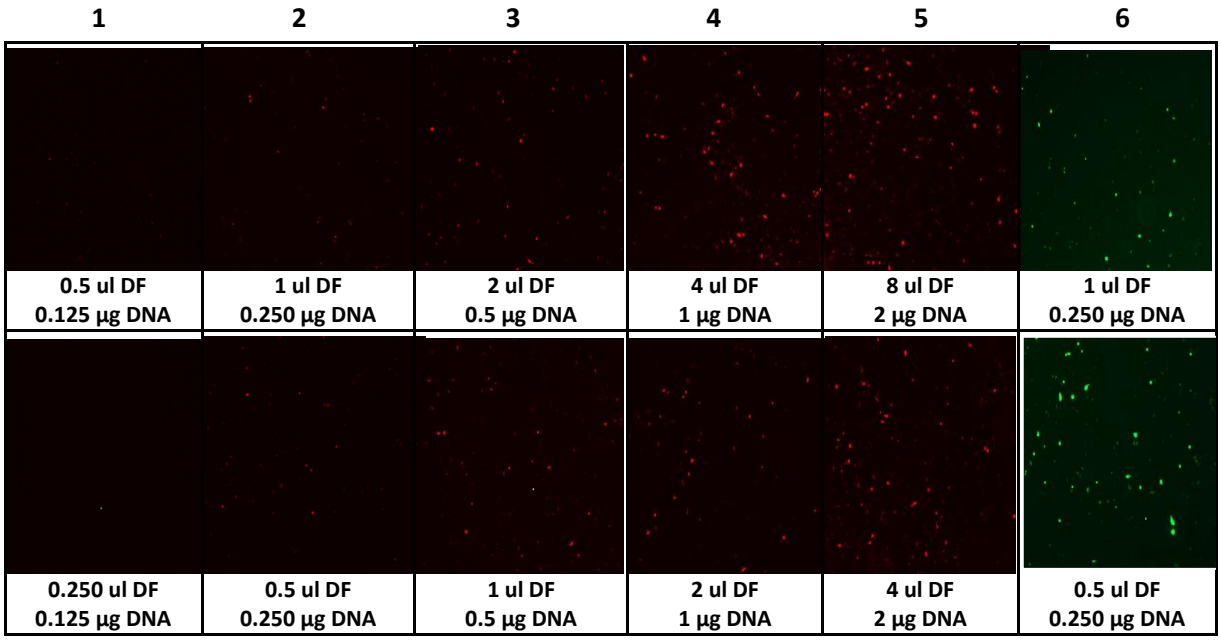

Figure 5.7 b: Expression of pDsRed-Monomer and pVect-OZ vectors in HeLa cells 24h post-transfection

RFP and GFP images from fluorescent microscopy at 4x magnification for pDsRed and pVect-OZ respectively;

Columns from left to right:

1-5 Expression of pDsRed-Monomer using different DNA concentrations and DF volumes at ¼ ratio (top row) and ½ (bottom row) for DNA/DF respectively;

6- Expression of pVect-OZ vector using one selected DNA concentration and DF volume at ¼ ratio (top row) and ½ ratio (bottom row);

In addition, the result showed that there was no difference in the expression of pDsRed-Monomer from both ratios as the transfection efficiency at each DNA and DF combination was nearly similar. Moreover, the expression of pVect-OZ in HeLa cells was higher as compared with the expression of pDsRed-Monomer. In column 6 from figure 5.7b, using 0.250µg DNA and 1 or 0.5µl DF showed higher expression as compared with the same combination of DNA and DF for the expression of pDsRed-Monomer (column 2 first and second row respectively).This expression was seen 24h post-transfection and was monitored also 48,72h post-transfection in order to check if the expression was increasing with time.

However, there was no difference in the expression with time between 24, 48 and 72h, and the transfection efficiency was almost the same.

Therefore, after this successful trial in getting high transfection efficiency in HeLa cells from the transfection of pVect-OZ and pDsRed-Monomer, the transfection of the three *phr* constructs in HeLa cells were done. But this trial was not successful because after the transfection many dead cells were observed as the cells were detached from the plate and the remaining attached cells were rounded up and seemed not healthy under light microscope.

The reason of this observation of dead cells was not known and therefore we started the troubleshooting to test each factor in the transfection procedure.

The toxicity from the DF reagent, possibility of plasmid miniprep contamination, medium contamination were all tested to find out the reason that killed the cells.

The reason was not from any of these tested factors because they were tested individually and the cells were healthy and attached after their addition Fig 5.7c.

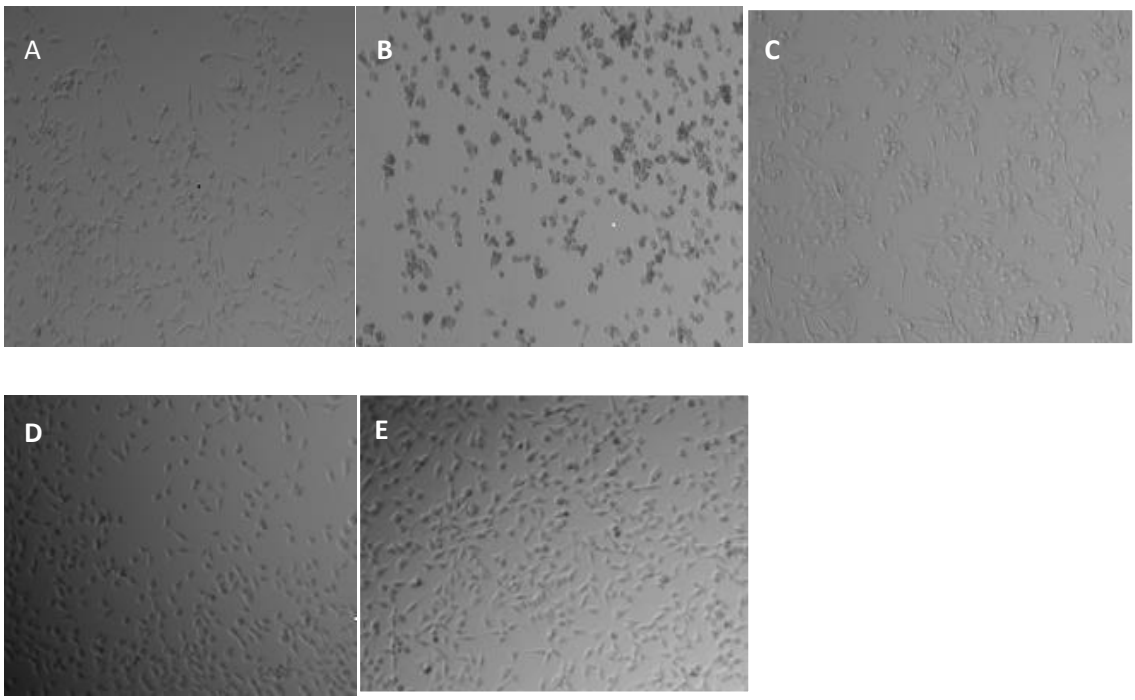

Figure 5.7c: Identification of factors responsible for toxicity during transfection in HeLa cells

Transmitted images for HeLa cells under light microscope at 4X magnification:

A- Untransfected HeLa cells;
B- Transfected cells with pDsRed-Monomer;
C- Addition of DF only to test toxicity;
D- Addition of Medium only to check contamination;
E- Addition of miniprep pDsRed-Monomer plasmid only to check contamination;

In Fig 5.7c, HeLa cells looked healthy with normal morphology under the microscope in the untransfected cells (A) and in all other tested factors like addition of DF only (C), possibility of medium contamination (D) and possibility of miniprep plasmid contamination (E). However, it was clear from this figure that after transfection (B) HeLa cells changed its morphology and became rounded up plus some cells were detached.

In order to check whether these cells were dead cells, HeLa cells were tested after transfection with Trypan Blue, a blue stain taken up by dead cells.

As can be seen from Fig 5.7d, unstained HeLa cells (A) and cells stained with Trypan Blue (B) showed different results. Two types of cells were seen after staining with Trypan Blue (B), dead cells that took the blue stain and dying cells which were rounded but not stained yet.

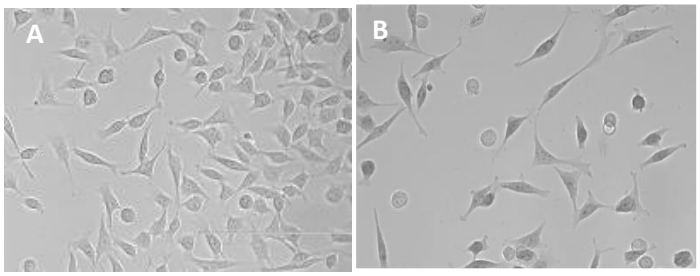

Figure 5.7d: Trypan Blue test in HeLa cells

Transmitted images from light microscopy at 20X magnification;
A- Unstained HeLa cells;
B- Stained HeLa cells with Trypan blue;

Therefore, this test confirmed that these HeLa cells were dead cells and hence we can not proceed in testing the expression in dead cells.

From previous trials on transfection (not mentioned here), cells looked healthy in 96 well plate after transfection. Therefore, the transfection plate was changed from 24 well to 96 well plate. In addition, and according to DreamFect protocol for transfection, they recommended changing the medium after 3-4h if some toxicity was observed and using serum free or reduced serum medium to increase the efficiency of transfection.

Therefore these points were taken into consideration when another trial of transfection was done. The expression of pDsRed-Monomer in a 96 well plate was monitored 24 and 48h post-transfection. Also quantification of cell death 48h post transfection by cell viability assay (MTT) was also done in this 96 well plate. The transfection efficiency in this successful trial was high (50-60 % according to photoQuad software) and the cells were alive after 48h of transfection.

The result of MTT assay for testing the cell viability in 96 well plate after changing the medium 3h post-transfection and using serum free medium was 99.8%. This level of viability was sufficient to perform the photorepair assay.

Figure 5.7e shows the successful trial of transfection of pDsRed-Monomer in HeLa cells with high transfection efficiency 48h post-transfection using 0.4 µg DNA plus 0.8 µl DF.

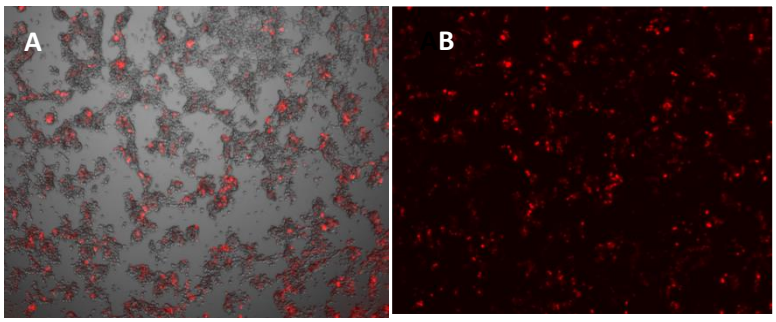

Figure 5.7e: Expression of pDsRed-Monomer in HeLa cells with high transfection efficiency

Images from florescent microscope at 4X magnification:

A- Overlay image;
B- RFP image;

After the successful expression of pDsRed-Monomer in HeLa cells and after the optimisation of transfection procedure to obtain high transfection efficiency, the transfection of the three *phr* constructs in HeLa cells was done.

RK*phr*-pDsRed, *S.sphr*-pDsRed, *E.coliphr*-pDsRed and pDsRed vector only were transfected into HeLa cells and the expression was checked 48h post-transfection. Figure 5.7f shows the result of transfection from the three *phr* constructs and pDsRed-Monomer.

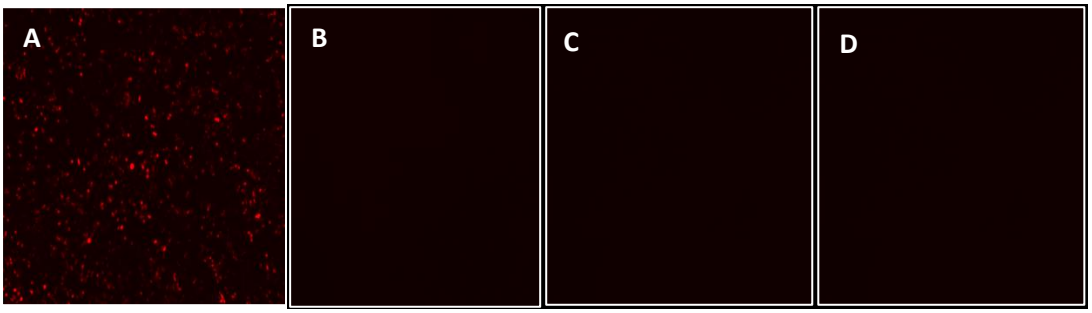

Figure 5.7f: Expression of pDsRed-Monomer and the three *phr* constructs in HeLa cells

RFP Images from florescent microscope at 4X magnification 48h post-transfection:

A- Expression of pDsRed-Monomer vector only;
B- Expression of RK*phr*-pDsRed;
C- Expression of *S.sphr*-pDsRed;
D- Expression of *E.coliphr*-pDsRed;

As can be seen from the figure above, the expression of pDsRed was only seen from the transfection of pDsRed-Monomer alone Fig 5.7f (A) but not from the transfection of any *phr* construct Fig 5.7f (B, C and D).

Photorepair assay in HeLa cells

The photorepair assay was conducted on all these transfected cells with different vectors and the average result of 3 independent experiments is shown in Fig 5.8.

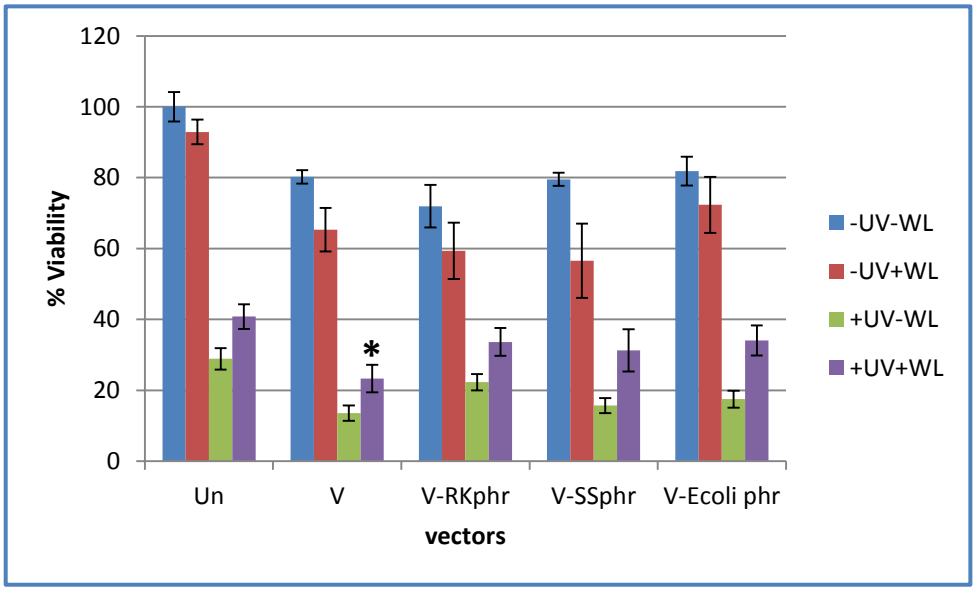

Figure 5.8: photoreactivation assay shows different viability from different transfected vectors in HeLa cells

HeLa cells expressing the photolyase gene from 3 different organisms *S. solfataricus* (V-ssphr), *E. coli* (V-Ecoliphr) and R. kangaroo (V-RKphr), in the pDS-Red monomer vector (+ *phr* cells). Photorepair (+UV+WL), dark repair (+UV-WL), white light alone (-UV+WL) and negative controls (-UV-WL) plus untransfected cells (Un). Data represents Mean +/- SEM from 3 independent experiments, each containing 4 replicates. A strike (*) indicates statistical difference at $p<0.05$ compared with the control (un transfected cells).

As seen from Fig 5.8, the percentage viability of HeLa cells in different transfected cells with different treatments, showed different viabilities. The average results of HeLa cell viability in both controls without UV radiation and with white light illumination for 30 min (-UV+WL) plus no white light illumination (-UV-WL) was higher than the viability of cells with 4 min UV radiation both in dark (+UV-WL) and under light illumination (+UV+WL). Moreover,

the viability of cells from the three transfected phr constructs of the three organisms was almost similar in (+UV+WL) when compared with the UN transfected cells with the same treatment, but higher than the transfected cells with the vector alone with the same treatment.

Two way ANOVA test was done (using GraphPad Prism 6) to test the significance of these variations in the percent viability. It was found that the variations between different treatments (+/- UV, +/- WL) was statistically significant ($p<0.0001$). Also the variations between the different tested groups (represented in the X axes), was also significant ($p=0.0212$).

However, when the differences in cell viability for the white repair (purple columns) was tested for the significance among different tested groups (X axes) by using one way ANOVA, the variations was not significant ($p=0.1061$). The same test was done for the dark repair (green columns) but it gave significant difference among different tested groups ($p=0.0005$).

Moreover, to test the variation of percent cell viability between two selected groups (from the X axes) with the same treatment (i.g +UV +WL), unpaired T-test was done using the same statistical program. Also this test showed no significant difference in cell viability between the transfected vector only (+UV+WL) and all other transfected vectors (all *phr* genes cloned into the vector) with the same treatments. The significant values were $p=0.0821$, 0.2839 and 0.0810 for V-RKphr (+UV+WL), V-SSphr (+UV+WL) and V-Ecoli (+UV+WL), respectively. But when the vector only (+UV+WL) was compared with the UN transfected cells at the same treatment, the difference in the cell percent viability was significant ($p=0.0041$).

The above was the comparison of white repair in different tested groups (X axes) with one of the controls, which is the white repair of V only. In addition, the other control used for this assay was the UN transfected HeLa cells which also showed no-significant difference compared to all other tested groups.

5.4 Discussion

The plasmid pDsRed-Monomer-N1 was selected and in order to clone the three *phr* genes into this vector, the start and the end of the each gene had to be determined. In fact the cloning of these genes was possible because their sequence was already published. *S. solfataricus phr* sequence was identified as described in chapter 2 whereas *Potorus triductylus* and *E. coli phr* sequences were obtained from pubmed website (www. Ncbi.nlm.nih.gov/pubmed). The template used for the amplification of *S. solfataricus phr* gene was *S. sofataricus phr*-pET28a, which was prepared as outlined in chapter 2. The rat kangaroo *phr*-PCY4B which was kindly donated from Prof. Carlos Menck from University of São Paulo, was used as a template for the amplification of Rat kangaroo (RK) phr gene. This vector drives the expression of RK *phr* gene by chicken β-actin promoter (Appendix 8). The *E. coli phr* amplification was obtained from the miniprepped plasmid of *E. coli* K12 strain (University of Bath).

The addition of NLS sequence in the forward primer design was necessary because this sequence will direct the protein into the nucleus and it was added at the N-terminus of each *phr* gene. According to a study done on identification of three conserved NLS in higher eukaryotes at the N-terminal region of human mismatch repair proteins MSH6 (Gassman *et al.* 2011), the shortest NLS sequence from this study (KRK) was chosen. This is because this sequence will add 9 basses in the flanking region of forward primer design, taking into account the addition of restriction sites plus ATG in the same primer. But the other two identified NLS sequence includes four and five amino acids which will add 12 and 15 nucleic acid bases, respectively. Long flanking region of primers design might affect the affinity of primer annealing to the desired gene, therefore the shortest NLS sequence was selected.

After the preparation of the three *phr* constructs in pDsRed-Monomer-N1 and verification of the gene sequences, selecting a human cell line for testing the expression of phr proteins was done.

In *vitro* mammalian cells offer an ideal system for the study of radiation effect on cells, because the cells are grown as a thin monolayer (Chu 1965). Therefore, they are also suitable for the study of UV radiation. UV light induces several types of DNA damage, which includes thymine dimerization, cross-linkage, etc. (review by Mclaren and Smith 1964). Thymine dimers in particular may account for a large proportion of UV lesions (Setlow and Setlow 1962). (Setlow and Setlow 1962) showed that UV light indeed induces thymine

dimers in the DNA of hamster cells and that the amount of dimer formation increases linearly with UV dose. In addition, it was reported that DNA damage causes several types of cellular damage, which involves cell death, delay in DNA synthesis and mitosis, etc. (Chu 1965).

Initially, to investigate the effect of photolyase expression in repairing UV damage in human cells, CRL 1360 cell line was chosen. This cell line is a fibroblast cell line obtained from a patient suffering from xeroderma pigmentosum (XP). It is well known that patients with this disease are hypersensitive to UV light and have deficiency in NER (Asahina *et al.* 1999). Therefore, this cell line is an ideal model to investigate the effect of photorepair, as any repair mechanism of UV damage observed in this cell line will result only from a photoreactivation mechanism.

However, the CRL 1360 cells were not UV sensitive as expected, but actually were resistant to UV radiation. The viability of these cells after UV treatment at different doses was about 80-90% 24h post-UV radiation (Fig 5.6c). Interestingly, (Cleaver 1972) found that cell fibroblasts from three XP patients showed normal UV sensitivity and normal repair mechanism as compared with the normal cells. It was concluded from this study that there are minority of XP cases with a biochemically distinct condition. In our study, CRL1360 cell line also behaves differently than the ordinary XP cells and as the previous study showed that some of these cells exhibit normal UV sensitivity, in this study CRL1360 cell line showed no hypersensitivity to UV light.

Therefore, and alternatively, HeLa cells were chosen and their sensitivity to UV light was tested. The result of cell viability 24h post-UV radiation using the same UV doses, showed high UV sensitivity as compared with CRL1360.

The observation that HeLa cell viability was almost similar at all tested UV doses (1-12 min) could refer to the use of single UV wavelength (254 nm). (Chu 1965) showed that acute effect of radiation on cell death was observed in cells exposed to high UV wavelength but at lower wavelengths, cell death occur after several hours of UV irradiation, So he concluded that the UV effect on cells is wavelength dependent but not dose dependent.

Moreover, the results showed also similar cell viability at all tested UV recovery times and this possibly due to the effect of UV radiation on cell division delay (Chu 1965). In other words, if the cells are not active and not dividing, their viability will be consistent at the tested durations. However, from Fig 5.6b we can see that 72h after UV irradiation the

viability of cells at 8min UV dose started to increase. This suggests that the delay in cell division in HeLa cells was observed up to 48h post-UV radiation and after that, the cells started to divide and showed slightly higher viability. Therefore, any tested UV dose and any 19-48h post UV recovery time can be chosen for the photorepair assay.

After confirming the sensitivity of HeLa cell to UV radiation and choosing 4min UV dose and 24h post-UV recovery time for the photorepair assay, transfection of *phr* genes into HeLa cells was done. The transfection method and type were selected for the reason that was explained at the beginning of this chapter. In addition, many reports on the transfection of photolyases cloned in specific vectors and the transfection of other genes cloned into pDsRed-Monomer-N1 were done by the lipofection method (Asahina *et al.* 1999; Chigancas *et al.* 2000; Upton *et al.* 2008; Khobta *et al.* 2010).

The three constructs of *Phr* genes from the three organisms plus the vector alone were transfected into HeLa cells and the expression of pDsRed protein (red fluorescent) was observed from the transfected vector only 48h-post transfection.

The reason behind the failure to observe red fluorescence with the phr-pDsRed constructs was unknown, the gene sequences from all three *phr* genes were checked and verified, and also the reading frame between the fusions of *phr* genes with DsRed was correct.

Knowing that protein folding in cells is a complex process (Mayssam and Barbara 2005), it is possible that the protein folding of DsRed was affected by the fusion with *phr* genes.

Moreover, it has been reported that DsRed has many disadvantages, such as strong oligomerization and slow maturation in which the red fluorescent can be seen only when the protein is fully ripen and this might take days (Baird *et al.* 2000). Also the red fluorescence can not be seen if there was a mutation in a single amino acid (Baird *et al.* 2000).

Furthermore and according to our knowledge, no photolyases were expressed as fusions with DsRed protein but it has been reported that *phr* genes were expressed successfully when they were cloned into pCY4B vector (Chigancas *et al.* 2000), pRc/RSV vector (Asahina *et al.* 1999), pEGFP-N1 plasmid (Chigancas *et al.* 2004).

Therefore, our results suggest that using DsRed to produce a tagged protein to indicate the expression of *phr* genes was not suitable, knowing that choosing the best fusion system for a particular protein is difficult (Terpe 2003).

The result of the photoreactivation assay in Fig. 5.8 showed the percent viability of HeLa cells, which was assessed by MTT assay 24h after UV treatment.

The effect of different treatments (+/- UV, +/- WL) on the cell viability was significant as indicated by two way ANOVA test. This was expected because it is well known that UV radiation induces CPD and 6-4pp lesions and the former ones are believed to be responsible for the majority of mutations induced by ultraviolet radiation in mammalian cells (You *et al.* 2001). Also these lesions were associated with inducing double strand breaks (DSB) in the DNA (Garinis *et al.* 2005). Because of that, these lesions might have a major effect on DNA replication and also the accumulation of this damage (if left unrepaired) might trigger apoptosis and cell death (Lo *et al.* 2005). This could explain the decrease in the percent cell viability of HeLa cells after UV treatment in both +/- WL (Green and Purple columns) as compared with the non UV treated cells (Red and Blue columns).

The data suggests a minor but not significant increase in the percent cell viability of the three transfected *phr* constructs into HeLa cells when compared with transfected cells with V only. This suggests that there is no photoreactivation detected in HeLa cells after the transfection of the three *phr* constructs, which may be a reflection of the lack of significant expression result. The absence of the red fluorescence from the expression of the protein which was tagged with DsRed suggests that the photolyase protein was either not expressed or not correctly folded.

The significance difference in the percent viability was only seen between the two controls (untransfected and V only) with the same treatments (+UV +WL). This reduction in the percent viability of the transfected cells with V only as compared with the un transfected cells suggests that there might be some toxicity from the pDsReD vector, which cannot be explained. This reduction in the viability was observed in HeLa cells transfected with all different vectors when compared with the un transfected cells.

In addition, it was observed from the same result in this Figure that the white repair (photoreactivation) represented in purple columns was higher than the dark repair in all tested groups. This may be explained by a phenomenon known as photoprotection, in which a reduction in UV damage can be seen if the illumination with white light was given before the UV treatment (Jagger 1960). This phenomenon was first discovered in 1956 by Weatherwax in *E. coli* cells (Weatherwax 1956). In this study, illumination of *E. coli* B with visible light

before UV treatments increased the survival from 10^{-3} to 10^{-1}. Also Miki observed photoprotection from killing in *E. coli* K12 strain (Miki 1956; Matsushita and Miki 1958).

So, this means that there is a difference between photoreactivation and photoprotection, in which the former is an enzymatically mediated reaction but the latter is not. Moreover, Jagger suggested another type of photoprotection given another description which is indirect photoreactivation, and in this type of photoprotection the light can be given either before or after UV treatments (see review by Jagger 2004). It was suggested that photoprotection mediated its action by inducing a growth and division delay, which will allow more time for the dark repair process (Takebe and Jagger 1969). This was reported by Jagger and Takebe in 1969, when they measured the action spectrum in *E.coli* B/r for growth and division delay by UVB radiation (Takebe and Jagger 1969).

In our study, the illumination of HeLa cells with white light for 30 min was done after UV treatments (indirect photoreactivation), but the whole experiment was done during the daylight. Therefore, it is possible that the cells acquired the photoprotection light from the daylight before UV treatment (photoprotection).

On the other hand, the difference in the dark repair (Green columns) among different tested groups was significant. This is probably because of the presence of an active NER mechanism in HeLa cells, and its activity can be varied in each tested group depending on the amount of UV damage induced and the amount of photoprotection light acquired.

Furthermore, successful expression of marsupial photolyase in HeLa cells and the repair of UV photoproducts was reported (Chigancas *et al.* 2000). This suggests that HeLa cells have the machinery for expressing the photolyase and that our choice in selecting HeLa cells as the mammalian cell line for evaluating the expression of photolyases from different organisms was appropriate.

However, the unsuccessful expression of the *phr* genes in HeLa cells from the three organisms might refer to the selection of an unsuitable vector.

Chapter 6- General discussion

The main aim of this PhD project was to identify and functionally characterize a putative *phr* gen(s) from a hyperthermophilic archaeon, *S. solfataricus*. Since the full genome sequence of this organism was annotated in 2001 from *S. solfataricus* P_2 strain it can be obtained from NCBI website, http://www.ncbi.nlm.nih.gov/. From that full sequence, it was possible to identify the putative *phr* gene sequence by a BLAST search of the whole genome sequence of *S. solfataricus* with the identified *phr* gene sequence of a species closely related to *S. solfataricus*, which is *S. tokodaii*. Both these archaeal organisms belong to the same genus which is *Sulfolobus*, and the similarity between them is more than 90% (Cavicchioli 2007). The BLAST search showed one sequence homologous to the *phr* gene sequence of *S. tokodaii*, with a similarity of 73%.

This identified *phr* gene sequence from *S. solfataricus* was then cloned into an expression vector in order to express it in *E. coli* cells. This allowed successful expression of the *S. solfataricus* photolyase in *E. coli* cells after lowering the growth incubation temperature to 24 ^{o}C, which is believed to slow down protein synthesis and allow more time for correct protein folding (Wu *et al.* 2008). This successful expression of *S. solfataricus* protein in *E. coli* cells is consistent with other studies where they demonstrated a functional expression of other photolyases in *E. coli* cells, such as the expression of *Potorous tridactylis* (Kato *et al.* 1994), *Arabidopsis thaliana* (Malhotra *et al.* 1995) and *Salmonella typhimurium* (Li and Sancar 1991) photolyases.

The photolyase protein was His tagged, and therefore was easily to purify on a His bind column. The purified protein was a greenish-yellow colour and its molecular mass was confirmed to be correct by SDS-PAGE gel and by HRMS analysis. Spectral analysis of the purified protein suggests the presence of FAD molecule (Sancar *et al.* 1987), since it showed a peak at 455 nm and we found that the ratio of the flavin to the protein was 2:1, respectively.

This result was expected because it was demonstrated from the crystal structure of *S. tokodaii* photolyase that it contains two FAD chromophores, one is acting as a catalytic cofactor and the second is acting as a light harvesting cofactor (Fujihashi *et al.* 2007). In addition, the similarity between *S. solfataricus* and *S. tokodaii* photolyase amino acid sequences is very high, which led us to speculate that their chromophores are also the same.

Furthermore, the absorption spectrum of *S. tokodaii* photolyase, which was taken directly after purification (Fujihashi *et al.* 2007), was very similar to the spectrum that we obtained for *S. solfataricus* photolyase under the same conditions Fig. 6.1.

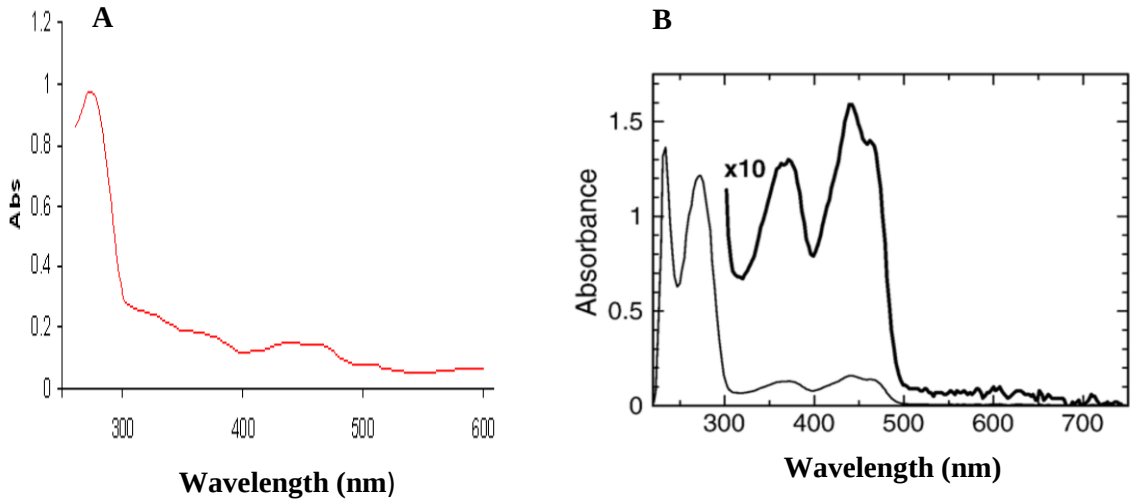

Figure 6.1 Spectral analysis of the purified proteins

A) Spectral analysis of the diluted (1:6) and purified *S. solfataricus* photolyase showing two peaks at 280 and 455 nm.
B) Spectral analysis of the purified *S. tokodaii* photolyase showing the same two peaks with the diluted version (Adapted from Fujihashi *et al.* 2007).

Therefore, based on what was mentioned above, our study suggests the presence of two FAD chromophores in *S. solfataricus* photolyase.

The *in vitro* assay used in characterizing the functional activity of the purified protein from *S. solfataricus* proved that this enzyme was able to repair CPD lesions. This is because this assay was based on using T4 endonuclease V enzyme, which recognizes only CPD lesions (Kraemer and DiGiovanna 2002). Also, it is known that the only photolyase that uses CPD photoproducts as substrates, is CPD photolyase. Therefore, this result suggests that the *phr* gene of *S. solfataricus* is coding for only CPD photolyase. Moreover, the photolyase that was identified from *S. tokodaii* was also from class I photolyases, which is CPD photolyase.

Since previous studies outlined an efficient light repair mechanism in *S. solfataricus* (Dorazi *et al.* 2007), in this study we proved the presence of an active CPD photolyase in *S. solfataricus* in removing UV-induced CPD lesions.

Furthermore, this study proved also that the purified protein was a hyperthermophilic enzyme as the optimum temperature for its activity was found to be at 90 ºC, which considered as an optimum temperature for the growth of this organism.

Also, in chapter 4, we determined the *S. solfataricus* photolyase concentration that was sufficient to show repair activity in removing UV damage as 7.7 µM, in the optimum temperature assay. Similarly, another study reported the use of 8 µM photolyase enzyme from *Saccharomyces cerevisiae*, and found that this concentration was efficient to remove the UV-induced dimers when human fibroblast cells were injected with the yeast photolyase (Roza *et al.* 1990).

After the successful expression of *S. solfataricus* photolyase in *E. coli* cells, its functional activity as a photoreactive enzyme in repairing UV lesions was examined *in vivo*.

The results obtained in chapter 2 for the transformation of a recombinant *phr* gene from *S. solfataricus* into *E. coli* cells showed very clear evidence for a functional activity of the transformed photolyase in a heterologous system, which grow at 37 ºC.

This finding stimulated us to look at the expression of this enzyme in human cells that lack the *phr* gene and are growing and functioning also at 37 ºC. It was of interest to look at the expression of an archaeal DNA repair enzyme in a eukaryotic system that shares a similarity in DNA repair mechanism (Kelman and White 2005; Aravind *et al.* 1999).

However, our attempt to express the photolyase in human HeLa cells was not successful. This might be due to the selection of an unsuitable mammalian expression vector (pDsRed Monomer) and a problem in the fusion of DsRed with *phr* gene. Our results suggest that DsRed was not suitable to use as a fusion tag for the expression of *phr* gene and it was described in chapter 5 more details about the disadvantages of using this fusion tag.

To conclude, in this study we managed to identify a *phr* gene and characterize an active photolyase from *S. solfataricus* in repairing UV-induced DNA lesions following illumination with visible light. Also the type of this enzyme was identified as Type I CPD photolyase from the *in vitro* assay.

We were able to express and purify the protein and showed that it was soluble protein and its spectrum suggests a presence of two FAD molecules.

In addition, the *S. solfataricus* photolyase showed functional activity when expressed in *E. coli* cells. Despite the optimum temperature for the activity of *S. solfataricus* as determined in this study to be 90 ºC, the *in vivo* assay result showed that the enzyme can function at 37 ºC.

In this study we were unable to express the *S. solfataricus* photolyase in HeLa cells, probably because of the selection of unsuitable mammalian expression vector.

Future work

Since the crystal structure of *S. solfataricus* photolyase is not known, it would be very valuable information to determine its structure. The structure would be expected to be closely similar to the *S. tokodaii* photolyase since they are closely related in amino acid sequence. This will allow us to understand more about the stability of hyperthermophilic enzymes, and also to confirm our finding about the presence of two FAD chromophores.

Another attempt on expressing the *E. coli* photolyase is also needed to make further comparisons between the activity of *S. solfataricus* and *E. coli* photolyases. This can be done by using the same concentration of both enzymes and examining the repair mechanism of UV damage followed by white light illumination. This would require changing some conditions in another trial in expressing *E. coli* photolyase, such as changing the growth incubation temperature and also the IPTG concentration.

HeLa cells have been shown to be suitable for expressing a recombinant marsupial photolyase gene (Chigancas *et al.* 2000). Thus, other attempts on expressing the *S. solfataricus* photolyase gene in the same cells can be made. However, choosing another mammalian expression vector in cloning the *phr* gene and evaluating its functional expression in repairing UV damage in HeLa cells would be worthwhile.

Bibliography

Adams, M.D., Kerlavage, A.R., Fleischmann, R.D., Fuldner, R.A., *et al*, 1995. Initial assessment of human gene diversity and expression patterns based upon 83-million nucleotides of cdna sequence. Nature, 377, pp. 3-&.

Adams, M.W.W., 1993. Enzymes and proteins from organisms that grow near and above 100 degrees C. Annual Review of Microbiology, 47, pp. 627-658.

Adimoolam, S. & Ford, J.M., 2003. p53 and regulation of DNA damage recognition during nucleotide excision repair. DNA Repair, 2, pp. 947-954.

Ahmad, M. & Cashmore, **A.R., 1993**. hy4 gene of *A-thaliana* encodes a protein with characteristics of a blue-light photoreceptor. nature, 366, pp. 162-166.

Allers, T. & Mevarech, M., 2005. Archaeal genetics - The third way. Nature Reviews Genetics, 6, pp. 58-73.

Ananthaswamy, H.N., Loughlin, S.M., Cox, P., Evans, R.L., *et al*., 1997. Sunlight and skin cancer: Inhibition of p53 mutations in UV-irradiated mouse skin by sunscreens. Nature Medicine, 3, pp. 510-514.

Aravind, L., Walker, D.R. & Koonin, E.V., 1999. Conserved domains in DNA repair proteins and evolution of repair systems. Nucleic Acids Research, 27, pp. 1223-1242.

Aravind, L. & Koonin, E.V., 1999. DNA-binding proteins and evolution of transcription regulation in the archaea. Nucleic Acids Research, 27, pp. 4658-4670.

Asahina, H., Han, Z., Kawanishi, M., Kato, T., *et al.*, 1999. Expression of a mammalian DNA photolyase confers light-dependent repair activity and reduces mutations of UV-irradiated shuttle vectors in xeroderma pigmentosum cells. Mutat Res. Netherlands, pp. 255-62.

Baird, G.S., Zacharias, D.A. & Tsien, R.Y., 2000. Biochemistry, mutagenesis, and oligomerization of DsRed, a red fluorescent protein from coral. Proceedings of the National Academy of Sciences of the United States of America, 97, pp. 11984-11989.

Baliga, N., Bjork, S., Bonneau, R., Pan, M., *et al.*, 2004. Systems level insights into the stress response to UV radiation in the halophilic archaeon Halobacterium NRC-1. Cold Spring Harbor Laboratory Press, pp. 1025-1035.

Barns, S.M., Delwiche, C.F., Palmer, J.D. & Pace, N.R., 1996. Perspectives on archaeal diversity, thermophily and monophyly from environmental rRNA sequences. Proceedings of the National Academy of Sciences of the United States of America, 93, pp. 9188-9193.

Berardesca, E., Bertona, M., Altabas, K., Altabas, V. & Emanuele, E., 2012. Reduced ultraviolet-induced DNA damage and apoptosis in human skin with topical application of a photolyase-containing DNA repair enzyme cream: Clues to skin cancer prevention. Molecular Medicine Reports, 5, pp. 570-574.

Blum, P., 2004, Archaea: Ancient microbs, extreme environments, and the origin of life.

Boone and Castenholz, 2001. Bergey's manual of systematic bacteriology. Bergey's manual of systematic bacteriology, pp. i-xxi, 1-721.

Boyce, R.P. & Howardflanders, P., 1964. Release of ultraviolet light-induced thymine dimers from DNA in *E. coli* k-12. proceedings of The National Academy of Sciences of The United States of America, 51, pp. 293-&.

Britt, A.B., 1996. DNA damage and repair in plants. Annual Review of Plant Physiology and Plant Molecular Biology, 47, pp. 75-100.

Brochier-Armanet, C., Boussau, B., Gribaldo, S. & Forterre, P., 2008. Mesophilic crenarchaeota: proposal for a third archaeal phylum, the Thaumarchaeota. Nature Reviews Microbiology, 6, pp. 245-252.

Brock, T.D., 1985. Life at high-temperatures. Science, 230, pp. 132-138.

Brock, T., Brock, K., Belly, R. & Weiss, R., 1972. Sulfolobus: a new genus of sulfur-oxidizing bacteria living at low pH and high temperature. Archives of Microbiology, 84, pp. 54-68.

Bult, C.J., White, O., Olsen, G.J., Zhou, L.X., *et al* 1996. Complete genome sequence of the methanogenic archaeon, Methanococcus jannaschii. Science, 273, pp. 1058-1073.

Cashmore, A.R., 2003. Cryptochromes: Enabling plants and animals to determine circadian time. Cell, 114, pp. 537-543.

Cavicchioli, R., 2007. Archaea. Washington, DC: American Society for Microbiology press.

Chao, C.C.K., 1993. Lack of DNA enzymatic photoreactivation in hela cell-free-extracts. febs letters, 336, pp. 411-416.

Chigancas, V., Miyaji, E.N., Muotri, A.R., Jacysyn, J.D., *et al*., 2000. Photorepair prevents ultraviolet-induced apoptosis in human cells expressing the marsupial photolyase gene. Cancer Research, 60, pp. 2458-2463.

Chigancas, V., Sarasin, A., Frederico, C. & Menck, F.M., 2004. CPD-photolyase adenovirus-mediated gene transfer in normal and DNA-repair-deficient human cells. Journal of Cell Science, 117, pp. 3579-3592.

Chu, E.H.Y., 1965. Effects of ultraviolet radiation on mammalian cells 1. Induction of chromosome abberations. Mutation Research, 2, pp. 75-94.

Cleaver, J.E., 1972. Xeroderma pigmentosum: variants with normal DNA repair and normal sensitivity to ultraviolet light. Journal of Investigative Dermatology, 58, pp. 124-8.

Dodson, M.L., Michaels, M.L. & Lloyd, R.S., 1994. Unified catalytic mechanism for DNA glycosylases. journal of biological chemistry, 269, pp. 32709-32712.

Dorazi, R., Gotz, D., Munro, S., Bernander, R. & White, M.F., 2007. Equal rates of repair of DNA photoproducts in transcribed and non-transcribed strands in *Sulfolobus solfataricus*. Molecular Microbiology, 63, pp. 521-529.

Duguet, M., 1993. The helical repeat of DNA at high-temperature. Nucleic Acids Research, 21, pp. 463-468.

Dulbecco, R., 1949. Reactivation of ultra-violet-inactivated bacteriophage by visible light. Nature, 163, p. 949.

Dulbecco, R., 1950. Experiments on photoreactivation of bacteriophages inactivated with ultraviolet radiation. Journal of Bacteriology, 59, pp. 329-47.

Eker, A.P.M., Dekker, R.H. & Berends, W., 1981. Photoreactivating enzyme from *streptomyces-griseus* .4. on the nature of the chromophoric cofactor in *streptomyces-griseus* photoreactivating enzyme. photochemistry and photobiology, 33, pp. 65-72.

Eker, A.P.M., Quayle, C., Chaves, I. & van der Horst, G.T.J., 2009. DNA Repair in Mammalian Cells. Cellular and Molecular Life Sciences, 66, pp. 968-980.

Elkins, J.G., Podar, M., Graham, D.E., Makarova, K.S., *et al*, 2008. A korarchaeal genome reveals insights into the evolution of the Archaea. Proceedings of the National Academy of Sciences of the United States of America, 105, pp. 8102-8107.

Forterre, P., Mirambeau, G., Jaxel, C., Nadal, M. & Duguet, M., 1985. High positive supercoiling *in vitro* catalyzed by an ATP and polyethylene glycol-stimulated topoisomerase from *sulfolobus-acidocaldarius*. EMBO journal, 4, pp. 2123-2128.

Friedberg, E., 2003. DNA damage and repair. Nature, 421, pp. 436-440.

Friedberg, E.C., 1995. Out of the shadows and into the light - the emergence of DNA-repair. trends in biochemical sciences, 20, pp. 381-381.

Friedberg, E.C., 2006. DNA repair and mutagenesis. 2nd ed. Washington, D.C.: ASM Press, pp. 1 online resource (xxix, 1118 p.).

Friedberg, E.C., 2001. How nucleotide excision repair protects against cancer. Nature Reviews Cancer, 1, pp. 22-33.

Friedberg, E.C., Walker, G.C. & Siede, W., 1995. DNA repair and mutagenesis. DNA repair and mutagenesis, pp. xvi+698p-xvi+698p.

Fröls, S., Gordon, P., Panlilio, M., Duggin, I., *et al.*, 2007. Response of the Hyperthermophilic Archaeon *Sulfolobus solfataricus* to UV Damage?†. Journal of Bacteriology, 189, pp. 8708-8718.

Fröls, S., White, M. & Schleper, C., 2009. Reactions to UV damage in the model archaeon *Sulfolobus solfataricus*. Biochemical Society Transactions, 37, p. 36.

Fujihashi, M., Numoto, N., Kobayashi, Y., Mizushima, A., *et al.*, 2007. Crystal structure of archaeal photolyase from *Sulfolobus tokodaii* with two FAD molecules: Implication of a novel light-harvesting cofactor. Journal of molecular biology, 365, pp. 903-910.

Galagan, J.E., Nusbaum, C., Roy, A., Endrizzi, M.G., *et al.*, 2002. The genome of *M-acetivorans* reveals extensive metabolic and physiological diversity. Genome Research, 12, pp. 532-542.

Garinis, G.A., Mitchell, J.R., Moorhouse, M.J., Hanada, K., *et al.*, 2005. Transcriptome analysis reveals cyclobutane pyrimidine dimers as a major source of UV-induced DNA breaks. Embo Journal, 24, pp. 3952-3962.

Garrett, R., & klenk, H., 2007. Archaea: Evolution, physiology, and Molecular Biology. blackwell publishing ltd.

Gassman, N.R., Clodfelter, J.E., McCauley, A.K., Bonin, K., *et al.*, 2011. Cooperative Nuclear Localization Sequences Lend a Novel Role to the N-Terminal Region of MSH6. *Plos One*, 6.

Gilchrest, B.A., Eller, M.S., Geller, A.C. & Yaar, M., 1999. The pathogenesis of melanoma induced by ultraviolet radiation. New England Journal of Medicine, 340, pp. 1341-1348.

Gribaldo, S. & Brochier-Armanet, C., 2006. The origin and evolution of Archaea: a state of the art. Philosophical Transactions of the Royal Society B-Biological Sciences, 361, pp. 1007-1022.

Grogan, D.W., 2000. The question of DNA repair in hyperthermophilic archaea. Trends in Microbiology, 8, pp. 180-185.

Grogan, D.W., 2004. Stability and repair of DNA in hyperthermophilic archaea. Current Issues in Molecular Biology, 6, pp. 137-144.

Guirouilh-Barbat, J., Huck, S., Bertrand, P., Pirzio, L., Desmaze, C., *et al*., 2004. Impact of the KU80 pathway on NHEJ-induced genome rearrangements in mammalian cells. Molecular Cell, 14, pp. 611-623.

Hamilton, K.K., Kim, P.M.H. & Doetsch, P.W., 1992. A eukaryotic DNA glycosylase lyase recognizing ultraviolet light-induced pyrimidine dimers. Nature, 356, pp. 725-728.

Hanawalt, P.C., 1994. Transcription-coupled repair and human-disease. science, 266, pp. 1957-1958.

Harm, H., 1978. Damage and repair in mammalian-cells after exposure to non-ionizing radiations .1. Ultraviolet and visible-light irradiation of cells of rat kangaroo (*potorous-tridactylus*) and determination of photorepairable damage invitro. Mutation Research, 50, pp. 353-366.

Harm, H., 1980. Damage and repair in mammalian-cells after exposure to non-ionizing radiations .2. Photoreactivation and killing of rat kangaroo cells (potorous-tridactylus) and herpes-simplex virus-1 by exposure to fluorescent white-light or sunlight. Mutation Research, 69, pp. 157-165.

Herndl, G.J., 1997. Role of ultraviolet radiation on bacterioplankton activity. In: Hader, ed. The effects of Ozone Depletion on Aquatic Ecosystems. Austin: Academic Press and R. G. Landes Company, pp. 143-154.

Hill, L.L., Ouhtit, A., Loughlin, S.M., Kripke, M.L., *et al*., 1999. Fas ligand: A sensor for DNA damage critical in skin cancer etiology. Science, 285, pp. 898-900.

Hitomi, K., Nakamura, H., Kim, S.T., Mizukoshi, T., *et al.*, 2001. Role of two histidines in the (6-4) photolyase reaction. Journal of Biological Chemistry, 276, pp. 10103-10109.

Hitomi, K., Okamoto, K., Daiyasu, H., Miyashita, H., *et al*., 2000. Bacterial cryptochrome and photolyase: characterization of two photolyase-like genes of Synechocystis sp PCC6803. Nucleic Acids Research, 28, pp. 2353-2362.

Hsu, D.S., Zhao, X.D., Zhao, S.Y., Kazantsev, A., *et al*., 1996. Putative human blue-light photoreceptors hCRY1 and hCRY2 are flavoproteins. Biochemistry, 35, pp. 13871-13877.

Huber, H., Hohn, M.J., Rachel, R., Fuchs, T., *et al*., 2002. A new phylum of Archaea represented by a nanosized hyperthermophilic symbiont. Nature, 417, pp. 63-67.

Huber, H., Hohn, M.J., Stetter, K.O. & Rachel, R., 2003. The phylum Nanoarchaeota: Present knowledge and future perspectives of a unique form of life. Research in Microbiology, 154, pp. 165-171.

Iwasa, T., Tokutomi, S. & Tokunaga, F., 1988. photoreactivation of halobacterium-halobium - action spectrum and role of pigmentation. photochemistry and photobiology, 47, pp. 267-270.

Iwatsuki, N., Joe, C.O. & Werbin, H., 1980. Evidence that deoxyribonucleic acid photolyase from baker's yeast is a flavoprotein. Biochemistry, 19, pp. 1172-6.

Jagger, J., 1960. photoprotection from ultraviolet killing in *Escherichia-coli-b*. radiation research, 13, pp. 521-539.

Jagger, J., 2004. Personal reflections on monochromators and action spectra for photoreactivation. Journal of Photochemistry and Photobiology B-Biology, 73, pp. 109-114.

Jans, J., Schul, W., Sert, Y., Rijksen, Y., *et al*., 2005. Powerful skin cancer protection by a CPD-photolyase transgene. Current Biology, 15, pp. 105-115.

Jiang, Y., Ke, C., Mieczkowski, P. & Marszalek, P., 2007. Detecting ultraviolet damage in single DNA molecules by atomic force microscopy. Biophysical journal, 93, pp. 1758-1767.

Johnson, J.L., Hammalvarez, S., Payne, G., Sancar, G.B., *et al*., 1988. identification of the 2nd chromophore of *Escherichia-coli* and yeast DNA photolyases as 5,10-methenyltetrahydrofolate. proceedings of the national academy of sciences of the united states of america, 85, pp. 2046-2050.

Kanai, S., Kikuno, R., Toh, H., Ryo, H. & Todo, T., 1997. Molecular evolution of the photolyase-blue-light photoreceptor family. Journal of Molecular Evolution, 45, pp. 535-548.

Kates, M., 1993. In the biochemistry of Archaea. In: M. Kates, D.J.Kushner & A.T. Matheson, eds. Archaebacteria. Amestrerdam: Elsevier, pp. 261-295.

Kato, R., Hasegawa, K., Hidaka, Y., Kuramitsu, S. & Hoshino, T., 1997. Characterization of a thermostable DNA photolyase from an extremely thermophilic bacterium, Thermus thermophilus HB27. Journal of bacteriology, 179, pp. 6499-6503.

Kato, T., Jr., Todo, T., Ayaki, H., Ishizaki, K., Morita, T., *et al.*, 1994. Cloning of a marsupial DNA photolyase gene and the lack of related nucleotide sequences in placental mammals. Nucleic Acids Research, 22, pp. 4119-4124.

Kelman, Z. & White, M.F., 2005. Archaeal DNA replication and repair. Current Opinion in Microbiology, 8, pp. 669-676.

Kelner, A., 1949a. Effect of Visible Light on the Recovery of *Streptomyces Griseus Conidia* from Ultra-violet Irradiation Injury. proceedings of the national academy of sciences of the united states of america , 35, pp. 73-9.

Kelner, A., 1949b. photoreactivation of ultraviolet-irradiated escherichia coli, with special reference to the dose-reduction principle and to ultraviolet-induced mutation. journal of bacteriology, 58, pp. 511-22.

Khobta, A., Anderhub, S., Kitsera, N. & Epe, B., 2010. Gene silencing induced by oxidative DNA base damage: association with local decrease of histone H4 acetylation in the promoter region. Nucleic Acids Research. England, pp. 4285-95.

Kikuchi, A. & Asai, K., 1984. Reverse gyrase - a topoisomerase which introduces positive superhelical turns into DNA. Nature, 309, pp. 677-681.

Kim, S.T. & Sancar, A., 1993. Photochemistry, photophysics, and mechanism of pyrimidine dimer repair by DNA photolyase. photochemistry and photobiology, 57, pp. 895-904.

Kim, S.T., Malhotra, K., Smith, C.A., Taylor, J.S. & Sancar, A., 1994. Characterization of (6-4)-photoproduct DNA photolyase. journal of biological chemistry, 269, pp. 8535-8540.

Kiontke, S., Geisselbrecht, Y., Pokorny, R., Carell, T., Batschauer, A. & Essen, L.-O., 2011. Crystal structures of an archaeal class II DNA photolyase and its complex with UV-damaged duplex DNA. EMBO Journal, 30, pp. 4437-4449.

Klaper, R., Frankel, S. & Berenbaum, M.R., 1996. Anthocyanin content and UVB sensetivity in *Brassica rapa*. Photochemistry and Photobiology, 63, pp. 811-813.

Klenk, H.P., Clayton, R.A., Tomb, J.F., White, O., *et al*., 1997. The complete genome sequence of the hyperthermophilic, sulphate-reducing archaeon Archaeoglobus fulgidus. Nature, 390, pp. 364-&.

Komori, H., Masui, R., Kuramitsu, S., Yokoyama, S., *et al*., 2001. Crystal structure of thermostable DNA photolyase: Pyrimidine-dimer recognition mechanism. Proceedings of the National Academy of Sciences, 98, p. 13560.

Kozubal, M.A., Romine, M., Jennings, R., Jay, Z.J., *et al*., 2013. Geoarchaeota: a new candidate phylum in the Archaea from high-temperature acidic iron mats in Yellowstone National Park. ISME Journal. England, pp. 622-34.

Kraemer, K.H. & DiGiovanna, J.J., 2002. Topical enzyme therapy for skin diseases? Journal of the American Academy of Dermatology, 46, pp. 463-466.

Kumar, S. & Hedges, S.B., 1998. A molecular timescale for vertebrate evolution. Nature, 392, pp. 917-920.

Lehmann, A.R., 1995. Nucleotide excision-repair and the link with transcription. trends in biochemical sciences, 20, pp. 402-405.

Leuko, S., Neilan, B.A., Burns, B.P., Walter, M.R. & Rothschild, L.J., 2011. Molecular assessment of UVC radiation-induced DNA damage repair in the stromatolitic halophilic archaeon, *Halococcus hamelinensis*. Journal of Photochemistry and Photobiology B-Biology, 102, pp. 140-145.

Ley, R.D., 1984. Photorepair of pyrimidine dimers in the epidermis of the marsupial *Monodelphis-domestica*. photochemistry and photobiology, 40, pp. 141-143.

Ley, R.D., 1993. Photoreactivation in humans. proceedings of the national academy of sciences of the united states of america, 90, pp. 4337-4337.

Ley, R.D., Applegate, L.A., Fry, R.J.M. & Sanchez, A.B., 1991. photoreactivation of ultraviolet radiation-induced skin and eye tumors of *Monodelphis-domestica*. cancer research, 51, pp. 6539-6542.

Li, Y.F. & Sancar, A., 1991. Cloning, sequencing, expression and characterization of DNA photolyase from *Salmonella-typhimurium*. nucleic acids research, 19, pp. 4885-4890.

Li, Y.F., Kim, S.T. & Sancar, A., 1993. Evidence for lack of DNA photoreactivating enzyme in humans. proceedings of the national academy of sciences of the united states of america, 90, pp. 4389-4393.

Li, X. & Heyer, W.-D., 2008. Homologous recombination in DNA repair and DNA damage tolerance. Cell Research, 18, pp. 99-113.

Lieber, M.R., 2010. The Mechanism of Double-Strand DNA Break Repair by the Nonhomologous DNA End-Joining Pathway. Annual Review of Biochemistry, Vol 79, 79, pp. 181-211.

Lima-Bessa, K., Armelini, M., Chiganças, V., Jacysyn, J., *et al*., 2007. CPDs and 6-4PPs play different roles in UV-induced cell death in normal and NER-deficient human cells. DNA repair.

Lindahl, T. & Wood, R.D., 1999. Quality control by DNA repair. Science. United States, pp. 1897-905.

Lo, H., Nakajima, S., Ma, L., Walter, B., *et al*., 2005. Differential biologic effects of CPD and 6-4 PP UV-induced DNA damage on the induction of apoptosis and cell-cycle arrest. BMC cancer, 5, p. 135.

Londei, P., 2005. Evolution of translational initiation: new insights from the archaea. Fems Microbiology Reviews, 29, pp. 185-200.

Lucas-Lledo, J. & Lynch, M., 2009. Evolution of mutation rates: phylogenomic analysis of the photolyase/cryptochrome family. Molecular Biology and Evolution.

Madigan, M.T. & Marrs, B.L., 1997. Extremophiles. Scientific American, 276, pp. 82-87.

Malhotra, K., Baer, M., Li, Y.F., Sancar, G.B. & Sancar, A., 1992. Identification of chromophore binding domains of yeast DNA photolyase. journal of biological chemistry, 267, pp. 2909-2914.

Malhotra, K., Kim, S.T., Batschauer, A., Dawut, L. & Sancar, A., 1995. Putative blue-light photoreceptors from *Arabidopsis-thaliana* and *Sinapis-alba* with a high-degree of sequence homology to dna photolyase contain the 2 photolyase cofactors but lack DNA-repair activity. biochemistry, 34, pp. 6892-6899.

Matsushita, H. & Miki, K., 1958. Prevention of and recovery from radiation damage in *Escherichia-coli*. radiation research, 9, pp. 150-150.

Mayssam, A.H. & Barbara, I., 2005. Protein oligomerization: How and why. Bioorganic & Medicinal chemistry, 13, pp. 5013-5020.

McCready, S. & Marcello, L., 2003. Repair of UV damage in Halobacterium salinarum. Biochemical Society Transactions, 31, pp. 694-698.

MCLAREN, A.D. & D, S., 1964. Photochemistry of Proteins and Nucleic Acids. Science, 147, pp. 496-497.

Menck, C.F.M., 2002. Shining a light on photolyases. Nature Genetics, 32, pp. 338-339.

Miki, K., 1956. Studies on the phage multiplication in induced lysogenic bacteria. II. Effects of visible light on the ultraviolet induction of *Escherichia coli* K12 (lambda). Japanese Jour Bact, 11, pp. 803-812.

Minato, S. & Werbin, H., 1971. Spectral properties of the chromophoric material associated with the deoxyribonucleic acid photoreactivating enzyme isolated from baker's yeast. Biochemistry, 10, pp. 4503-8.

Minato, S. & Werbin, H., 1972. Excitation and fluorescence spectra of the chromophore associated with the DNA-photoreactivating enzyme from the blue-green alga Anacystis nidulans. Photochemistry and Photobiology, 15, pp. 97-100.

Mitchell, D.L. & Karentz, D., 1993. The induction and repair of DNA photodamage in the environment. Environmental UV photobiology, pp. 345-377.

Muller, F., Brissac, T., Le Bris, N., Felbeck, H. & Gros, O., 2010. First description of giant Archaea (Thaumarchaeota) associated with putative bacterial ectosymbionts in a sulfidic marine habitat. Environmental Microbiology, 12, pp. 2371-2383.

Ng, W.V., Kennedy, S.P., Mahairas, G.G., Berquist, B., *et al.*, 2000. Genome sequence of Halobacterium species NRC-1. Proceedings of the National Academy of Sciences of the United States of America, 97, pp. 12176-12181.

Novick, A. & Szilard, L., 1949. Experiments on light-reactivation of ultra-violet inactivated bacteria. Proceedings of the National Academy of Sciences of the United States of America, 35, pp. 591-600.

Ogrunc, M., Becker, D.F., Ragsdale, S.W. & Sancar, A., 1998. Nucleotide excision repair in the third kingdom. Journal of Bacteriology, 180, pp. 5796-5798.

Olsen, G.J. & Woese, C.R., 1996. Lessons from an Archaeal genome: What are we learning from Methanococcus jannaschii? Trends in Genetics, 12, pp. 377-379.

Ozer, Z., Reardon, J.T., Hsu, D.S., Malhotra, K. & Sancar, A., 1995. The other function of DNA photolyase: Stimulation of excision repair of chemical damage to DNA. Biochemistry, 34, pp. 15886-15889.

Pang, Q.S. & Hays, J.B., 1991. UV-b-inducible and temperature-sensitive photoreactivation of cyclobutane pyrimidine dimers in *Arabidopsis-thaliana*. *plant physiology*, 95, pp. 536-543.

Park, H.W., Kim, S.T., Sancar, A. & Deisenhofer, J., 1995. Crystal structure of DNA photolyase from *Escherichia coli*. Science, 268, pp. 1866-72.

Partch, C.L. & Sancar, A., 2005. Photochemistry and photobiology of cryptochrome blue-light photopigments: The search for a photocycle. Photochemistry and Photobiology, 81, pp. 1291-1304.

Patrick, M.H., 1977. Studies on thymine-derived UV photoproducts in DNA .1. formation and biological role of pyrimidine adducts in DNA. photochemistry and photobiology, 25, pp. 357-372.

Pegg, A.E., 2000. Repair of O(6)-alkylguanine by alkyltransferases. Mutation Research, 462, pp. 83-100.

Perugino, G., Vettone, A., Illiano, G., Valenti, A., Ferrara, M.C., *et al.*, 2012. Activity and Regulation of Archaeal DNA alkyltransferase conserved protein involved in repair of DNA alkylation damage. Journal of biological chemistry, 287, pp. 4222-4231.

Posnick, L., & Samson, L., 2001. DNA repair. Encyclopedia of Life Sciences.

Roza, L., Vermeulen, W., Henegouwen, J., Eker, A.P.M., *et al.*, 1990. Effects of microinjected photoreactivating enzyme on thymine dimer removal and DNA-repair synthesis in normal human and xeroderma-pigmentosum fibroblasts. cancer research, 50, pp. 1905-1910.

Rupert, C.S., 1960. Photoreactivation of transforming DNA by an enzyme from bakers' yeast. Journal of General Physiology, 43, pp. 573-95.

Rupert, C.S., 1962a. Photoenzymatic repair of ultraviolet damage in DNA. I. Kinetics of the reaction. Journal of General Physiology, 45, pp. 703-24.

Rupert, C.S., 1962b. Photoenzymatic repair of ultraviolet damage in DNA. II. Formation of an enzyme-substrate complex. Journal General Physiology, 45, pp. 725-41.

Rupert, C.S., Goodgal, S.H. & Herriott, R.M., 1958. Photoreactivation *in vitro* of ultraviolet-inactivated *Hemophilus influenzae* transforming factor. Journal General Physiology, 41, pp. 451-71.

Sachadyn, P., 2010. Conservation and diversity of MutS proteins. Mutation Research, 694, pp. 20-30.

Sakofsky, C.J., Runck, L.A. & Grogan, D.W., 2011. Sulfolobus Mutants, Generated via PCR Products, Which Lack Putative Enzymes of UV Photoproduct Repair. Archaea-an International Microbiological Journal.

Sakumi, K. & Sekiguchi, M., 1990. Structures and functions of DNA glycosylases. Mutation Research, 236, pp. 161-172.

Salerno, V., Napoli, A., White, M.F., Rossi, M. & Ciaramella, M., 2003. Transcriptional response to DNA damage in the archaeon *Sulfolobus solfataricus*. Nucleic Acids Research, 31, pp. 6127-6138.

Sancar, A. & Sancar, G.B., 1984. *Escherichia coli* DNA photolyase is a flavoprotein. Journal of Molecular Biology, 172, pp. 223-7.

Sancar, A. & Sancar, G.B., 1988. DNA-repair enzymes. Annual Review of Biochemistry, 57, pp. 29-67.

Sancar, A., 1994. Structure and function of DNA photolyase. Biochemistry, 33, pp. 2-9.

Sancar, A., 1996a. DNA excision repair. Annual Review of Biochemistry, 65, pp. 43-81.

Sancar, A., 1996b. No "End of History" for photolyases. Science, 272, pp. 48-9.

Sancar, A., 2003. Structure and function of DNA photolyase and cryptochrome blue-light photoreceptors. Chemical Reviews, 103, pp. 2203-2237.

Sancar, A., 2008. Structure and Function of Photolyase and *in Vivo* Enzymology: 50th Anniversary. Journal of Biological Chemistry, 283, p. 32153.

Sancar, G.B. & Smith, F.W., 1989. interactions between yeast photolyase and nucleotide excision repair proteins in *Saccharomyces-cerevisiae* and *Escherichia-coli*. molecular and cellular biology, 9, pp. 4767-4776.

Sancar, G.B., 1990. DNA photolyases - physical-properties, action mechanism, and roles in dark repair. mutation research, 236, pp. 147-160.

Sancar, G.B., 2000. Enzymatic photoreactivation: 50 years and counting. Mutation Research. Netherlands, pp. 25-37.

Sancar, G.B., Jorns, M.S., Payne, G., Fluke, D.J., *et al*., 1987. Action mechanism of *Escherichia-coli* DNA photolyase .3. photolysis of the enzyme-substrate complex and the absolute action spectrum. journal of biological chemistry, 262, pp. 492-498.

Sancar, G.B., Smith, F.W., Lorence, M.C., Rupert, C.S. & Sancar, A., 1984. sequences of the *Escherichia-coli* photolyase gene and protein. journal of biological chemistry, 259, pp. 6033-6038.

Sancar, G.B., Smith, F.W. & Heelis, P.F., 1987. Purification of the yeast PHR1 photolyase from an *Escherichia coli* overproducing strain and characterization of the intrinsic chromophores of the enzyme. Journal of Biological Chemistry, 262, pp. 15457-65.

Sancar, G.B., Smith, F.W. & Sancar, A., 1985. Binding of Escherichia-coli DNA photolyase to UV-irradiated DNA. Biochemistry, 24, pp. 1849-1855.

Saxena, C., Sancar, A. & Zhong, D.P., 2004. Femtosecond dynamics of DNA photolyase: Energy transfer of antenna initiation and electron transfer of cofactor reduction. Journal of Physical Chemistry B, 108, pp. 18026-18033.

Schenborn, E.T. & Goiffon, V., 2000. DEAE-dextran transfection of mammalian cultured cells. Methods in Molecular Biology, 130, pp. 147-53.

Schild, D., Johnston, J., Chang, C. & Mortimer, R.K., 1984. Cloning and mapping of *Saccharomyces cerevisiae* photoreactivation gene PHR1. Molecular and Cellular Biology, 4, pp. 1864-70.

Schul, W., Jans, J., Rijksen, Y., Klemann, K., *et al*., 2002. Enhanced repair of cyclobutane pyrimidine dimers and improved UV resistance in photolyase transgenic mice. The EMBO Journal, 21, p. 4719.

Seeberg, E., Eide, L. & Bjoras, M., 1995. The base excision-repair pathway. Trends in Biochemical Sciences, 20, pp. 391-397.

Setlow, J.K., Boling, M.E. & Bollum, F.J., 1965a. The chemical nature of photoreactivable lesions in DNA. Proceedings of The National Academy of Sciences of the United States of America, 53, pp. 1430-6.

Setlow, R.B. & Carrier, W.L., 1964. Disappearance of thymine dimers from DNA - error-correcting mechanism. Proceedings of The National Academy of Sciences of The United States of America, 51, pp. 226-&.

Setlow, R.B. & Setlow, J.K., 1962. Evidence that ultraviolet-induced thymine dimers in DNA cause biological damage. Proceedings of The National Academy of Sciences of The United States of America, 48, pp. 1250-7.

Setlow, R.B., Carrier, W.L. & Bollum, F.J., 1965b. Pyrimidine dimers in UV-irradiated poly dI:dC. Proceedings of The National Academy of Sciences of The United States of America, 53, pp. 1111-8.

She, Q., Singh, R.K., Confalonieri, F., Zivanovic, Y., *et al*., 2001. The complete genome of the crenarchaeon *Sulfolobus solfataricus* P2. Proceedings of the National Academy of Sciences of the United States of America, 98, pp. 7835-7840.

Shinohara, A. & Ogawa, T., 1995. Homologous recombination and the roles of double-strand breaks. Trends in Biochemical Sciences, 20, pp. 387-391.

Sinha, R.P. & Hader, D.P., 2002. UV-induced DNA damage and repair: a review. Photochemical and Photobiological Sciences, 1, pp. 225-36.

SMITH, K.C., 1964. Photochemistry of the nucleic acids. Photophysiology, 2, pp. 329-388.

Soehnge, H., Ouhtit, A. & Ananthaswamy, H.N., 1997. Mechanisms of induction of skin cancer by UV radiation. Frontiers in Bioscience, 2, pp. D538-551.

Song, Q., Tang, W., Ji, X., Wang, H. & Guo, Q., 2007. Do Photolyases Need To Provide Considerable Activation Energy for the Splitting of Cyclobutane Pyrimidine Dimer Radical Anions? Chemistry-A European Journal, 13.

Stege, H., Roza, L., Vink, A., Grewe, M., *et al*., 2000. Enzyme plus light therapy to repair DNA damage in ultraviolet-B-irradiated human skin. National Academy of Sciences, pp. 1790-1795.

Sugasawa, K., Ng, J.M.Y., Masutani, C., Iwai, S., van der Spek, P.J., *et al*. 1998. Xeroderma pigmentosum group C protein complex is the initiator of global genome nucleotide excision repair. Molecular Cell, 2, pp. 223-232.

Sutherland, B.M. & Hausrath, S.G., 1980. Insertion of *E. coli* photoreactivating enzyme into V79 hamster cells. Nature, 286, pp. 510-511.

Takahashi, S., Nakajima, N., Saji, H. & Kondo, N., 2002. Diurnal change of cucumber CPD photolyase gene (CsPHR) expression and its physiological role in growth under UV-B irradiation. Plant and Cell Physiology, 43, pp. 342-349.

Takebe, H. & Jagger, J., 1969. Action spectrum for growth delay induced in *Escherichia coli b/r* by far-ultraviolet radiation. journal of bacteriology, 98, pp. 677-&.

Takeuchi, Y., Murakami, M., Nakajima, N., Kondo, N. & Nikaido, O., 1996. Induction and repair of damage to DNA in *cucumber cotyledons* irradiated with UV-B. Plant and Cell Physiology, 37, pp. 181-187.

Tamada, T., Kitadokoro, K., Higuchi, Y., Inaka, K., *et al*., 1997. Crystal structure of DNA photolyase from *Anacystis nidulans*. Nature Structural Biology, 4, pp. 887-891.

Tanaka, K., Sekiguchi, M. & Okada, Y., 1975. Restoration of ultraviolet-induced unscheduled DNA-synthesis of xeroderma pigmentosum cells by concomitant treatment with bacteriophage-t4 endonuclease V and hvj (sendai-virus). Proceedings of The National Academy of Sciences of The United States of America, 72, pp. 4071-4075.

Terpe, K., 2003. Overview of tag protein fusions: from molecular and biochemical fundamentals to commercial systems. Applied Microbiology and Biotechnology, 60, pp. 523-533.

Thoma, F., 1999. Light and dark in chromatin repair: repair of UV-induced DNA lesions by photolyase and nucleotide excision repair. Embo Journal, 18, pp. 6585-6598.

Thompson, C.L. & Sancar, A., 2002. Photolyase/cryptochrome blue-light photoreceptors use photon energy to repair DNA and reset the circadian clock. Oncogene, 21, pp. 9043-9056.

Thresher, R.J., Vitaterna, M.H., Miyamoto, Y., Kazantsev, A., *et al*., 1998. Role of mouse cryptochrome blue-light photoreceptor in circadian photoresponses. Science, 282, pp. 1490-4.

Todo, T., 1999. Functional diversity of the DNA photolyase blue light receptor family. Mutation Research-DNA Repair, 434, pp. 89-97.

Todo, T., Ryo, H., Yamamoto, K., Toh, H., *et al*., 1996. Similarity among the Drosophila (6-4)photolyase, a human photolyase homolog, and the DNA photolyase-blue-light photoreceptor family. Science, 272, pp. 109-112.

Todo, T., Takemori, H., Ryo, H., Ihara, M., *et al*., 1993. A new photoreactivating enzyme that specifically repairs ultraviolet light-induced (6-4)photoproducts. Nature, 361, pp. 371-374.

Ueda, T., Kato, A., Kuramitsu, S., Terasawa, H. & Shimada, I., 2005. Identification and characterization of a second chromophore of DNA photolyase from *Thermus thermophilus* HB27. Journal of Biological Chemistry, 280, pp. 36237-36243.

Upton, J.W., Kaiser, W.J. & Mocarski, E.S., 2008. Cytomegalovirus M45 cell death suppression requires receptor-interacting protein (RIP) homotypic interaction motif (RHIM)-dependent interaction with RIP1. Journal of Biological Chemistry. United States, pp. 16966-70.

Ussery, D. W., 2001. DNA denaturation.

Van den Burg, B., 2003. Extremophiles as a source for novel enzymes. Current Opinion in Microbiology, 6, pp. 213-218.

Vande Berg, B.J. & Sancar, G.B., 1998. Evidence for dinucleotide flipping by DNA photolyase. Journal of Biological Chemistry, 273, pp. 20276-20284.

VanderSpek, P.J., Kobayashi, K., Bootsma, D., Takao, M., *et al.*, 1996. Cloning, tissue expression, and mapping of a human photolyase homolog with similarity to plant blue-light receptors. Genomics, 37, pp. 177-182.

Vanhouten, B., 1990. Nucleotide excision repair in *Escherichia-coli*. microbiological reviews, 54, pp. 18-51.

Wang, S.Y., 1976. Photochemistry and photobiology of nucleic-acids vol II biology. wang, shih yi (ed.). photochemistry and photobiology of nucleic acids, vol. II. biology. xv+430p. illus. academic press: new york, N.Y., U.S.A.; London, England. isbn 0-12-734602-3, pp. xv-430.

Weatherwax, R.S., 1956. Desensitization of *Escherichia-coli* to ultraviolet light. Journal of Bacteriology, 72, pp. 124-125.

Weber, S., 2005. Light-driven enzymatic catalysis of DNA repair: a review of recent biophysical studies on photolyase. Biochimica Et Biophysica Acta-Bioenergetics, 1707, pp. 1-23.

White, R.H., 1984. Hydrolytic stability of biomolecules at high temperatures and its implication for life at 250 degrees C. Nature, 310, pp. 430-2.

Woese, C.R. & Fox, G.E., 1977. Phylogenetic structure of prokaryotic domain - primary kingdoms. Proceedings of The National Academy of Sciences of The United States of America, 74, pp. 5088-5090.

Woese, C.R., Kandler, O. & Wheelis, M.L., 1990. Towards a natural system of organisms - proposal for the domains archaea, bacteria, and eucarya. Proceedings of The National Academy of Sciences of The United States of America, 87, pp. 4576-4579.

Wood, E.R., Ghane, F. & Grogan, D.W., 1997. Genetic responses of the thermophilic archaeon *Sulfolobus acidocaldarius* to short-wavelength UV light. Journal of Bacteriology, 179, pp. 5693-5698.

Wood, R.D., 1997. Nucleotide excision repair in mammalian cells. Journal of Biological Chemistry, 272, pp. 23465-23468.

Ward, J.F., 1988. DNA damage produced by ionizing-radiation in mammalian-cells - identities, mechanisms of formation, and reparability. Progress in Nucleic Acid Research and Molecular Biology, 35, pp. 95-125.

Worthington, E.N., Kavakli, I.H., Berrocal-Tito, G., Bondo, B.E. & Sancar, A., 2003. Purification and characterization of three members of the photolyase/cryptochrome family blue-light photoreceptors from *Vibrio cholerae*. Journal of Biological Chemistry, 278, pp. 39143-39154.

Wu, Y., Zhou, Y., Song, J., Hu, X., Ding, Y. & Zhang, Z., 2008. Using green and red fluorescent proteins to teach protein expression, purification, and crystallization. Biochemistry and Molecular Biology Education, 36, pp. 43-54.

Wulff, D.L. & Rupert, C.S., 1962. Disappearance of thymine photodimer in ultraviolet irradiated DNA upon treatment with a photoreactivating enzyme from baker's yeast. Biochemal and Biophysical Research Communications, 7, pp. 237-40.

Yamamoto, J., Tanaka, Y. & Iwai, S., 2009. Spectroscopic analysis of the pyrimidine(6-4)pyrimidone photoproduct: insights into the (6-4) photolyase reaction. Organic & Biomolecular Chemistry, 7, pp. 161-166.

Yamamoto, K., Fujiwara, Y. & Shinagawa, H., 1983. Evidence that the phr+ gene enhances the ultraviolet resistance of *Escherichia-coli* reca strains in the dark. molecular & general genetics, 192, pp. 282-284.

Yarosh, D., Klein, J., O'Connor, A., Hawk, J., *et al.*, 2001. Effect of topically applied T4 endonuclease V in liposomes on skin cancer in xeroderma pigmentosum: a randomised study. Lancet, 357, pp. 926-929.

Yasuhira, S. & Yasui, A., 1992. Visible light-inducible photolyase gene from the goldfish *carassius-auratus*. journal of biological chemistry, 267, pp. 25644-25647.

Yasui, A. & McCready, S.J., 1998. Alternative repair pathways for UV-induced DNA damage. Bioessays. England, pp. 291-7.

Yasui, A., Eker, A.P.M., Yasuhira, S., Yajima, H., *et al.*, 1994. A new class of DNA photolyases present in various organisms including aplacental mammals. EMBO journal, 13, pp. 6143-6151.

Yasui, A., Takao, M., Oikawa, A., Kiener, A., *et al.*, 1988. Cloning and characterization of a photolyase gene from the cyanobacterium *Anacystis-nidulans*. Nucleic Acids Research, 16, pp. 4447-4463.

You, Y.H., Lee, D.H., Yoon, J.H., Nakajima, S., *et al.*, 2001. Cyclobutane pyrimidine dimers are responsible for the vast majority of mutations induced by UVB irradiation in mammalian cells. Journal of Biological Chemistry. United States, pp. 44688-94.

You, Y.H., Szabo, P.E. & Pfeifer, G.P., 2000. Cyclobutane pyrimidine dimers form preferentially at the major p53 mutational hotspot in UVB-induced mouse skin tumors. Carcinogenesis, 21, pp. 2113-7.

Yuan, Q., Metterville, D., Briscoe, A.D. & Reppert, S.M., 2007. Insect cryptochromes: Gene duplication and loss define diverse ways to construct insect circadian clocks. Molecular Biology and Evolution, 24, pp. 948-955.

Zhao, X.D., Liu, J.Q., Hsu, D.S., Zhao, S.Y., *et al.*, 1997. Reaction mechanism of (6-4) photolyase. Journal of Biological Chemistry, 272, pp. 32580-32590.

Zillig, W., Stetter, K.O., Wunderl, S., Schulz, W., *et al.*, 1980. The *sulfolobus-caldariella* group - taxonomy on the basis of the structure of DNA-dependent RNA-polymerases. archives of microbiology, 125, pp. 259-269.

Zwetsloot, J.C.M., Vermeulen, W., Hoeijmakers, J.H.J., Yasui, A., *et al.*, 1985. Microinjected photoreactivating enzymes from Anacystis and Saccharomyces monomerize dimers in chromatin of human-cells. mutation research, 146, pp. 71-77.

Appendix

1. *S. solfataricus phr* gene sequence (1302 bp):

GTGCTCTGCCTATTTATATTTAGAAGAGATCTGAGACTAGACGACAATAC
TGGATTAATTAAAGCTTTAGAGGATTGCGAGAAAGTTATTCCAGCGTTTA
TATTAGATCCTAGACAAGTCGGTAATGAAAACGAATACAAATCAGAGTTT
GCCATAAACTTCATGATTAATTCATTGAATGAGCTAAATGACGAGTTAAG
AAAAAGAGGATCCAGACTTTATGTCTACTTCGGACTAGCTGAGGAGGTAA
TAAAGAACTTACTTAAAGATGTTGATGCAGTTTATCTAAATGAGGATTAT
ACTCCATTTAGTAAAATGAGGGACGAAAGAATTCGCAAGTACTGTGAAGA
TACCGGAAAAATTATGAAATCTTTTGAGGATTACTTACTCACATCAAAGA
ACGATTTTAAAAACTATAGGAACTTCACAACATTTTATAATGTAGTAAAA
AATAAACAAATAAAGAAACCAGTTCAAAATAATTATACAAATTACTATAA
AAATTCTTTAGGTGACGAGCATGAATTACCACCTAGACAAGGAGAACGAG
GAGGAAGAAAAGAGGGCATTAAATTAATAGAGAGAGCAAGGCAAATTAAT
TACGATAGGAAAGATTTCGTAGCAGAGGATAATAGAACTTTTCTTTCACC
CCATCTGAAATTTGGAACCTTGTCAATTAGAGAGGTTTATTATTCTCTAT
TAGACAGTCAAGCTATAATTAGGCAGTTATACTGGAGGGATTTCTATACT
TTATTGGCTTACTATAATGAGAGAGTATTTCATGAACCGTTAAAAAGGGA
ATATAATTGCATTGAGTGGGAGAACAATGAAAGGCTATTTCAAGCTTGGC
TTGAGGGAAAAACTGGATATCCAATAATAGATGCTGGAATGAGACAATTG
AACCGGACTGGTGATATGCCGAACAGAGTTAGAATGTTAACCGCATTTTT
CCTAGTTAAGGTTCTTATAATTGATTGGAGGATAGGTGAGAAATACTTTG
CAAGTAAATTAATTGATTATGATCCTTCGGTTAACAATGGAAACTGGCAA
TGGATAGCCTCTGTAGGTACTGATTATATATTTAGAGTATTTGACCCTTG
GAAACAACAGGTTACATATGATCCGGAGGCAAAGTATATAAAAAGGTGGG
TAGATGAATTGGAAAGCTATGACGCAGAGATCATACATAATGCATACAAA
TATACTCTGAAGAGCTACCCTAAACCTATAGTAGATTGGAGAATAAGGGT
AAATCTCGCAAAGAGACTTTACGAGGTATGTAGGAAATCTAAAATAAAAT
AG

2. *S. solfataricus phr* protein sequence (54 KDa):

```
         10          20          30          40          50          60
MGSSHHHHHH SSGLVPRGSH MASMLCLFIF RRDLRLDDNT GLIKALEDCE KVIPAFILDP

         70          80          90         100         110         120
RQVGNENEYK SEFAINFMIN SLNELNDELR KRGSRLYVYF GLAEEVIKNL LKDVDAVYLN

        130         140         150         160         170         180
EDYTPFSKMR DERIRKYCED TGKIMKSFED YLLTSKNDFK NYRNFTTFYN VVKNKQIKKP

        190         200         210         220         230         240
VQNNYTNYYK NSLGDEHELP PRQGERGGRK EGIKLIERAR QINYDRKDFV AEDNRTFLSP

        250         260         270         280         290         300
HLKFGTLSIR EVYYSLLDSQ AIIRQLYWRD FYTLLAYYNE RVFHEPLKRE YNCIEWENNE

        310         320         330         340         350         360
RLFQAWLEGK TGYPIIDAGM RQLNRTGDMP NRVRMLTAFF LVKVLIIDWR IGEKYFASKL

        370         380         390         400         410         420
IDYDPSVNNG NWQWIASVGT DYIFRVFDPW KQQVTYDPEA KYIKRWVDEL ESYDAEIIHN

        430         440         450
AYKYTLKSYP KPIVDWRIRV NLAKRLYEVC RKSKIK
```

Sequence in red indicates the additional amino acids residues that was added from the pET28a vector at the N-terminal region of the protein in order to His tag the protein.

3. Primers sequences for cloning *S. solfataricus phr* gene in pGEM-T for expression in *E. coli* cells

a. Forward primer (SSforNheI):

5' CTAG*CTAGCATGCTCTGCCTATTTATA 3'

*NheI cut site

b. Reverse primer (SSrevSacI):

5' CGAGCT*CCTATTTTATTTTAGATTTCCTACA 3'

* SacI cut site

4. pGEM-T Easy Vector

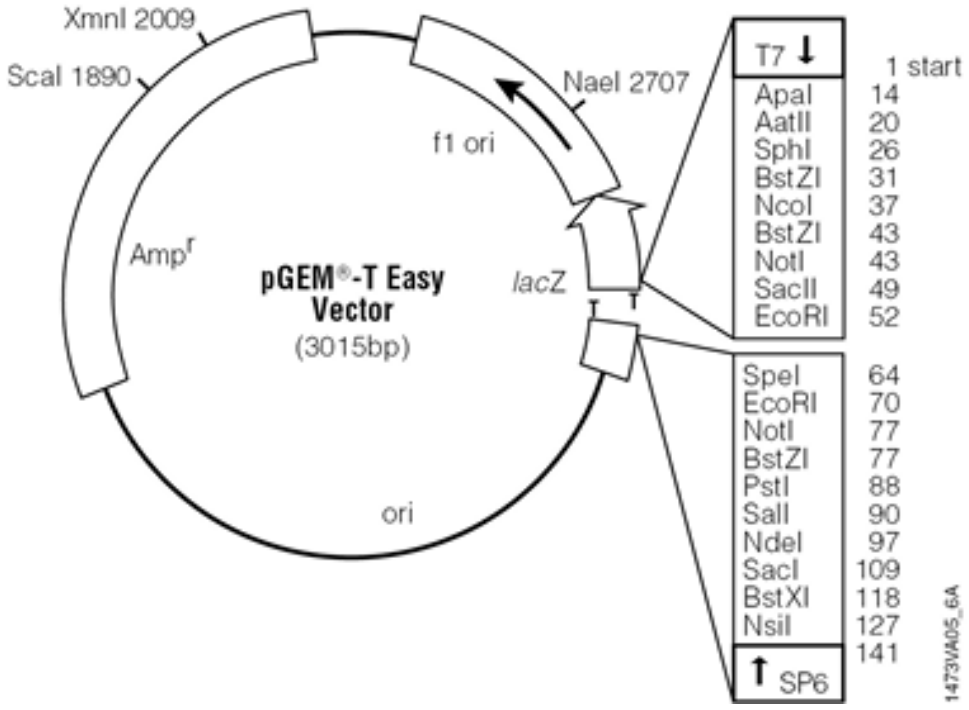

5. pET28a vector

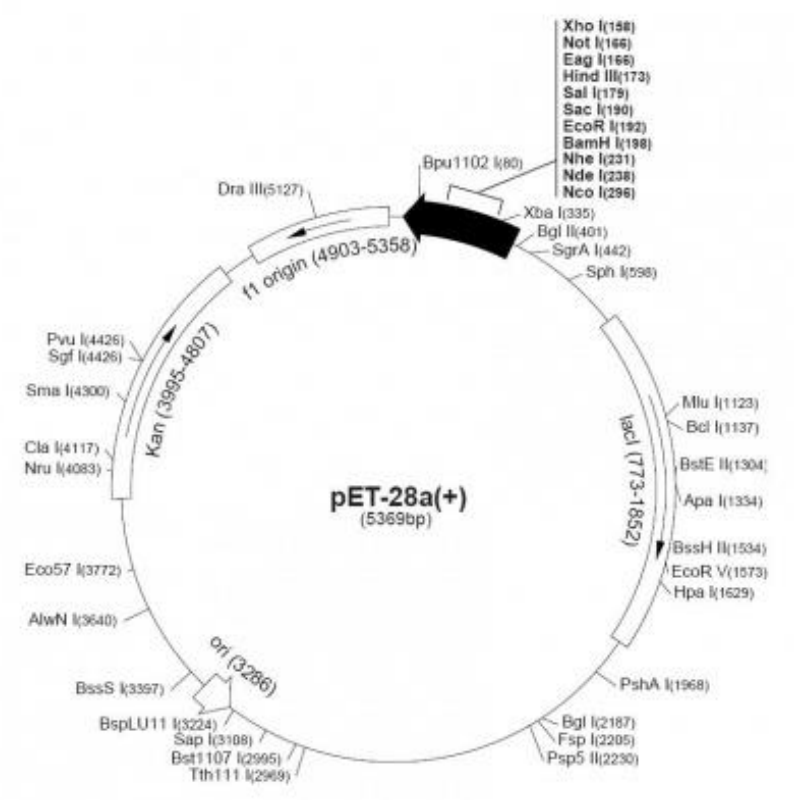

6. pDsRed monomer mammalian expression vector map

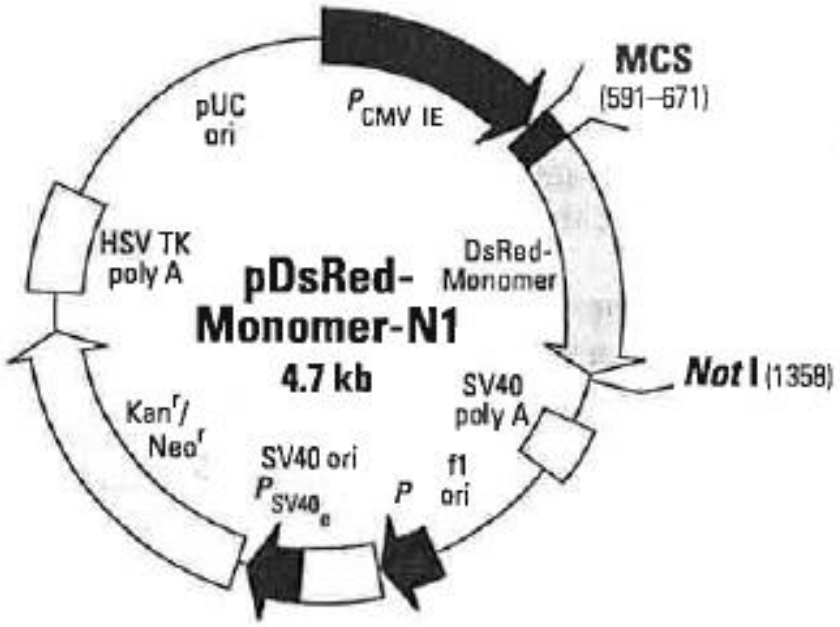

7. Primers sequences of 3 *phr* genes from SS, RK and *E. coli* for cloning in pGEM-T vector in order for express in mammalian cells

a. Forward primer sequence for SS *phr* (SSphr-stopforNheI):

5' CTAG*CTAGCCATGAAGCGTAAGGTGCTCTGCCTATT 3'

b. Reverse primer sequence for SS *phr* (SSphr-stoprevKpnI):

5' CGGTAC*CCTATTTTATTTTAGATTTCCTACA 3'

c. Forward primer sequence for RK *phr* (RK-stoprforNheI):

5' CTAG*CTAGCCATGAAGCGTAAGGTGGACTCCAAAAAGAG 3'

d. Reverse primer sequence for RK *phr* (RK-stoprevSacI):

5' CGAGCT*CATCTGCAGGGCTGATCTTTCGTTC 3'

e. Forward primer sequence for *E. coli phr* (Ecoli-stopforSacI):

5' CGAGCT*CATGAAGCGTAAGGTGACTACCCATCTGGT 3'

f. Reverse primer sequence for *E. coli phr* (Ecoli-stoprevKpnI):

5' CGGGGTAC*CTTTCCCCTTCCGCGC 3'

Red sequences indicate incorporated restriction sites into the flanking region of both forward and reverse primers. Blue sequences indicate the incorporated NLS sequences in the forward primers correspond to the amino acid sequence (KRK).

8. pCY4B vector map

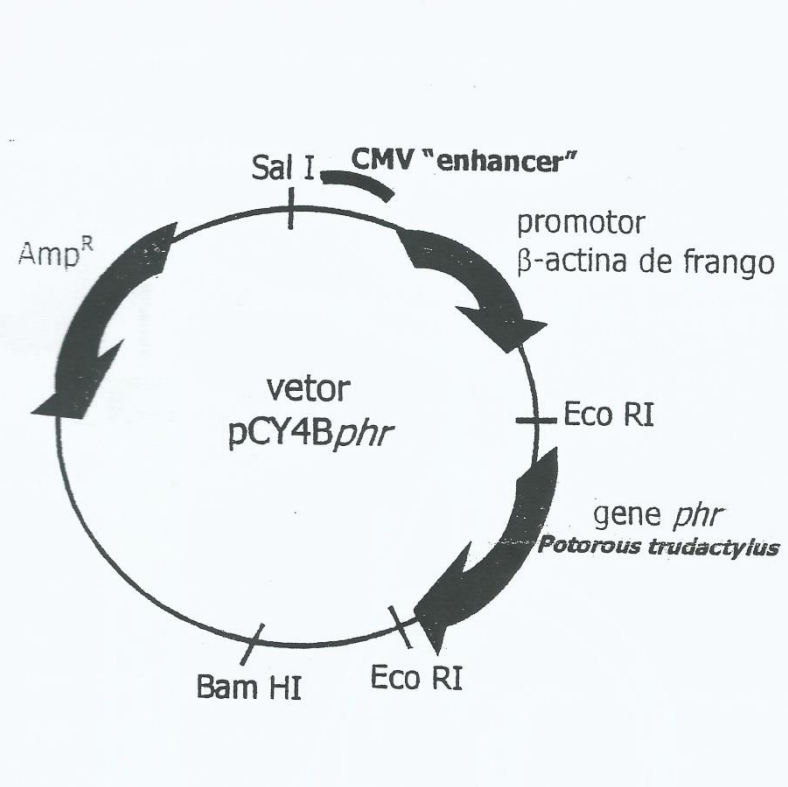

9- Amino acid sequence alignment of *S. solfataricus* photolyase with the identified crystal structurs of photolyase from different organisms.

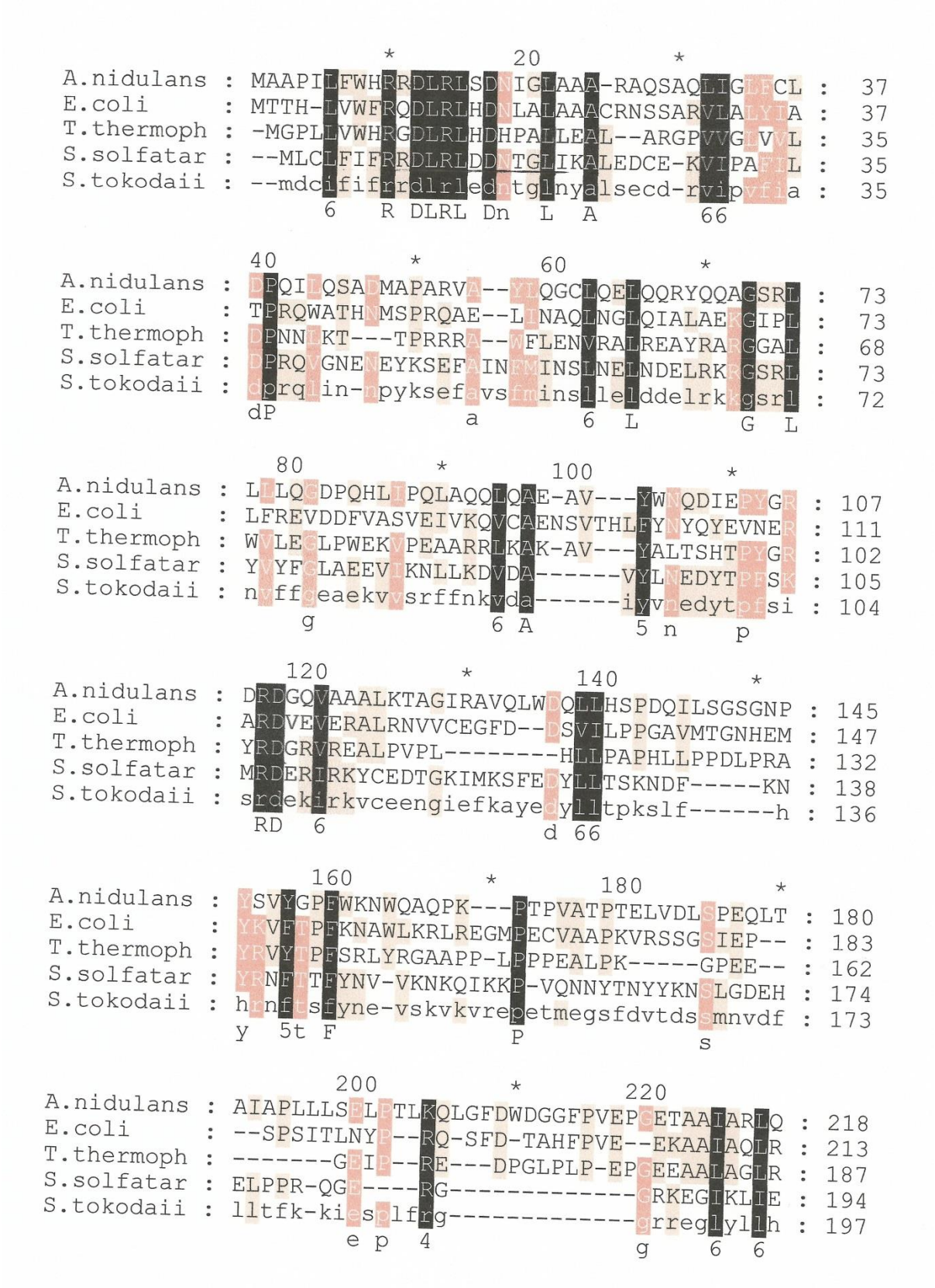

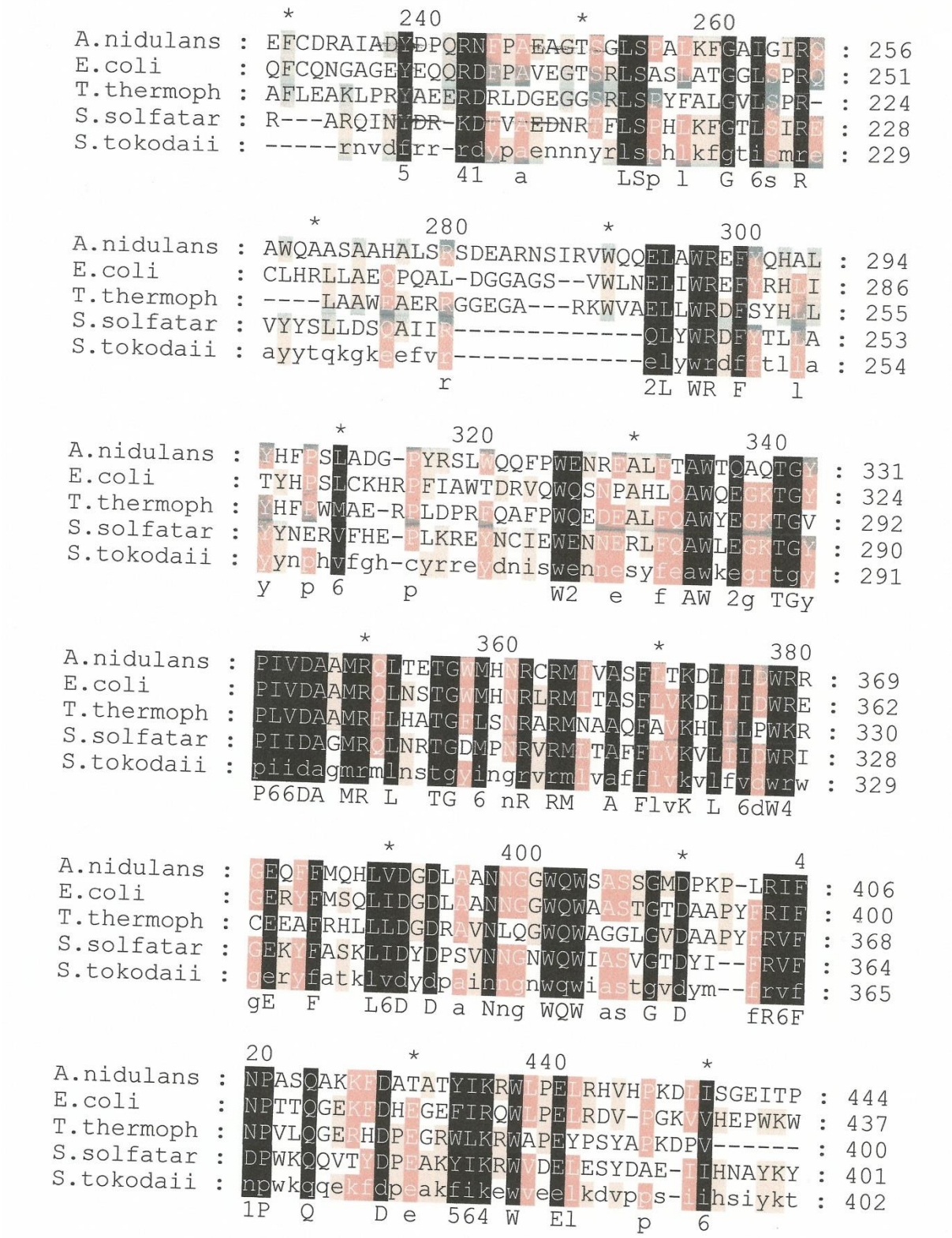
A.nidulans
E.coli
T.thermoph
S.solfatar
S.tokodaii
240
260
280
300
320
340
360
380
400
440

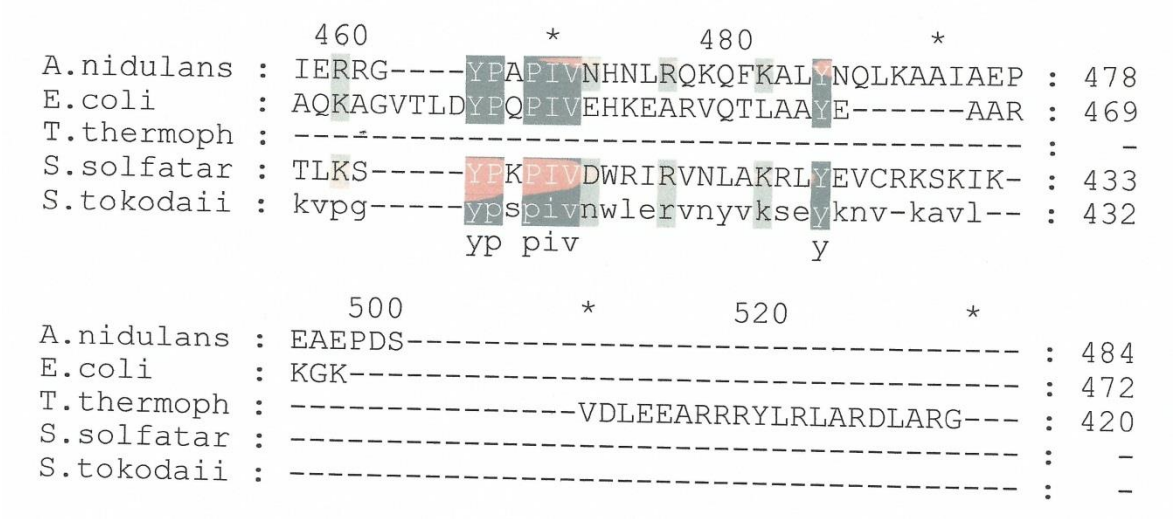

GI number for *A. nidulans*: 118595452

GI number for *E. coli*: 1651311

GI number for *T. thermophilus*: 55978183

GI number for *S. solfataricus*: 13815773

GI number for *S. tokodaii*: 499287596

10. Amino acid sequence alignment of the identified *s. solfataricus phr* gene in this study (S .sphriden) with the annotated *phr* sequence for *S. solfataricus* P2 by She et al 2001 (S. sphrP2).

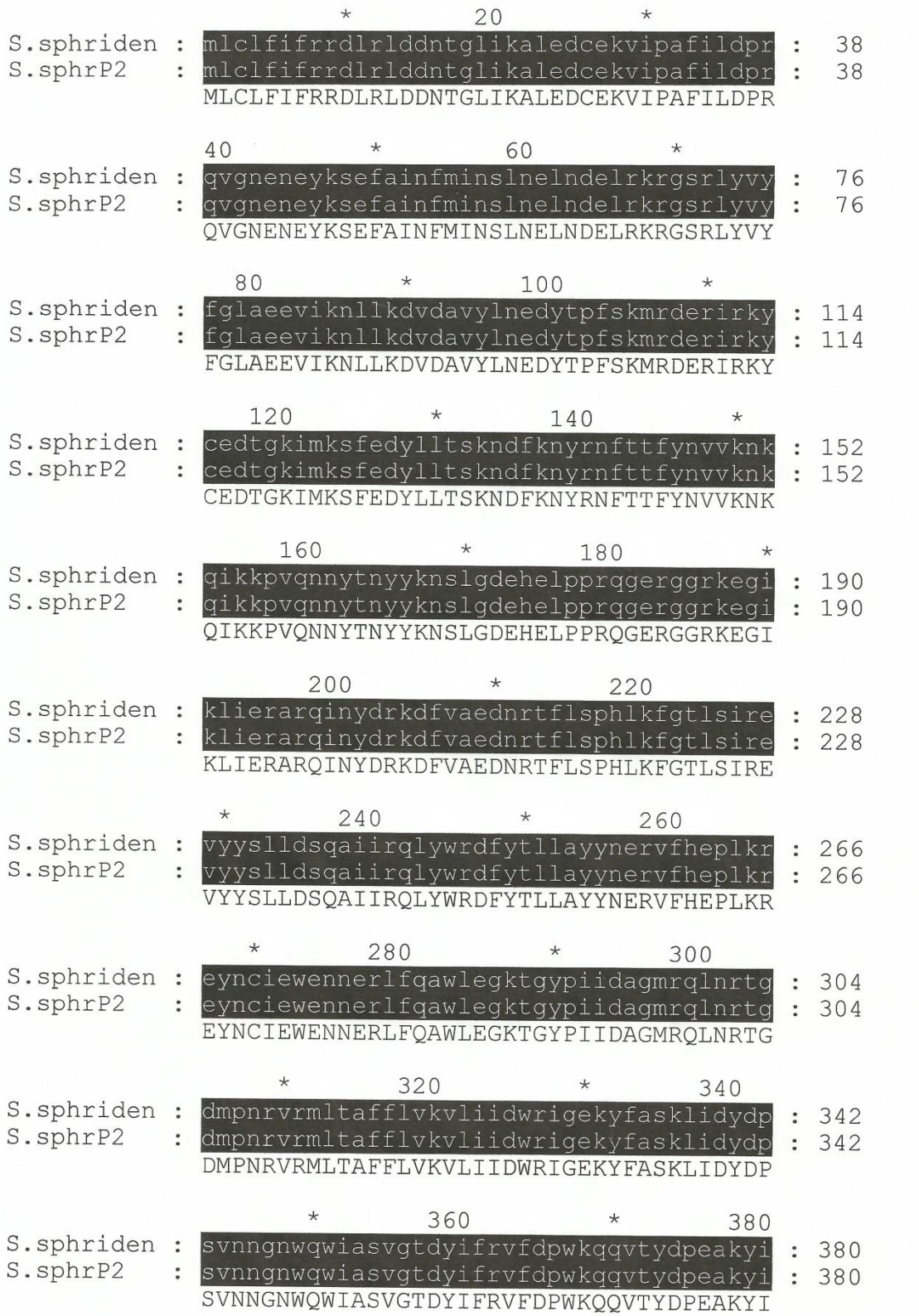
* 20 *
S.sphriden : mlclfifrrdlrlddntglikaledcekvipafildpr : 38
S.sphrP2 : mlclfifrrdlrlddntglikaledcekvipafildpr : 38
MLCLFIFRRDLRLDDNTGLIKALEDCEKVIPAFILDPR
40 * 60 *
S.sphriden : qvgneneyksefainfminslnelndelrkrgsrlyvy : 76
S.sphrP2 : qvgneneyksefainfminslnelndelrkrgsrlyvy : 76
QVGNENEYKSEFAINFMINSLNELNDELRKRGSRLYVY
80 * 100 *
S.sphriden : fglaeeviknllkdvdavylnedytpfskmrderirky : 114
S.sphrP2 : fglaeeviknllkdvdavylnedytpfskmrderirky : 114
FGLAEEVIKNLLKDVDAVYLNEDYTPFSKMRDERIRKY
120 * 140 *
S.sphriden : cedtgkimksfedylltskndfknyrnfttfynvvknk : 152
S.sphrP2 : cedtgkimksfedylltskndfknyrnfttfynvvknk : 152
CEDTGKIMKSFEDYLLTSKNDFKNYRNFTTFYNVVKNK
160 * 180 *
S.sphriden : qikkpvqnnytnyyknslgdehelpprqgerggrkegi : 190
S.sphrP2 : qikkpvqnnytnyyknslgdehelpprqgerggrkegi : 190
QIKKPVQNNYTNYYKNSLGDEHELPPRQGERGGRKEGI
200 * 220
S.sphriden : klierarqinydrkdfvaednrtflsphlkfgtlsire : 228
S.sphrP2 : klierarqinydrkdfvaednrtflsphlkfgtlsire : 228
KLIERARQINYDRKDFVAEDNRTFLSPHLKFGTLSIRE
* 240 * 260
S.sphriden : vyyslldsqaiirqlywrdfytllayynervfheplkr : 266
S.sphrP2 : vyyslldsqaiirqlywrdfytllayynervfheplkr : 266
VYYSLLDSQAIIRQLYWRDFYTLLAYYNERVFHEPLKR
* 280 * 300
S.sphriden : eynciewennerlfqawlegktgypiidagmrqlnrtg : 304
S.sphrP2 : eynciewennerlfqawlegktgypiidagmrqlnrtg : 304
EYNCIEWENNERLFQAWLEGKTGYPIIDAGMRQLNRTG
* 320 * 340
S.sphriden : dmpnrvrmltafflvkvliidwrigekyfasklidydp : 342
S.sphrP2 : dmpnrvrmltafflvkvliidwrigekyfasklidydp : 342
DMPNRVRMLTAFFLVKVLIIDWRIGEKYFASKLIDYDP
* 360 * 380
S.sphriden : svnngnwqwiasvgtdyifrvfdpwkqqvtydpeakyi : 380
S.sphrP2 : svnngnwqwiasvgtdyifrvfdpwkqqvtydpeakyi : 380
SVNNGNWQWIASVGTDYIFRVFDPWKQQVTYDPEAKYI

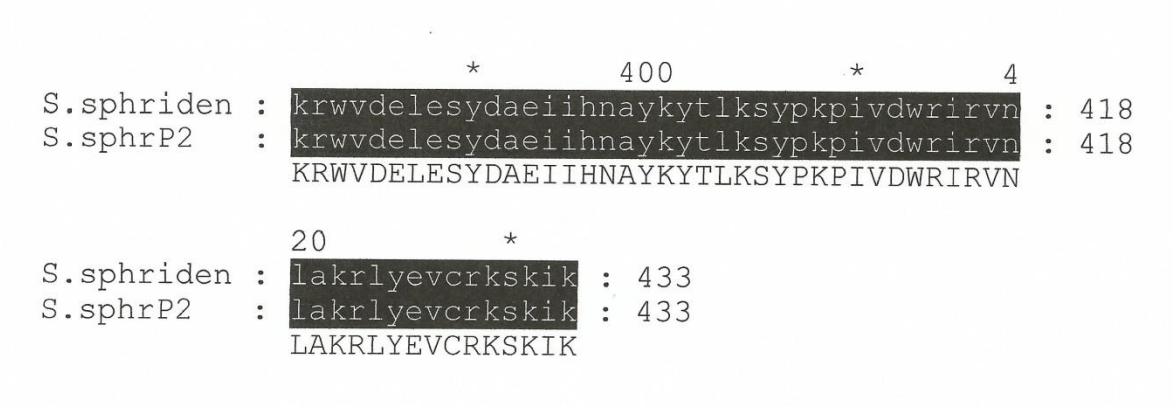
* 400 * 4
S.sphriden : krwvdelesydaeiihnaykytlksypkpivdwrirvn : 418
S.sphrP2 : krwvdelesydaeiihnaykytlksypkpivdwrirvn : 418
KRWVDELESYDAEIIHNAYKYTLKSYPKPIVDWRIRVN
20 *
S.sphriden : lakrlyevcrkskik : 433
S.sphrP2 : lakrlyevcrkskik : 433
LAKRLYEVCRKSKIK